Ph.D. Dissertation of Science

Relationship between upper-ocean variability and tuna catches in the tropical western Indian and Pacific Oceans

열대서인도양과 열대서태평양 상층 해양 변동성과 다랑어류 어획량 사이의 관계

August 2023

School of Earth and Environmental Sciences

Graduate School

Seoul National University

Jihwan Kim

Relationship between upper-ocean variability and tuna catches in the tropical western Indian and Pacific Oceans

Supervisor: Hanna Na, Professor

Submitting a Ph.D. Dissertation of Science
May 2023

School of Earth and Environmental Sciences
Graduate School
Seoul National University
Jihwan Kim

Confirming the Ph.D. Dissertation written by
Jihwan Kim
July 2023

Chair	Yang-Ki Cho	(인)
Vice Chair	Hanna Na	(인)
Examiner	SungHyun Nam	(인)
Examiner	Young-Gyu Park	(인)
Examiner	Sukyung Kang	(인)

Abstract

Relationship between upper-ocean variability and tuna catches in the tropical western Indian and Pacific Oceans

Jihwan Kim
School of Earth and Environmental Sciences
The Graduate School
Seoul National University

Tuna catches are strongly influenced by physical ocean environmental variables, including sea surface temperature, thermocline depth, and current velocity. Therefore, it is crucial to understand the relationship between ocean environmental variability and tuna catches in order to explain the changes in tuna fisheries. This dissertation investigated the statistical relationship between ocean environmental variability and annual catches of skipjack (*Katsuwonus pelamis*), yellowfin (*Thunnus albacares*), and bigeye (*Thunnus obesus*) tuna, the most abundant tuna species in the tropical western Indian and Pacific Oceans, where the largest tuna catches were recorded over 25 years.

The statistical relationship between ocean environmental variability and annual tuna catches in the southwestern tropical Indian Ocean (SWTIO) suggests that the catches of yellowfin and bigeye tuna

in the northern region of the SWTIO increase as the thermocline and 20° C isotherm deepen. Further analysis reveals that the favorable ocean conditions for tuna catches develop during El Niño years and persist in the following years. However, it is difficult to explain the changes in the tuna catches in the southern region of the SWTIO based on the relationship with ocean environmental variability, mainly because the variance of ocean environmental variables is relatively weak.

In the Western Central Pacific (WCP), annual catch amounts of skipjack tuna increase under La Niña-like conditions in the western region, whereas El Niño-like conditions are associated with increased skipjack tuna catches in the eastern region, indicating a zonal difference. Moreover, compared to the skipjack tuna catch amount, the yellowfin and bigeye tuna catch amounts exhibit opposite characteristics in terms of their statistical relationship with the ocean environmental variables.

The predictability of the annual catch amount was examined for the skipjack tuna in the WCP. The results show that subsurface temperature or near-surface salinity can be a good predictor of the catch variability, which suggests potential predictability of the annual catch amounts of other tuna species, such as yellowfin and bigeye tuna.

This dissertation contributes to understanding the statistical relationship between ocean environmental variables and tuna catches, which could assist in the sustainable management of tuna fisheries. It also highlights that the potential predictability of the catch amount would increase over the regions with stronger environmental variability.

Keyword: Tuna catches, El Niño-Southern Oscillation, Southwestern Tropical Indian Ocean, Western Central Pacific Ocean

Student Number: 2019-28546

Table of Contents

List of Figures

List of Tables

1. Introduction

The tuna fishing industry is a major player in the global economy with a rich history spanning several centuries. It has been instrumental in the development of many countries, providing critical support to local economies, creating jobs, and ensuring a steady supply of fresh protein for communities (Remolà & Gudmundsson, 2018). The industry's economic reach is vast, with an estimated $40 billion in economic activity generated globally in 2018 (Figure 1.1) (Gibbon & Galland, 2020)

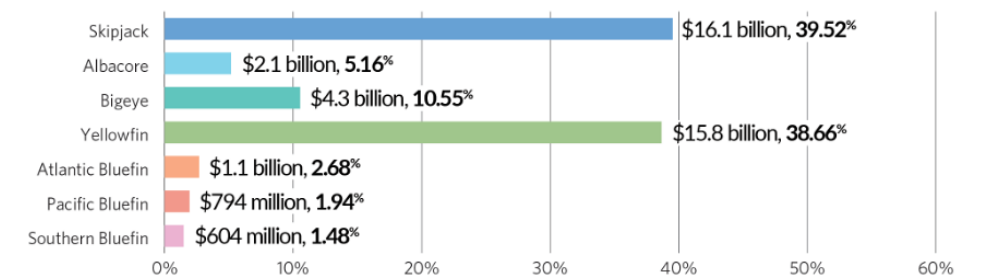

Figure 1.1 The total end tuna values of each species in 2018. Retrieved from https://www.pewtrusts.org/en/research-and-analysis/reports/2020/10/netting-billions-2020-a-global-tuna-valuation.

The collection of access fees from foreign fishing fleets operating in a country's Exclusive Economic Zone (EEZ) is a key aspect of the industry's impact (Williams & Terawasi, 2010). This underscores the

importance of the tuna fishing industry to the global economy and is a significant source of funding for many countries. Ensuring the continued success of the tuna fishing industry depends on understanding the current and future availability of tuna species in each EEZ. This requires careful monitoring and management to maintain the health of tuna populations and ensure the long-term viability of the industry. In conclusion, the tuna fishing industry is an important player in the global economy, providing vital support to local economies, creating jobs, and ensuring a steady supply of fresh protein.

The skipjack tuna (*Katsuwonus pelamis*), yellowfin tuna (*Thunnus albacares*), and bigeye tuna (*Thunnus obesus*) are three highly prized species of tuna found in tropical and temperate oceanic waters around the world (Williams & Terawasi, 2010; Table 1.1). These species are members of the Scombridae family, which also includes mackerels and bonitos, and are known for their exceptional swimming abilities and predatory instincts (Remolà & Gudmundsson, 2018). These tunas are not only important to the ocean ecosystem as top predators, but also play an important role in the global economy through their commercial value in fisheries.

Table 1.1 The physiologies of skipjack tuna (*Katsuwonus pelamis*), yellowfin tuna (*Thunnus albacares*), and bigeye tuna (*Thunnus obesus*).

	Life Span	Maturity Age	Optimal Growth Temperature	Diet
Skipjack tuna	5 years	10 months	19–26°C	Small organisms from upper layers (thermocline)
Yellowfin tuna	7 years	2 years	26–31°C	Small organisms from upper and middle layers
Bigeye tuna	Over 10 years	2 years	27°C (juvenile) – 10°C (adult)	Small organisms from upper layers (juvenile) and mesopelagic prey (adult)

The skipjack tuna is the smallest of the three species and is distinguished by its yellowish-brown dorsal side and white ventral side (Brill, 1994; Langley et al., 2009). It grows to an average length of 36 inches and is typically found in upper oceanic waters less than 100 meters deep, with an optimal temperature range of 19-26° C and oxygen levels greater than 3.75 ml/L (Brill, 1994; Senina et al., 2018). It feeds on small organisms found in the upper layers of the ocean and prefers warm waters (Ashida et al., 2009; Senina et al., 2018).

The yellowfin tuna is larger than the skipjack tuna and is found in tropical and subtropical oceans throughout the world (Tremblay-Boyer et al., 2017). It is found at mid-depths and feeds on small organisms in the upper and middle layers (Schaefer et al., 2011; Senina

et al., 2018). Its optimum temperature range for larvae is 26-31° C and it can survive in waters with lower oxygen levels than the skipjack tuna (Schaefer & Oliver, 1998; Wexler et al., 2011; Nicol et al., 2022). It feeds on small organisms found in the upper and middle layers of the ocean (Senina et al., 2018).

The bigeye tuna is the largest of the three species and has a longer life span, older age at maturity, and lower natural mortality than the skipjack (Brill, 1994; Hampton & Gunn, 1998; Farley et al., 2017). Juvenile bigeye tuna is often found in the surface layer with skipjack tuna, but as they mature, they explore deeper layers and have a wider temperature range, from 27° C for the youngest to 10° C for the oldest (Lehodey et al., 2010). This species has a better thermoregulatory system and can survive in waters with lower levels of oxygen than either the skipjack or the yellowfin tuna (Evans et al., 2008; Schaefer & Fuller, 2010). The bigeye tuna feeds on small organisms from the upper layers during the juvenile period and on mesopelagic prey during the adult period (Senina et al., 2018).

In summary, skipjack, yellowfin, and bigeye tuna play a critical role in the ocean ecosystem as top predators and also impact the global economy through their importance in the fishing industry.

Valued for their swimming and hunting abilities, these species vary in size, body shape, coloration, and feeding habits. For their conservation and the continued success of the fishing industry, understanding the unique characteristics and habitat requirements of each species is essential.

These three tuna species are primarily caught using longline and purse seine fishing techniques. Longline (LL) fishing can last for several weeks, with lines containing thousands of hooks and bait (Figure 1.2) (Nakano et al., 1997; Morato et al., 2010).

The LL method is commonly used in the deep ocean to target adult yellowfin and bigeye tuna which are typically found in deeper waters (Lehodey, 2000). The purse-seine (PS) method is a surface gear that uses a square net or circle of netting to encircle schools of juvenile tuna with its larger mesh sizes, making it an effective method for catching pelagic, small-sized juvenile tuna species such as skipjack tuna and juvenile yellowfin and bigeye tuna found in relatively shallow waters (shallower than about 200 meters) (Figure 1.3) (Green, 1967).

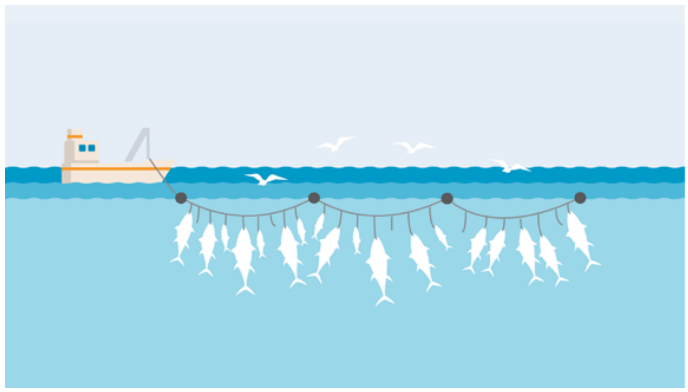

Figure 1.2 Schematic of the LL fishing method. Retrieved from https://www.msc.org/what-we-are-doing/our-approach/fishing-methods-and-gear-types/longlines.

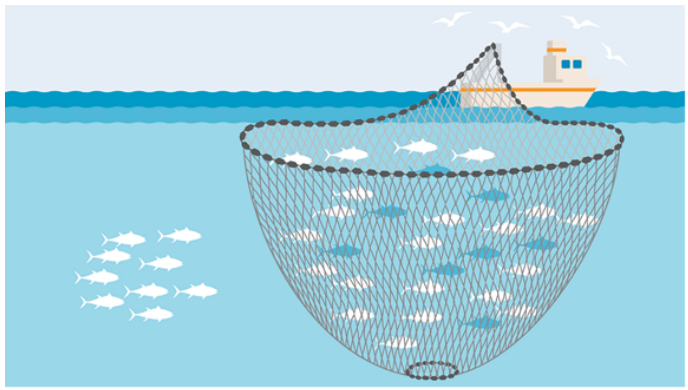

Figure 1.3 same as Figure 1.2, but for the PS fishing method. Retrieved from https://www.msc.org/what-we-are-doing/our-approach/fishing-methods-and-gear-types/purse-seine.

The El Niño-Southern Oscillation (ENSO) has a significant impact on tuna populations by affecting the distribution, biomass, and availability of micronekton, a key food source for tuna (Lehodey et al., 2011; Bell et al., 2013; Senina et al., 2018). This can lead to shifts in population dynamics and productivity, resulting in increased mortality and reduced production in tuna fisheries (Lehodey et al., 2011). The sensitivity of tuna to changes in their trophic sources is well known, and a decrease in micronekton during ENSO events can severely impact the health of tuna populations (Lehodey et al., 2011). Previous studies suggest that the distribution of skipjack tuna is linked to the zonal shift of the equatorial Pacific warm pool, which is influenced by ENSO (Figure 1.4) (Lehodey et al., 1997). During El Niño, the western equatorial Pacific warm pool expands eastward, shifting the habitat of skipjack tuna eastward. On the other hand, during La Niña, the warm pool contracts westward, causing the skipjack habitat to shift westward. This leads to changes in the spatial distribution of skipjack catches in response to ENSO.

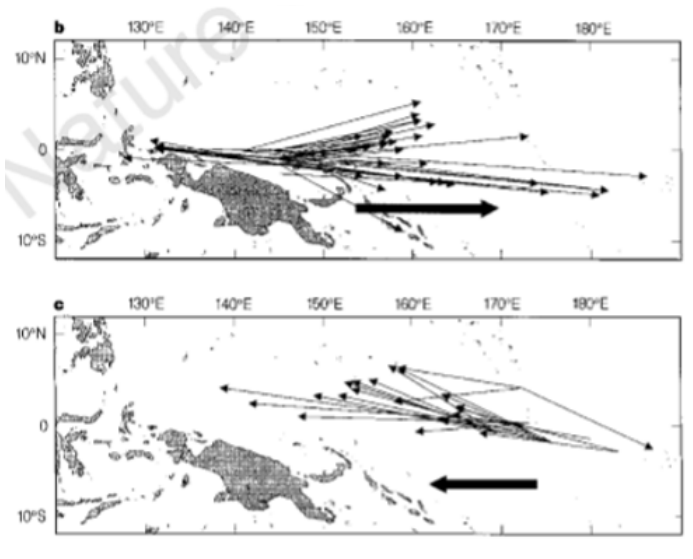

Figure 1.4 Displacements of tagged skipjack tuna. (top) Tuna released May 1991, recaptured before February 1992 (El Niño years). (bottom) Tuna released March 1992, recaptured before October 1992 (La Niña years) (Figure adapted from Lehodey et al., 1997).

The thermocline acts as a barrier to vertical migration for juvenile tuna, but adult yellowfin and bigeye tuna can dive below the thermocline to access mesopelagic prey (Schaefer & Fuller, 2010; Aoki et al., 2020). ENSO can have a significant impact on the habitat of adult tuna, resulting in changes in their catchability. The variability in thermal structure caused by ENSO can lead to a shallowing of the thermocline in the western Pacific during El Niño, resulting in increased catchability for the surface tuna fishery (Lehodey, 2000; Harley et al., 2011). This can lead to higher yields for fishermen targeting adult tuna in these areas. On the other hand, during La Niña, the thermocline deepens, reducing the catchability of yellowfin and

bigeye tuna and leading to lower yields for fishermen.

It's important to note that the effect of ENSO on the catchability of different tuna species caught by different fishing techniques also depends on the depth of the thermocline. This is because the thermocline can act as a physical barrier, making it more difficult to target and catch adult tuna, especially those caught by purse seine fishing techniques. In addition, the migration patterns of adult tuna can also be influenced by ENSO, which can further affect their catchability.

The interdependence between ocean environmental conditions and tuna populations is a well-established phenomenon that has been observed in several ocean basins, reinforcing the critical importance of its consideration in the management of tuna fisheries. This is because each ocean basin has its own unique physical and biological characteristics that have a profound effect on the distribution, migration patterns, and behavior of tuna. For example, the western Indian Ocean is known for its strong coastal upwelling that occurs along the eastern coasts of African countries such as Madagascar, Africa, and Sumatra (Saji et al., 1999; POSEIDON et al., 2014; Varghese et al., 2019). This upwelling results in an abundant supply of nutrients that lead to a thriving population of phytoplankton and

zooplankton, which serve as the foundation of the food chain that supports the growth and prosperity of tuna populations (Hermes and Reason, 2008). The Indian Ocean Dipole, a climatic event that causes oceanic and atmospheric perturbations, can enhance or diminish the effects of upwelling, thus affecting the overall productivity of the western Indian Ocean and the availability of tuna in the region (Kumari et al., 1993; Mohri and Nishida, 2000; Ménard et al., 2007; Lan et al., 2013). In the North Atlantic, the 20° C isotherm depth is a useful predictor of the distribution of bigeye tuna (Lan et al., 2018). This is because the 20° C isotherm is known to be a preferred habitat for bigeye tuna, providing an optimal thermal environment for feeding, growth, and reproduction (Lan et al., 2018). Changes in the depth of the 20° C isotherm can affect the distribution and catchability of bigeye tuna because the shallow depth of the isotherm can increase the catchability of bigeye tuna caught by fishing gear such as longlines (Nakano et al., 1997; Morato et al., 2010).

Thus, it's clear that ocean environmental variability and its impact on the distribution and abundance of tuna populations is an important aspect of tuna management and conservation. Climate variability, including ENSO and IOD, can have a significant impact on the distribution, migration, and behavior of tuna, affecting their

catchability and productivity. As a result, effective tuna management and conservation require that fishers, policymakers, and researchers consider these effects and the specific ocean conditions of each ocean basin when making tuna management and conservation decisions to effectively manage these valuable resources and ensure the sustainability of tuna populations.

Recently, the overexploitation of tuna stocks has raised serious concerns about the sustainability of these fish populations, which play a critical role in the ocean ecosystem and the livelihoods of millions of people around the world (Ritchie & Roser, 2021). The declining biomass of these fish species has led to a reduction in total catch and an increase in fishing efforts, resulting in higher economic and social costs for the fishing industry and the communities that depend on it.

To mitigate the effects of overfishing, it is essential to understand the factors contributing to the decline of tuna populations and the interactions between fisheries and the ocean environment. This requires a thorough examination of the relationship between fishery productivity and ocean environmental variability, as well as the influence of other human activities, such as fishing gear selectivity and migration patterns of the species.

In conclusion, it is essential to address the decline of tuna populations by examining the relationship between fishing and environmental variability to ensure the sustainability of these valuable resources. This requires a multidisciplinary approach that integrates knowledge from marine biology, ecology, oceanography, and fisheries science.

By examining the interplay between ocean environmental variables (e.g, temperature, salinity, current, DO, etc.) and fishery productivity, this dissertation will help identify tuna catch variability undulated by climate variability and inform strategies for sustainable management. This dissertation aims to provide a comprehensive and up-to-date understanding of the relationship between fishery productivity and ocean environmental variables in the tropical Pacific and Indian Oceans.

Chapter 2 focuses on the southwestern tropical Indian Ocean, another important region for tuna populations. This region is characterized by strong coastal upwelling and the Indian Ocean Dipole, a climate phenomenon that can significantly affect environmental variability and, in turn, fishery productivity. By analyzing available data on yellowfin and bigeye tuna catches, this chapter examines the

relationship between ocean environmental variability and fishery productivity in the southwestern tropical Indian Ocean.

Chapter 3 shifts the focus to the western central Pacific Ocean, home to some of the world's largest tuna fisheries. This region is characterized by strong ocean currents and warm sea surface temperatures that create a productive environment for tuna populations. Through an analysis of available data, this chapter examines the relationship between ocean environmental variability and the productivity of tuna fisheries in the western central Pacific, including catches of skipjack, yellowfin, and bigeye tuna, and evaluates the potential predictability of the annual catches of skipjack tuna in the FSM.

The results of this dissertation will provide valuable insights for the development of strategies aimed at the sustainable management and conservation of these important fishery resources. In addition, it will contribute to the broader field of ocean science and fisheries management by elucidating the relationship between tuna catches and the variability of ocean environmental factors, and by presenting statistical predictive results derived from this relationship.

2. Relationship between upper-ocean variability and tuna catches in the southwestern tropical Indian Ocean

2.1. Introduction

The western tropical Indian Ocean is a valuable fishing ground for pelagic tuna due to the high biological productivity associated with monsoons and upwelling near the equator (POSEIDON et al., 2014; Varghese et al., 2019). In addition, the Southwest Tropical Indian Ocean (SWTIO) is one of the fishing grounds for yellowfin tuna (YFT; *Thunnus albacares*) and bigeye tuna (BET; *Thunnus obesus*). Four EEZs (Republic of Seychelles, Republic of Mauritius, Tromelin Island, and Reunion Island) are included in the SWTIO (Figure 2.1a; from north to south). YFT and BET are among the dominant species caught in this area (Figure 2.1b). In the Indian Ocean, the Indian Ocean Dipole (IOD) is known to influence upwelling conditions (Saji et al., 1999). During the negative phase of the IOD, the increase in YFT catches in the western Indian Ocean (including the marginal and high seas) has been reported to be associated with a shoaling of near-surface isotherms and an increase in primary production and food availability (Kumari et al., 1993; Mohri and Nishida, 2000; Ménard et al., 2007; Lan et al., 2013).

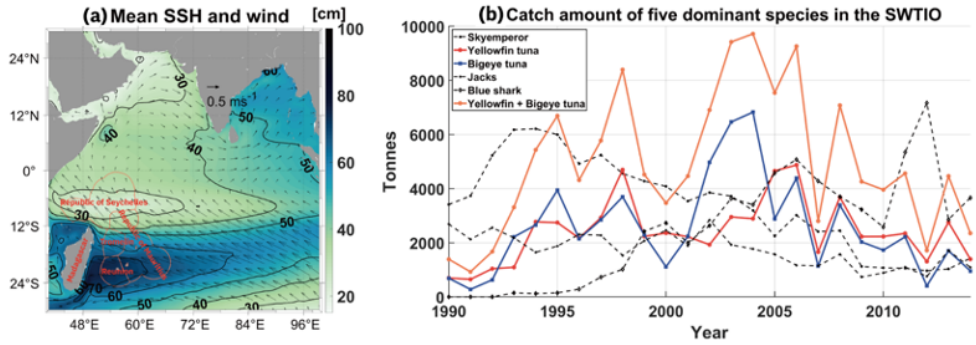

Figure 2.1 (a) Mean SSH (color shading and contours) and wind velocity (vectors) in the tropical Indian Ocean for 1990–2014. Red contour lines illustrate the boundaries of the four exclusive economic zones (the Republic of Seychelles, the Republic of Mauritius, Tromelin Island, and Reunion Island) in the SWTIO. (b) The annual catch amounts of the five dominant species (skyemperor, yellowfin tuna, bigeye tuna, jacks, and blue shark) in the SWTIO during 1990–2014. The red and blue lines denote the catch amounts of yellowfin tuna and bigeye tuna, respectively, and the orange line denotes the catch amount of Thunnus genus (yellowfin tuna + bigeye tuna).

The isotherm depths show a meridional difference between the northern (0° -12° S, EEZ of the Republic of Seychelles) and the southern SWTIO (12° S-25° S, EEZs of the Republic of Mauritius, Tromelin Island, and Reunion Island). The mean sea surface height (SSH) in the northern region is relatively low compared to that in the southern region (Figure 2.1a). This meridional difference in SSH is mainly due to a pronounced upwelling in the northern SWTIO, called the Seychelles-Chagos Thermocline Ridge (SCTR, 5° -10° S) (Hermes and Reason, 2008; Vialard et al., 2009). Therefore, isotherms, including the thermocline and D20, are shallower in the northern region. Changes in isotherm depths and the associated upwelling variability could play an important role in the interannual variability of YFT and BET catches in SWTIO.

The upwelling conditions develop due to both local wind forcing and remote forcing via westward propagation of upwelling Rossby waves, which tend to occur during the negative phase of IOD and ENSO years (Marsac and Le Blanc, 1999; Lehodey et al., 2006; Ménard et al., 2007; Lan et al., 2013; Lan et al., 2020). However, due to meridional differences in the ocean environment, upwelling conditions would evolve differently throughout the SWTIO. Accordingly, the relationship between YFT catch and thermocline depth previously reported in the

Indian Ocean (Lan et al., 2013) could be different in the northern and southern regions of the SWTIO.

This chapter aimed to investigate the meridional differences in the relationships between the YFT and BET catches and the ocean environmental variability in the SWTIO by analyzing the interannual variability of the catch amount during 1990–2014 (25 years). To understand the local and remote influences on the upper ocean (< 400 m) variability, temperature, salinity, and ocean currents were studied in the broader tropical Indian Ocean. This comprehensive analysis of the various ocean environmental variables, beyond temperature variability, will clarify the link between the catch amounts in the SWTIO and climate variability, including the IOD and ENSO.

2.2. Materials and methods

This chapter investigated the temporal variability of YFT and BET catch amounts in the northern region (the Republic of Seychelles) and the southern region (the Republic of Mauritius + Tromelin Island + Reunion Island) of the SWTIO (Figure 2.1a). The annual catch amounts of the four EEZs were obtained from Sea Around Us (SAU, http://www.seaaroundus.org) for 1990-2014 (Boistol et al., 2011; Le Manach et al., 2015a; Le Manach et al., 2015b; Le Manach et al., 2015c). The catch data were based on officially reported data from the Food and Agriculture Organization of the United Nations (http://www.fao.org/fishery/statistics/en), but were improved by including unreported catches and major discards (Pauly and Zeller, 2015; Pauly and Zeller, 2016). However, the unreported catch amounts of YFT and BET are more than one order smaller than the reported catch amounts in the four EEZs. For example, the unreported YFT catch amount in the Republic of Seychelles is about 15 tonnes on average during 1990-2014.

The monthly sea surface height and upper 400 m temperature, salinity, and current velocity were obtained from the Simple Ocean Data Assimilation (SODA) 3.4.2, with a spatial resolution of 0.5° × 0.5°

for 1988-2016 (Carton et al., 2018). The relationship between the tuna catches and the ocean environment was analyzed for the overlapping period, that is, 1990-2014, and the extra years, i.e., 1998-1999 and 2015-2016, were used to examine the lead-lag relationship with the climate indices. The thermocline depth and D20 were calculated from the SODA 3.4.2 data at each grid point, after conducting vertical linear interpolation of the temperature every 1 m. Monthly mean 10 m wind velocity and total precipitation were obtained for the same period (1988-2016) with a horizontal resolution of 0.25° × 0.25° from ERA5, which is the fifth-generation atmospheric reanalysis from the European Centre for Medium-Range Weather Forecasts. The ERA5 is based on 4D-Var data assimilation using global observation data (Hersbach et al., 2020). Monthly mean net primary production and chlorophyll concentration in the upper 400 m of the ocean were obtained for 1993-2016 with a resolution of 0.25° × 0.25° from the Global Ocean Biogeochemistry Hindcast from Mercator-Ocean, provided by the Copernicus Marine Environment Monitoring System Service. This biogeochemical hindcast is based on the PISCES biogeochemical model, available on the Nucleus for European Modelling of the Ocean modeling platform (Perruche et al., 2019).

The CSEOF analysis (Kim et al., 1996; Kim and North, 1997; see

Appendix) is used for the ocean environmental variables. Regression analysis can be used to understand the physical relationship between the target and the predictor. This results in a spatial pattern of predictor and target variables corresponding to their physical evolution.

The relationship between the ocean environment in the SWTIO and the IOD and ENSO was investigated using the same regression analysis, but using the monthly PC time series of the environmental variables, as the Indian Ocean Dipole Mode Index (DMI) and the Multivariate ENSO Index (MEI) are available as monthly means (Saji et al., 1999; Zhang et al., 2019). The regression analysis was also conducted by employing time lags between the ocean environmental variables and climate indices because the IOD and ENSO exhibit low-frequency variabilities that last longer than a year. A series of lagged regression analyses were conducted with time lags of ± 1 year (e.g., 1989-2013 and 1991-2015) and ±2 years (e.g., 1988-2012 and 1992-2016), targeting the DMI and MEI.

2.3. Results

Figure 2.2 shows the zonally averaged mean and standard deviation of temperature, salinity, and zonal and meridional current velocity The mean thermocline depth is shallower in the northern region (northern: ~66 m, southern: ~87 m), which is associated with the SCTR, and the peak of the SCTR (shallowest thermocline depth) is observed at approximately 8° S (Figure 2.2a). The mean D20 is shallower (~91 m) and closer to the thermocline depth in the northern region, but the mean D20 is significantly deeper (~163 m) in the southern region. In the northern region, the near-surface layer (< D20) is more saline, but the deeper layer (> D20) is more saline in the southern region (Figure 2.2b). The fresh near-surface water in the southern region comes from the Indonesian Throughflow in the equatorial eastern Indian Ocean (Gordon et al., 1997; Makarim et al., 2019). The mean zonal currents exhibit meridionally opposite directions, reflecting the southeastward-flowing South Equatorial Counter Current (SECC) north of the SCTR (north of approximately 8° S) and the southwestward-flowing South Equatorial Current (SEC) south of the SCTR (Figure 2.2c-d).

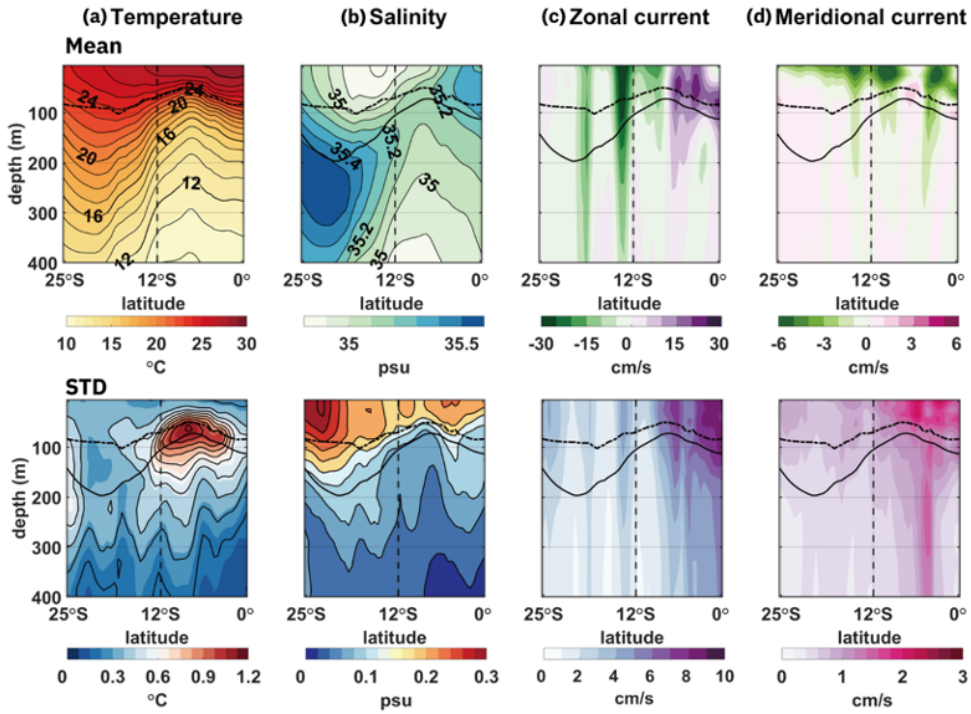

Figure 2.2 Meridional distribution of the (top) means and (bottom) standard deviations of the ocean environmental variables for 1990–2014, zonally averaged from 54°E to 60°E in the SWTIO. The standard deviations were calculated from the annual means of the variables. Each column represents a different variable: (a) temperature, (b) salinity, (c) zonal current velocity, and (d) meridional current velocity. The thick dashed/dotted lines and solid lines indicate the mean thermocline depth and 20°C isotherm depth (D20), respectively. The vertical dashed lines denote 12°S, the boundary between the northern and southern regions of the SWTIO.

The temporal variations of the environmental variables also exhibit Due to the strong subsurface upwelling variability in the SCTR, the standard deviation of temperature in the upper ocean (< 400 m) is larger near the thermocline depth and D20 in the northern region. In both regions, salinity displays significant variability from the surface to the thermocline depth, which is deeper in the southern region. The standard deviations of the zonal and meridional currents are larger in the northern region, where the SECC flows southeast. The different ocean environmental conditions in the northern and southern regions shown in Figure 2.2 may contribute to the YFT and BET catch variability in the SWTIO.

Figure 2.3 shows the annual catch of YFT and BET in the SWTIO for 1990-2014. The YFT and BET catch amounts exhibit similar variability throughout the SWTIO, except for a few years in the early 2000s (Figure 2.3a). This similarity between YFT and BET catches is also observed separately in the northern and southern regions (Figure 2.3b-c). In the northern region, both YFT and BET catches were larger in the 1990s and early 2000s compared to the late 2000s and early 2010s. In the southern region, however, catches were smaller in the 1990s than in later years. The difference in YFT and BET catch variability does not appear to be as significant as the difference in

catch variability between the northern and southern regions.

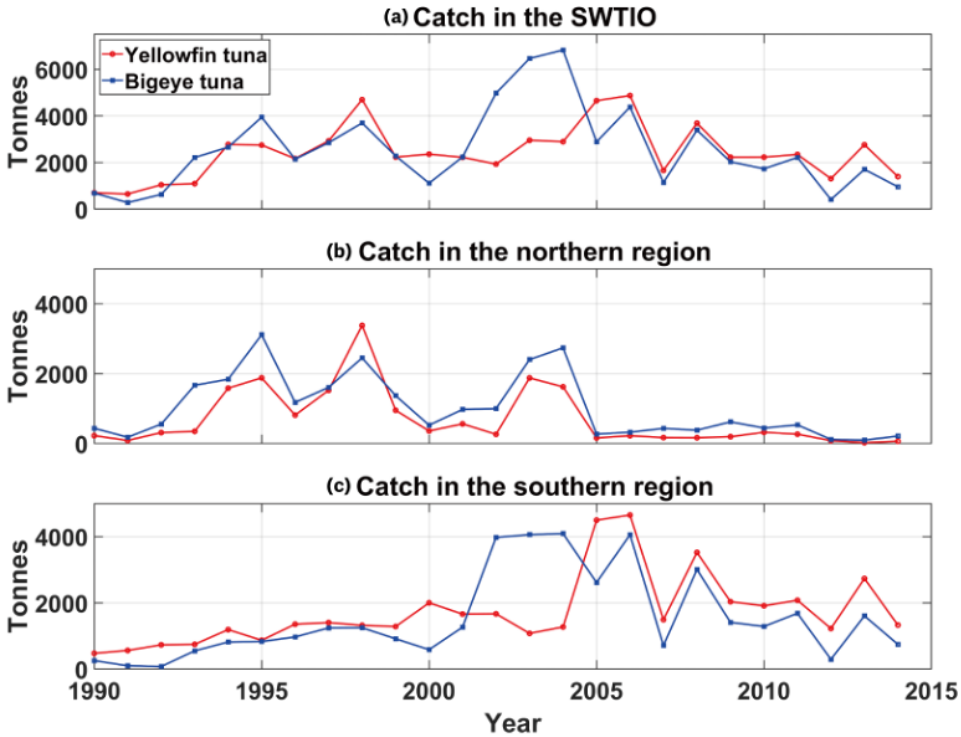

Figure 2.3 (a) The annual catch amounts of yellowfin tuna and bigeye tuna during 1990–2014 in the four exclusive economic zones (EEZs) of the entire SWTIO. (b) The same as (a), but only for the northern region of the SWTIO. (c) The same as (b), but only for the southern region of the SWTIO.

Figure 2.4 illustrates the regressed anomalies of ocean conditions during the increase in YFT and BET in the northern and southern regions of the SWTIO. The R-squared values of the regression for each variable and each depth are presented in Figure 2.5. The temperature conditions during the increase of YFT and BET catches in the northern region represent strong positive anomalies near the mean thermocline depth and D20 in the northern region (top two rows in Figure 2.4a). They also display the negative anomalies below the thermocline depth and D20 in the northern SCTR. The temperature anomalies indicate the deeper isotherms in the southern SCTR and the shallower isotherms in the northern SCTR, hence the flattening of the isotherms in the SCTR during the increase in the catch in the northern region. The flattening of the isotherms indicates the suppression of the subsurface upwelling in the SCTR. On the contrary, the temperature conditions, during the increase of YFT and BET catches in the southern region, represent relatively weak positive anomalies in the southern region (bottom two rows in Figure 2.4a).

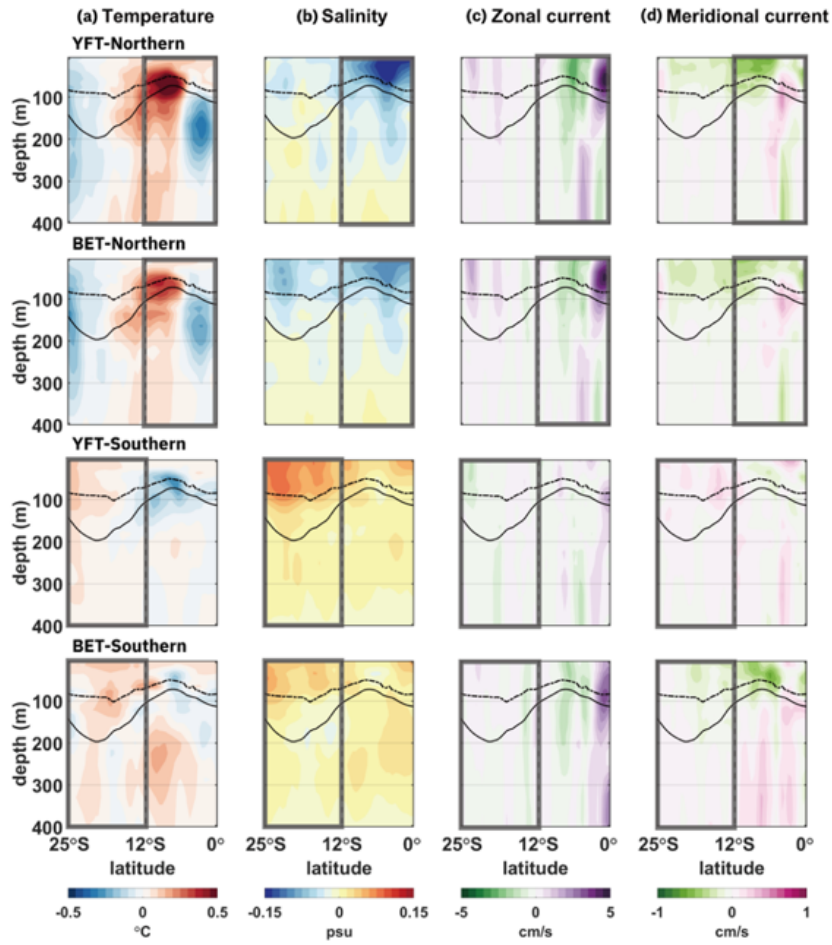

Figure 2.4 Meridional distributions of the regressed and reconstructed anomalies of the ocean environmental variables during 1990–2014. Target time series are the annual catch amounts of YFT and BET in the northern (top two rows) and southern (bottom two rows) regions; the target time series are referred as YFT-Northern, BET-Northern, YFT-Southern, and BET-Southern, respectively. The anomalies are presented after zonal averages from 54°E to 60°E. Each column represents a different variable: (a) temperature (shading intervals: 0.05°C), (b) salinity (shading intervals: 0.015 psu), (c) zonal current velocity (shading intervals: 0.5 cm/s), and (d) meridional current velocity (shading intervals: 0.1 cm/s). The thick dashed/dotted lines and solid lines indicate the mean thermocline depth and D20, respectively. The gray boxes indicate the northern or southern region of the SWTIO, denoting the region of each target time series.

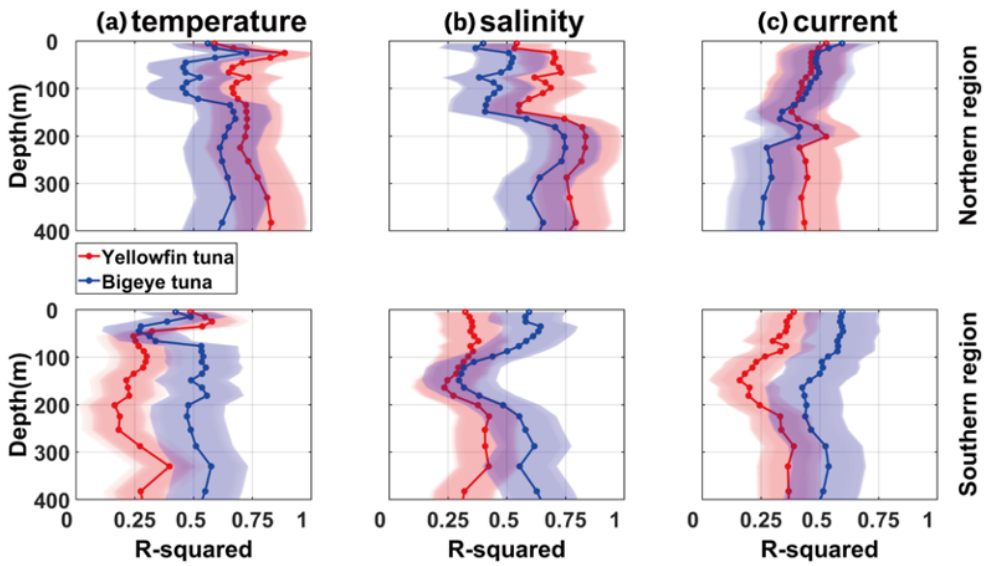

Figure 2.5 The R-squared values of the regression for 1990–2014 from the (a) temperature, (b) salinity, and (c) current velocity at each depth in the tropical Indian Ocean, targeting the YFT (red) and BET (blue) catches in the entire SWTIO (top), northern (middle) and southern (bottom) regions of the SWTIO. The shadings display the 95% confidence intervals of the R-squared values for each depth.

The salinity conditions during the increase of YFT and BET catches in the northern region exhibit similar anomalies with the near-surface (< D20) freshening in the northern region (top two rows in Figure 2.4b). This freshening in the northern region is consistent with an increase in precipitation in this region (top row in Figure 2.6). On the other hand, the positive salinity anomalies and the decrease of precipitation in the southern region are detected during the increase of YFT and BET catches in the southern region (bottom two rows in

Figure 2.4b and middle row in Figure 2.6). The negative anomalies in the north and the positive anomalies in the south contribute to the similar near-surface salinity ranges of 34.8-35.2 psu, which is within the favorable salinity range for an increase in YFT and BET catches reported in the Indian Ocean (Song et al., 2008; Song et al., 2009). The current velocity conditions in the northern region during the increase of the YFT and the BET catches show westward anomalies at the latitude near the SCTR upwelling peak and eastward anomalies north of the peak (top two rows in Figure 2.4c-d). It shows the equatorward shift of the SEC compared to the mean current velocity in Figure 2.2c-d. The equatorward shift is consistent with the eastward wind anomalies near the equator during the increase in YFT and BET catches in the northern region (top row in Figure 2.6). The regressed current velocity anomalies targeting the YFT and BET catches in the southern region are relatively smaller (bottom two rows in Figure 2.4c-d), similar to the results of the temperature regression.

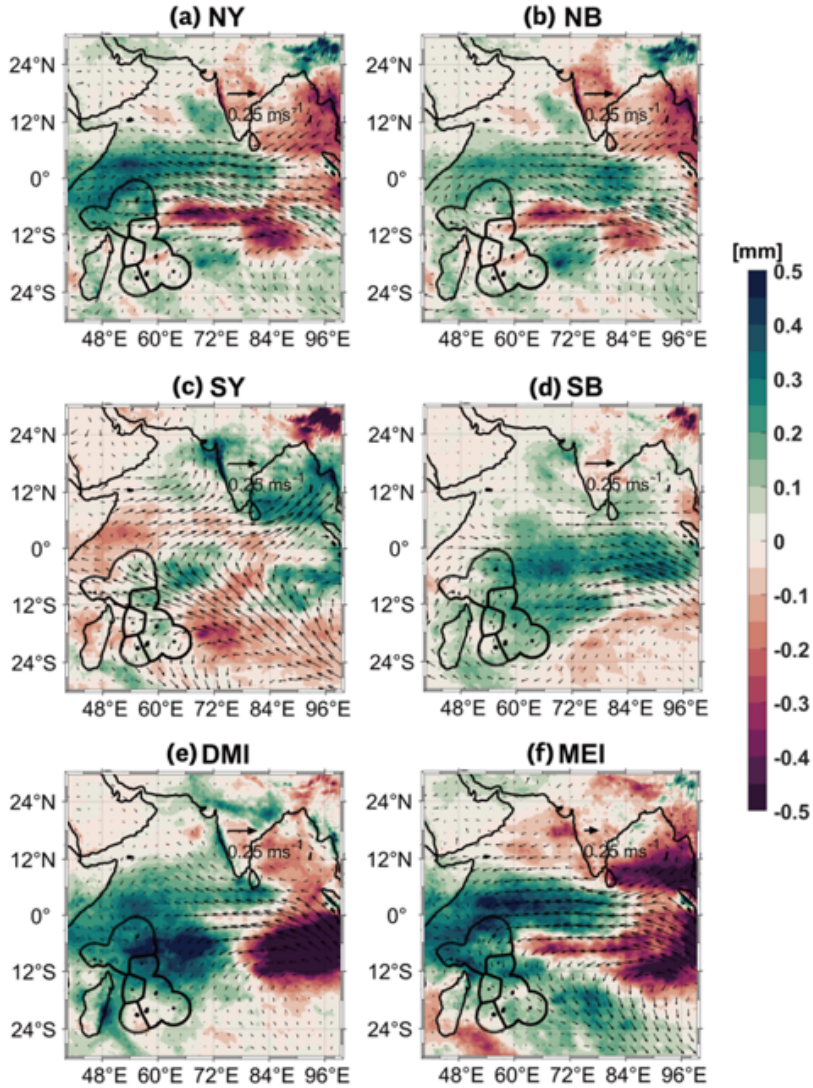

Figure 2.6 The regressed and reconstructed anomalies of the total precipitation (color) and 10-m wind velocity (vector) in the tropical Indian Ocean during 1990–2014 with respect to: (a) the catch amounts of yellowfin tuna in the northern region (NY), (b) the catch amounts of bigeye tuna in the northern region (NB), (c) the catch amounts of yellowfin tuna in the southern region (SY), (d) the catch amounts of bigeye tuna in the southern region (SB), (e) the normalized DMI, and (f) the MEI.

Figure 2.7 illustrates the ocean environmental conditions in the SWTIO during the positive phase of IOD and ENSO. The R-squared values of the regressions are shown in Figure 2.8. Strong positive temperature anomalies are observed near the thermocline depth and D20 in the northern region during the positive phase of both IOD and ENSO, indicating the suppression of SCTR upwelling (Figure 2.7a). The current velocity conditions show an equatorward shift of the SEC during the positive phase of both IOD and ENSO (Figure 2.7c-d).

However, the salinity conditions are different between the positive phase of the IOD and the ENSO (Figure 2.7b). During the positive phase of the IOD, the salinity anomalies show different signs between the northern and southern regions (top of Figure 2.7b). The dipole-like pattern of the salinity anomaly was previously reported as a salinity IOD mode originating from the eastern tropical Indian Ocean (Zhang et al., 2016). On the other hand, during the positive phase of ENSO, the salinity condition reflects a general near-surface freshening in both the northern and southern regions (bottom of Figure 2.7b). The regression of precipitation generally shows consistent patterns with the regressed salinity anomalies (bottom row in Figure 2.6).

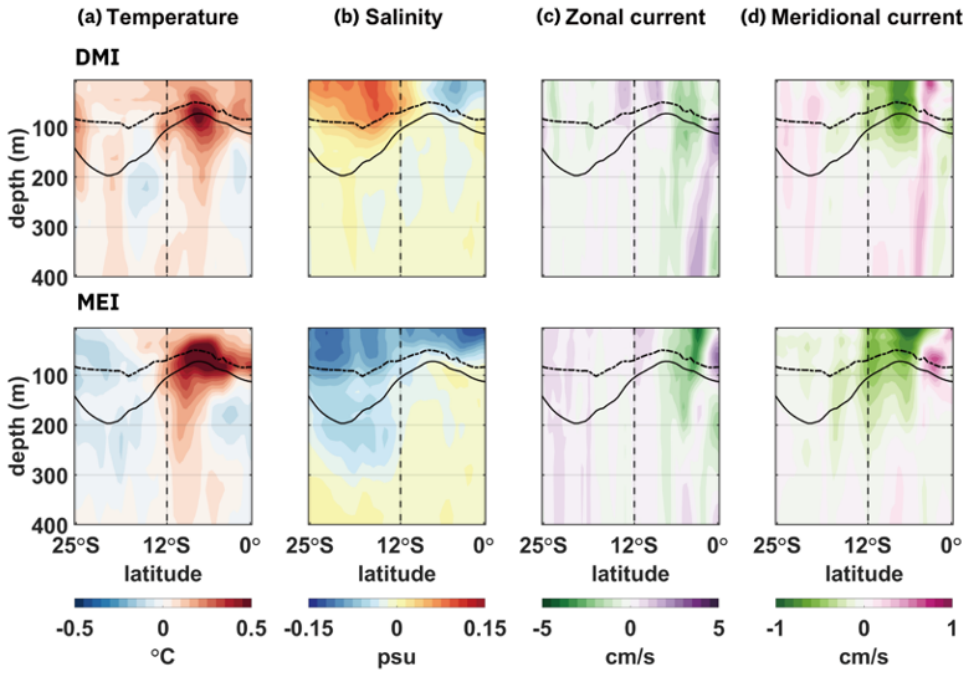

Figure 2.7 Meridional distribution of the regressed and reconstructed anomalies of the ocean environmental variables with respect to the normalized DMI (top) and normalized MEI (bottom) for 1990–2014. The anomalies are presented after zonal averages from 54°E to 60°E. Each column represents a different variable: (a) temperature (shading intervals: 0.05°C), (b) salinity (shading intervals: 0.015 psu), (c) zonal current velocity (shading intervals: 0.5 cm/s), and (d) meridional current velocity (shading intervals: 0.1 cm/s). The thick dashed/dotted lines and solid lines indicate the mean thermocline depth and D20, respectively. The vertical dashed lines denote 12°S, the boundary between the northern and southern regions of the SWTIO.

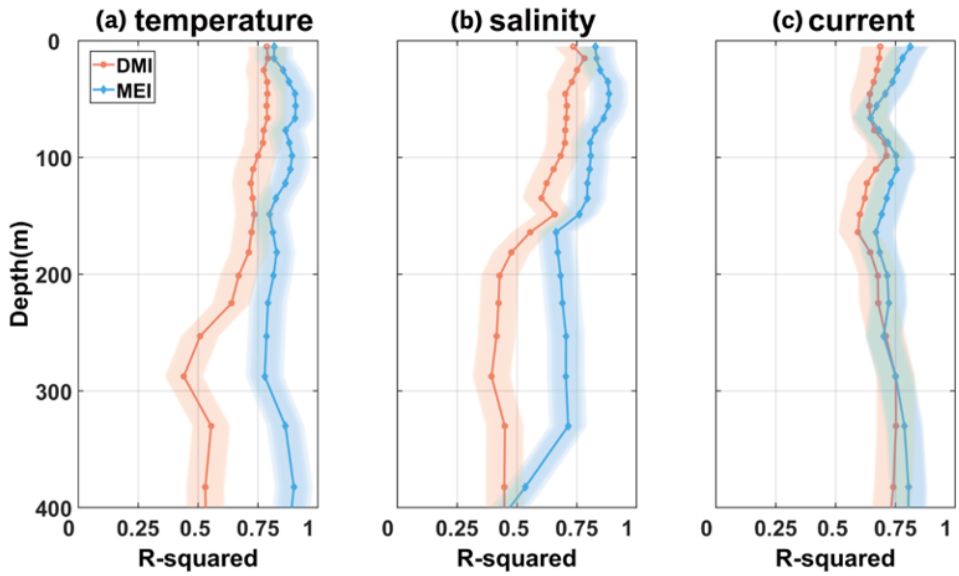

Figure 2.8 The R-squared values of the regression targeting the normalized indices of the DMI and the MEI for 1990–2014. The predictor variables are the (a) temperature, (b) salinity, and (c) current velocity at each depth in the tropical Indian Ocean. The positive sign of the lags denotes that climate indices lead the ocean environment. The shadings display the 95% confidence intervals of the R-squared values for each depth.

2.4. Discussion

The southern region exhibits lower temporal variability in both temperature and current velocity compared to the northern region (see Figure 2.2, bottom panel). In addition, the regressed anomalies of temperature and current velocity show relatively weak associations with the catch in the southern region, indicating challenges in identifying favorable fishing conditions. The R-squared values for the southern region are also lower than those for the northern region, suggesting difficulties in investigating favorable ocean conditions for fishing in regions with weaker natural variability (Figure 2.5). Despite the greater variability in ocean conditions in the northern region, primarily influenced by the presence of the Seychelles-Chagos Thermocline Ridge as a permanent upwelling region, the variability in catch amounts does not exceed that of the southern region.

The results in this chapter indicate that the magnitude of the ocean environmental variability contributes to explaining the relationship between variability in the ocean environment and the catch amounts. However, establishing a specific relationship between the magnitude of ocean environmental variability and catch variability remains inconclusive. Therefore, factors other than the magnitude of

environmental variability should be considered in explaining catch variability.

According to the results in this chapter, the relatively small variability of the ocean environment in the southern region of the SWTIO made it difficult to explain the favorable ocean conditions for the tuna catches. In comparison, the relatively large variability of the ocean environment in the northern region of the SWTIO showed that the favorable ocean condition associated with the catch is statistically significant. Therefore, factors other than the physical ocean environmnetal variables should be considered when explaining the catch in the southern region. One of these factors is the existence of competing ocean areas. The northern region and the southern region are competing ocean areas, and the amplitude of environmental variability in the northern region is greater than in the southern region. Therefore, the migration of tuna is expected to occur more actively in the northern region than in the southern region, and the migration of tuna in the southern region is expected to occur relatively passively (in response to the variability in the northern region). As a result, the variability in catch in the northern region may be the main influence on the variability in catch in the southern region (a relatively passive fishing area).

Figure 2.5 shows the R-squared values of the regression for each tuna species. The R-squared values for YFT in the northern region show statistical significance, while those in the southern region are not statistically significant. This indicates the challenges associated with explaining the variability in YFT catch using ocean environmental variables in the southern region. However, there is a slight difference when considering the R-squared values for BET in both the northern and southern regions. The R-squared values for BET suggest similar levels of explanatory power using ocean environmental variables in both regions. The varied responses of different tuna species in each region indicate the complexity involved in investigating the variability of ocean environmental factors and their relationship to catch amounts. Consequently, this may lead to a greater discrepancy in explaining the variability of YFT catches compared to BET catches using ocean environmental variables in this chapter. Therefore, it is crucial to approach the examination of ocean conditions related to the target species with caution in each region.

The SCTR upwelling is suppressed during the increase in the catch in the northern region, where the natural background variability is strong. Previous studies have suggested that upwelling-induced shallower isotherms are associated with increases in YFT and BET

catches in the western Indian Ocean (Marsac and Le Blanc, 1999; Lehodey et al., 2006; Ménard et al., 2007; Lan et al., 2020). This seems reasonable because upwelling generally increases near-surface productivity, which would be favorable for pelagic tuna (Hermes and Reason, 2008; Vialard et al., 2009). However, the regression results illustrate a meridional flattening of the isotherms, indicating the suppression of SCTR upwelling (top two rows in Figure 2.4). This discrepancy can be explained by the different ocean environments of the subsurface upwelling in the northern SWTIO.

Figure 2.9 shows the mean and regressed anomalies of net primary production and chlorophyll concentration targeting tuna catches in the SWTIO for 1993-2014 (22 years). The R-squared values of the regression for each depth are shown in Figure 2.10. In the northern region, mean net primary production is higher in the near-surface layer, and mean chlorophyll concentration exhibits a maximum near D20 and the thermocline depth. The regressed anomalies, targeting the catch variability in the northern SWTIO, illustrate both positive and negative anomalies at different depths and latitudes. However, the depth-integrated anomalies are generally positive north of the peak of the SCTR, but negative to the south, which contributes to the area-averaged anomalies becoming close to zero.

This suggests that there is no significant increase in biological activity as YFT and BET catches increase. A plausible hypothesis would be that in the northern SWTIO, where the mean biological activity is high, upwelling suppression may vertically extend the favorable habitat for pelagic tuna even without an increase in biological activity. The deepening of the isotherms itself could contribute to an extension of the fishing grounds and thus increase the YFT and BET catches. The overall suppression of the SCTR upwelling and the equatorward shift of the SEC appears to occur during the positive phase of both the IOD and the ENSO. Despite the similarities, the salinity state during the positive phase of the IOD is significantly different (top of Figure 2.7b). This indicates that the ocean environmental conditions during the increase in the catch in the northern region are more similar to those during the El Niño years (positive phase of ENSO) than those during the positive phase of IOD. The direct correlation coefficients between the MEI and the YFT and BET catches in the northern region are 0.29 and 0.30, respectively, while those between the DMI and the YFT and BET catches in the northern region are 0.18 and 0.06, respectively. The correlation coefficients between the climate indices and catches in the southern region are all insignificant.

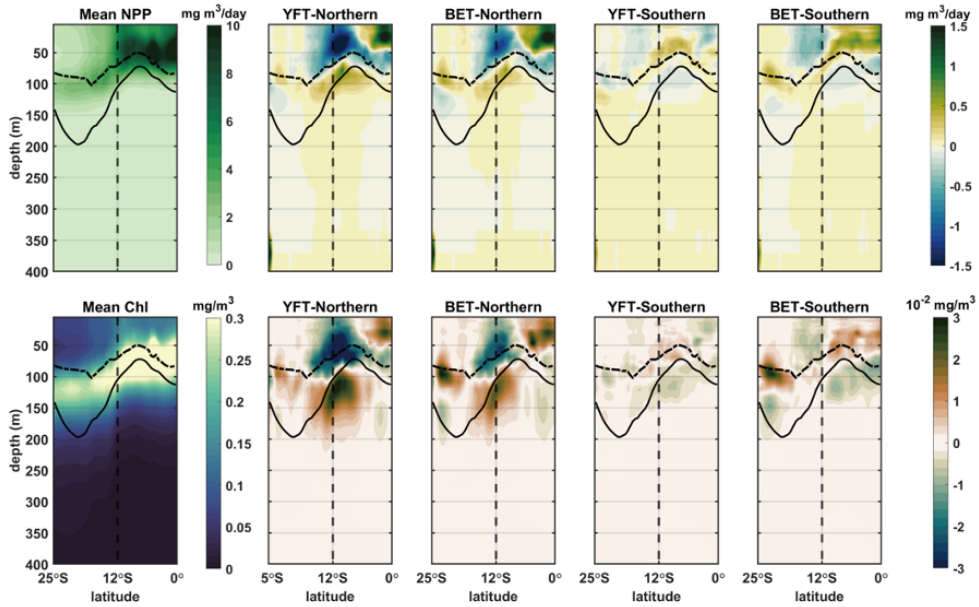

Figure 2.9 Meridional distribution of the mean (first column) and the regressed and reconstructed anomalies of the NPP (upper row) and Chl (lower row) during 1993–2014. Target time series are the annual catch amounts of YFT and BET in the northern (second and third columns) and southern (fourth and last columns) regions of the SWTIO. The anomalies are presented after zonal average from 54°E to 60°E. The thick dashed/dotted lines and solid lines indicate the mean thermocline depth and D20, respectively.

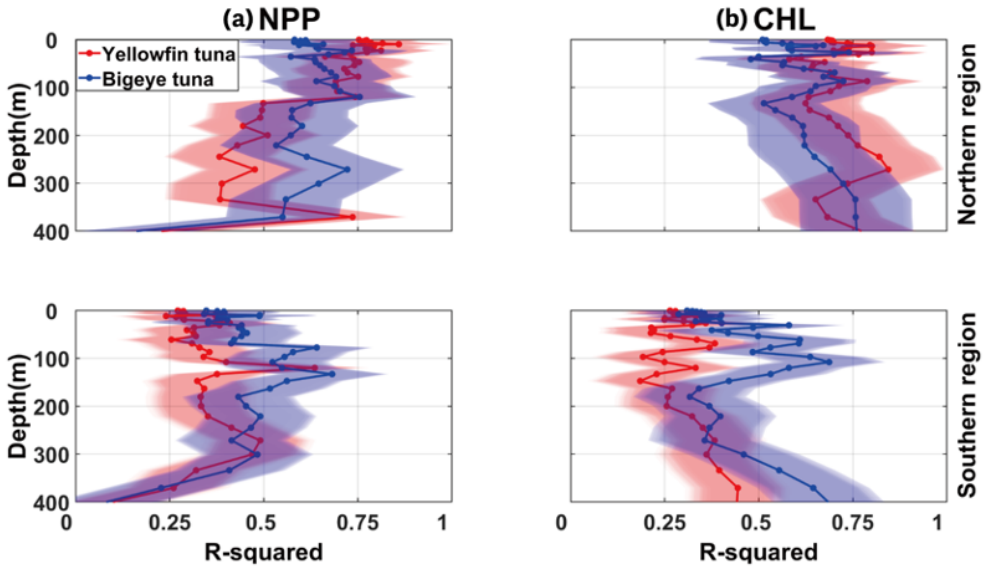

Figure 2.10 The R-squared values of the regression for 1993–2014 from the (a) NPP and (b) CHL at each depth in the tropical Indian Ocean, targeting the YFT (red) and BET (blue) catches in the entire SWTIO (top), northern (middle) and southern (bottom) regions of the SWTIO. The shadings display the 95% confidence intervals of the R-squared values for each depth.

The lagged regression results between catch variability and climate indices also suggest a possible closer relationship with ENSO than with IOD (Figure 2.11-12). The R-squared values of the regression for each depth are shown in Figure 2.13. The clear temperature anomalies from the zero-lag regression in Figure 2.7 develop in the northern region during El Niño years and continue in the following years, while the temperature anomalies almost disappear one year after positive IOD years. The direct correlation coefficients between the MEI and the YFT and BET catches in the northern region are 0.53 and 0.52, respectively, using the one-year lag. Those of the DMI are all insignificant, which may support the closer relationship between ENSO and catch variability in the northern region. Finally, this chapter used annual catch as the target time series, not normalized by-catch Considering this limitation, this chapter limited the analysis period after the 1990s, assuming that the possible changes in catch effort and fishing methods do not significantly affect the relationship between catch and ocean environmental variability for recent decades (1990-2014). The temporal changes in catch effort and fishing methods can be considered "anthropogenic" factors and become a source of regression error in finding a relationship with "natural" ocean environmental variability. The reliable use of catch data for specific

EEZs in recent decades in place of CPUE data has also been demonstrated for skipjack tuna in the western tropical Pacific (Kim et al., 2020).

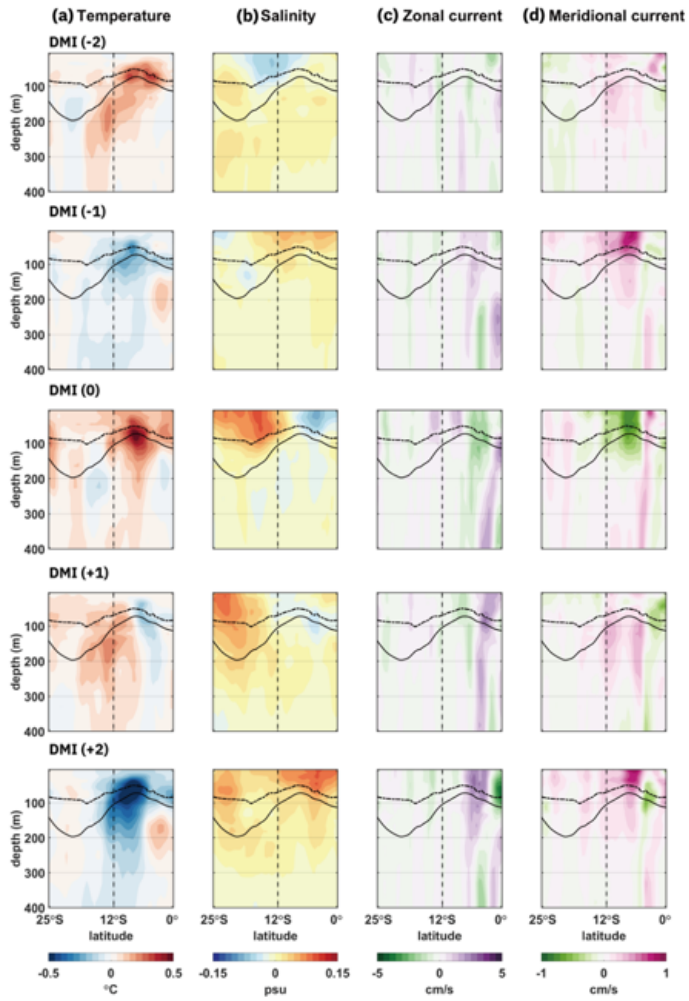

Figure 2.11 Meridional distribution of the regressed and reconstructed anomalies of the ocean environmental variables with respect to the normalized DMI. The target indices are for 1990–2014, and the ocean environmental variables are for 1988–2016, applying time lags of ±2 years. Numbers in parenthesis indicate the time lags, and positive values denote that the DMI leads the ocean environmental variables. The anomalies are based on the zonal averages from 54°E to 60°E. Each column represents a different variable: (a) temperature, (b) salinity, (c) zonal current velocity, and (d) meridional current velocity. The thick dashed/dotted and solid lines indicate the mean thermocline depth and D20, respectively. The vertical dashed lines denote 12°S, the boundary between the northern and southern regions of the SWTIO.

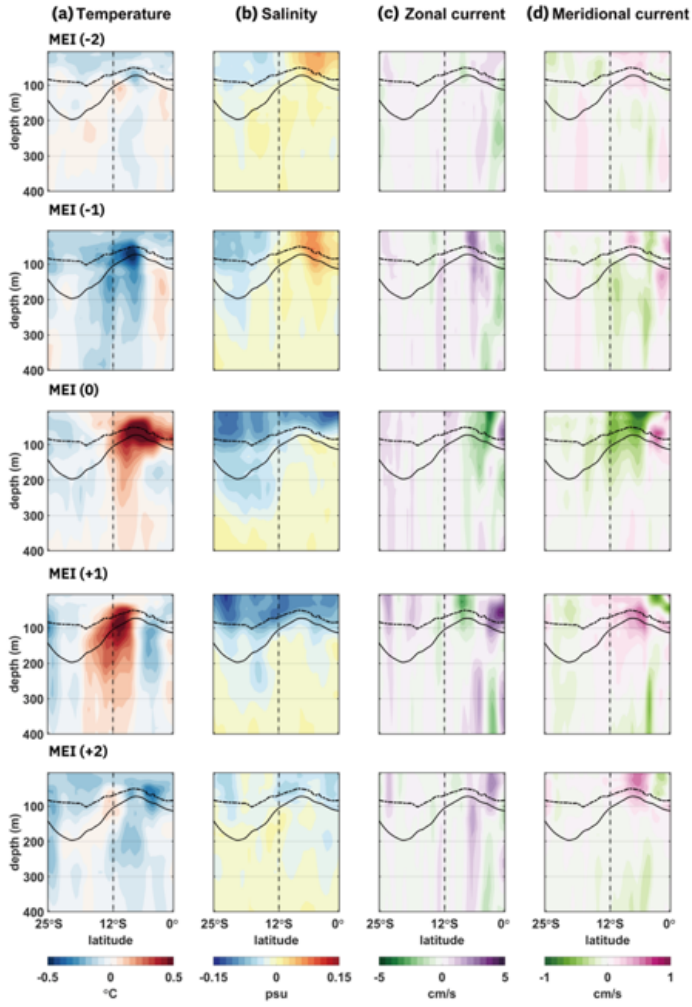

Figure 2.12 same as Figure 2.11, but for the normalized MEI.

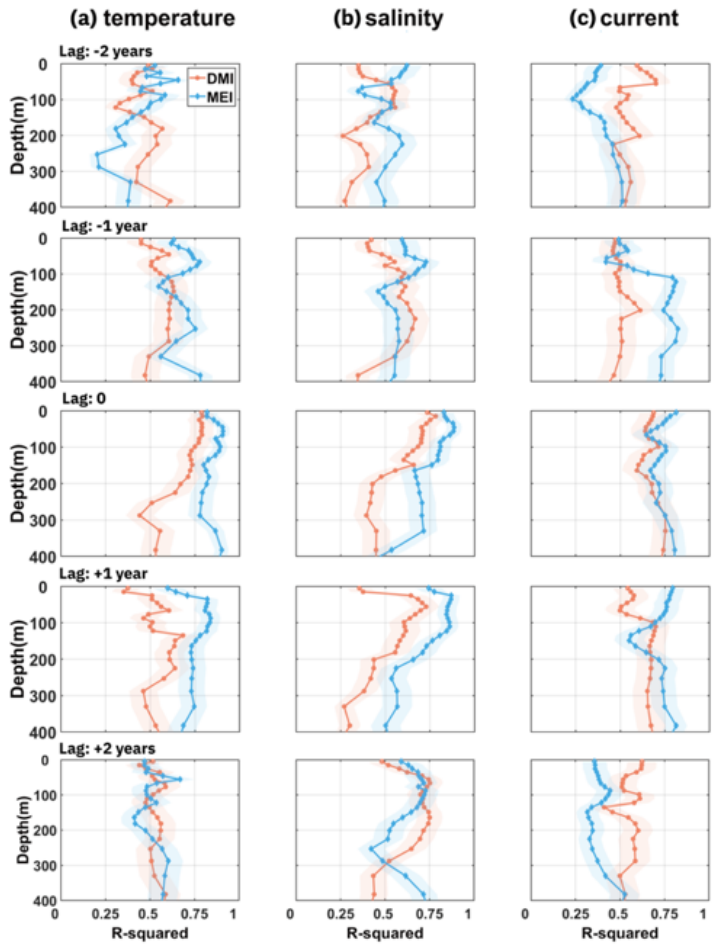

Figure 2.13 The R-squared values of the lagged regression (lags: -2 years, -1 year, 0, +1 year and +2 years, respectively, from top to bottom) targeting the normalized DMI and the MEI for 1990–2014. The predictor variables are the (a) temperature, (b) salinity, and (c) current velocity at each depth in the tropical Indian Ocean. The positive sign of the lags denotes that climate indices lead the ocean environment. The shadings display the 95% confidence intervals of the R-squared values for each depth.

Between 2001 and 2004, BET catches increased in both the northern and southern regions, while YFT catches increased in the northern region but decreased in the southern region during the same period (Figure 2.3). Excluding this period (2001–2004), the remaining 21 years exhibited similar variability in YFT and BET catches. It is plausible that the expansion of BET habitat occurred not only in the northern region, but also to some extent in the southern region, leading to an increase in BET catches in the southern region. However, given that YFT and BET catches have shown consistent patterns since 2005, it becomes challenging to explain the continued presence of BET in the southern region from 2001 to 2004 based solely on their relationships with physical oceanographic variables. Therefore, further studies are required to explore the biological dynamics associated with the BET habitat.

Significantly, catches of YFT and BET in the northern region have declined since 2005, as shown in Figure 2.3. Figure 2.14 shows the yearly averaged third mode of temperature anomaly and the second mode of salinity anomaly at 200 m depth, which have significant R-squared values in relation to the catches in the northern region of the SWTIO during the period 1990–2014.

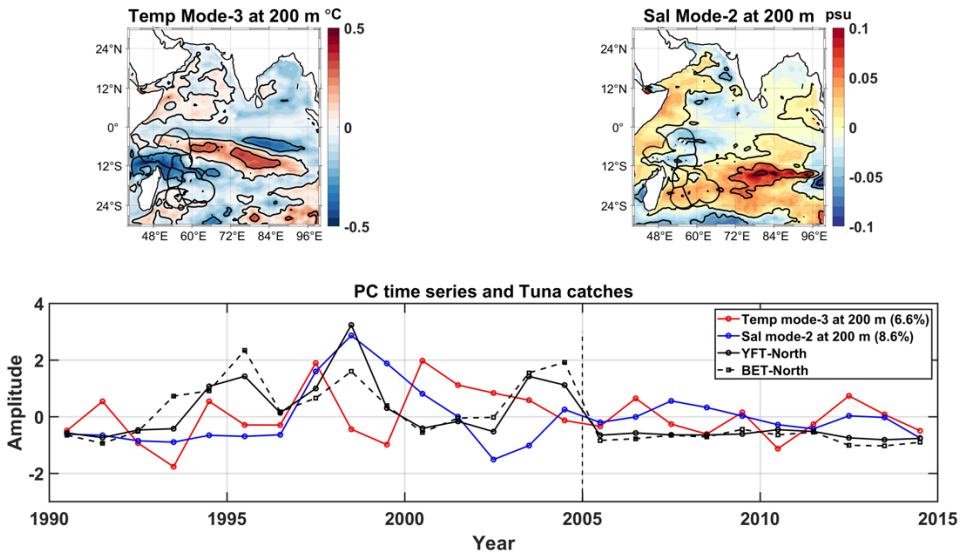

Figure 2.14 The yearly averaged third mode of temperature anomaly and the second mode of salinity anomaly at a depth of 200 m, respectively. The upper panel displays the cyclostationary loading vectors, while the lower panel presents their principal component (PC) time series alongside tuna catches in the northern region of the SWTIO during the period of 1990–2014.

The third mode of temperature anomaly at 200 m depth shows a broad cold anomaly in the SWTIO, with a warm anomaly extending approximately from 50° E to 95° E near the equator. The prominent cold anomaly is located in the middle of the SWTIO. Considering the SCTR, this mode indicates suppressed upwelling in the SCTR, which is associated with an increase in the catches in the northern region of the SWTIO. The PC time series of this mode shows more variability before 2005, while its variability decreases after 2005. The second

mode of salinity anomaly at 200 m depth shows a significant positive anomaly from 12° S to 25° S, with a slight freshening in the northern region of the SWTIO. The freshening in the northern region corresponds to an increase in the catches in this area. Similar to the temperature mode, the PC time series of the salinity mode shows more variability before 2005 and less variability thereafter.

The amplitude variability observed in the ocean environmental variables indicates a significant change in the overall ocean condition after 2005. Simultaneously, YFT and BET catches show significant decreases after 2005. These comprehensive changes can be attributed to long-term ocean environmental variability.

Figure 2.15 presents mean temperature and temperature anomalies for two different periods: 1990-2004 and 2005-2014 in the SWTIO. The former period illustrates a generally cold ocean environment, while the latter period illustrates a generally warm ocean environment. A large-scale and long-term change in the ocean environment, occurred around 2004-2005, known as a regime shift, may have contributed to the sharp decline in the catches in the northern region since 2005. This decline is consistent with the overall warming trend of the ocean environment in the SWTIO. Consequently,

it may suggest that tuna catches in the SWTIO are influenced not only by interannual variability, such as ENSO, but also by long-term variability, such as the Pacific Decadal Oscillation. To understand the variability of tuna catches in the SWTIO, it is important to consider the relationship between the catches and the ocean environment on a long-term time scale.

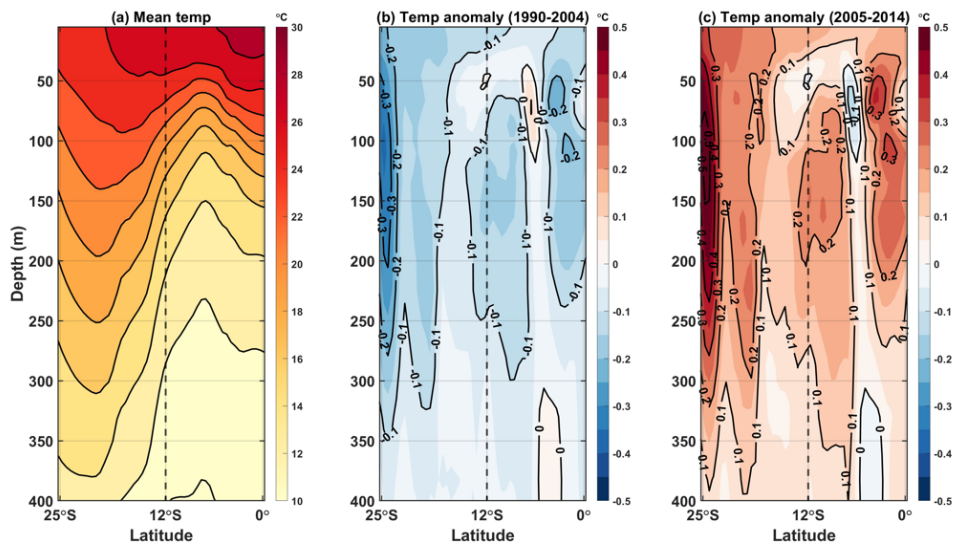

Figure 2.15 Mean temperature and temperature anomaly in the SWTIO. (a) mean temperature during the period of 1990–2014, (b) temperature anomaly during the period of 1990–2004, and (c) same as (b) but for the 2005–2014. The vertical dashed lines denote 12°S, the boundary between the northern and southern regions of the SWTIO.

2.5. Conclusions

This chapter has presented the ocean environmental conditions during the increase of YFT and BET catches in the SWTIO on an interannual time scale. The favorable ocean environment is only pronounced in the northern region, where the subsurface upwelling variability over the SCTR is pronounced. The meridional flattening of the isotherms, resulting in the suppression of the subsurface upwelling, is associated with the increase in both YFT and BET catches in the northern region. This is in contrast to previous studies in the western Indian Ocean, which suggested an increase in upper ocean productivity in the fishery during upwelling, suggesting a complex relationship between ocean conditions and catch variability. The regressed anomalies in the southern region are relatively weak when examining their relationship with tuna catches. This suggests that it may be difficult to determine the favorable ocean conditions for the catches in the southern region. In addition, the R-squared values for the relationship between the ocean environment and the catches in the southern region are smaller than those in the northern region, suggesting that it may be difficult to investigate favorable ocean conditions in regions where natural variability is low. The ocean environmental conditions associated with the increase in YFT and BET

catches in the northern region appear to develop during El Niño years and persist into the following year. The significant relationship between catch and ENSO with a one-year lag suggests the possible predictability of YFT and BET catches for sustainable fisheries in the SWTIO.

3. Relationship between upper-ocean variability and tuna catches in the western central Pacific Ocean

3.1. Introduction

The countries of the Pacific Island region are critically dependent on the fishing industry for the maintenance of their economies. The collection of exclusive economic zone (EEZ) access fees from foreign fishing fleets contribute significantly to these countries' financial resources, and the fish processing industry also provides employment for local people (Williams and Terawasi, 2011). The five island nations, Federated States of Micronesia (FSM), Marshall Islands (MS), Kiribati (Ki), Nauru (Na), and Tuvalu (Tu), are located in the Western Central Pacific (WCP), a subdivision 71 assigned by the Food and Agriculture Organization of the United Nations (FAO, 2013) (Figure 3.1). Skipjack tuna (Katsuwonus pelamis; SKJ), yellowfin tuna (Thunnus albacares; YFT), and bigeye tuna (Thunnus obesus; BET) are three tuna species commonly found in various oceans and have been the most abundant in recent decades in the WCP (Williams & Terawasi, 2010; Remolà & Gudmundsson, 2018) (Figure 3.2).

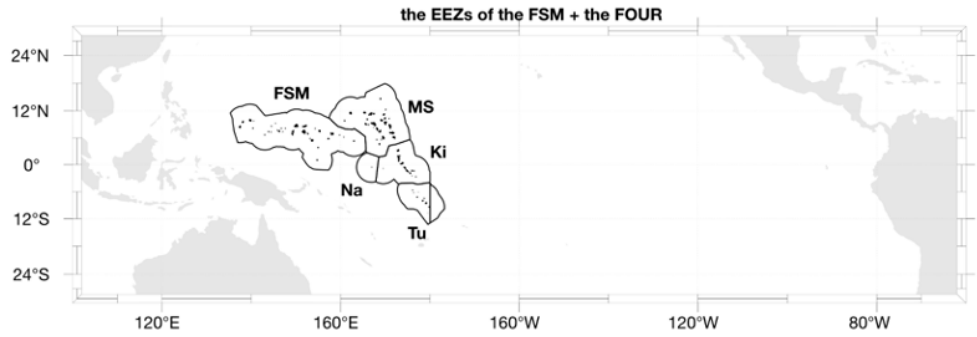

Figure 3.1 The exclusive economic zones (EEZs) of the FSM and the FOUR in the WCP.

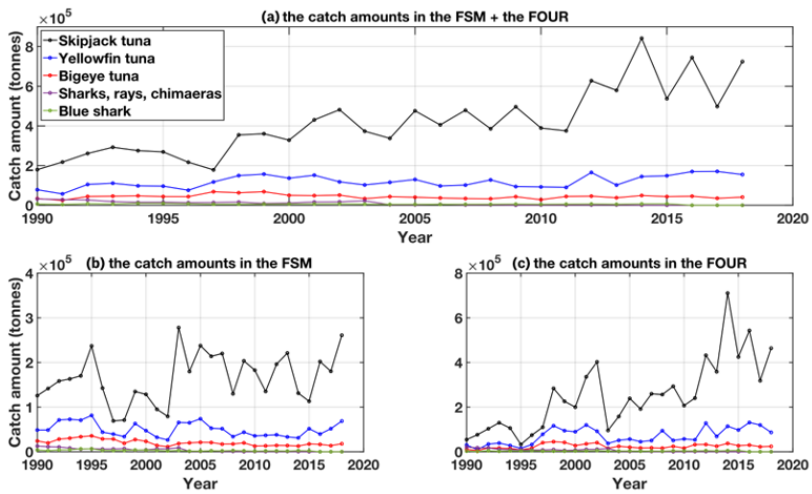

Figure 3.2 (a–c) The catch amounts of the five dominant species in the EEZs of each nation during 1990–2018: (a) the sum of catch amounts in the FSM and FOUR, (b) the catch amounts in the FSM, and (c) the catch amounts in the FOUR.

A significant proportion of the SKJ, YFT, and BET caught in the EEZs of the FSM, located in the western part of the WCP, and the FOUR (Marshall Islands, Kiribati, Nauru, and Tuvalu) are taken using the purse seine (PS) method (Figure 3.3). Specifically, the PS method was reported to be responsible for over 99% of the SKJ caught in the FSM and FOUR, with approximately 90% of the YFT and 70% of the BET also caught by this method. In addition, a relatively smaller proportion of these tuna species are caught using the longline (LL) method over the period 1990–2018, with approximately 12% of the YFT and 30% of the BET being caught using this method in the FSM and 10% of the YFT and 31% of the BET being caught using this method in the FOUR (not shown).

The spatial distribution of SKJ catches in the WCP is influenced by ENSO, as their habitat expands eastward during El Niño and contracts westward during La Niña (Lehodey et al., 1997). The EEZ of FSM is located in the western part of the WCP, so SKJ catches in the FSM would increase (decrease) when the warm pool and ITCZ contract (expand) westward during La Niña (El Niño) (Lehodey et al., 1997). Variability in the thermal structure associated with ENSO has been observed to affect the vertical extent of YFT and BET habitats, thereby affecting the catchability of adult tuna in the surface layer

(Lehodey, 2000; Harley et al., 2011). During El Niño years, vertical habitat compression of the YFT and BET occurs due to shallowing of the vertical thermal structure and increases catchability for the surface tuna fishery in the western Pacific (Marsac & Le Blanc, 1998; Lu et al., 2001; De Anda-Montañez et al., 2004). In contrast, regions such as the FSM could experience a deepening of this habitat during La Niña years, which could reduce YFT and BET catchability.

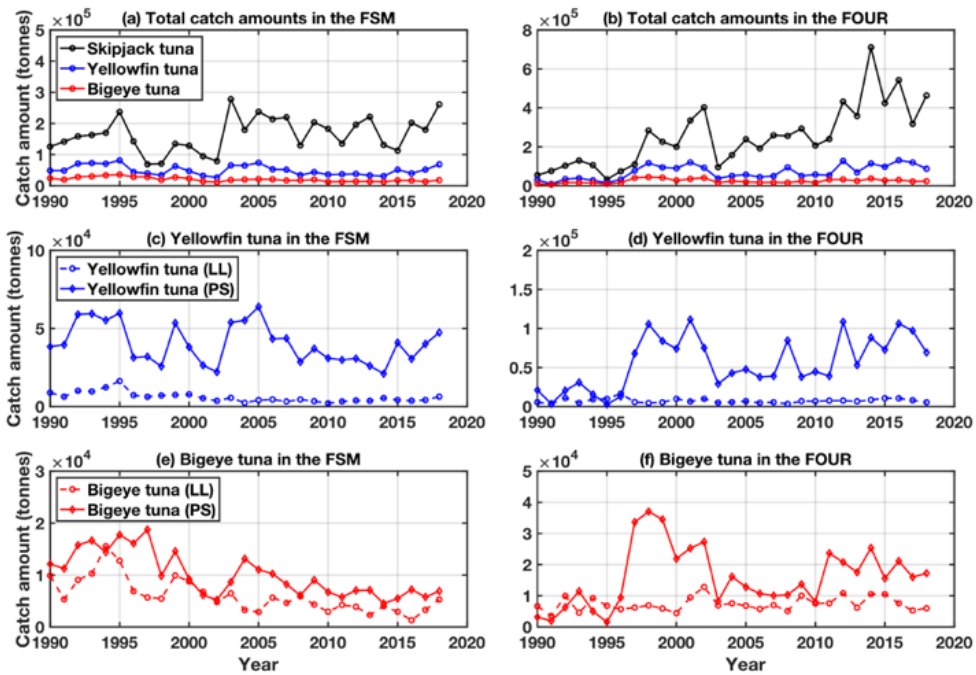

Figure 3.3 The catch amounts of the SKJ (black), the YFT (blue), and the BET (red) in the EEZs of the FSM and the FOUR during 1990–2018: the total catch amounts of tuna species (a, b), the catch amounts of the yellowfin tuna caught by the LL (dotted lines) and the PS (solid lines) fishing methods (c, d), and the catch amounts of the bigeye tuna caught by the LL and the PS (e, f).

ENSO has also been shown to affect the catchability of tuna using different fishing techniques, such as LL and PS methods, by affecting the thermocline depth (Lehodey et al., 1997; Lehodey, 2000; Lennert-Cody & Hall, 2000; Syamsuddin et al., 2013; Abascal et al., 2018). The LL method is typically used in deep ocean waters to target deep-sea tuna species (Nakano et al., 1997; Morato et al., 2010), while the PS method is used to target pelagic, small-sized juvenile tuna in waters shallower than about 200 m (Green, 1967). For example, during El Niño years, higher SKJ captured by the PS method is observed in Pacific Island countries and territories in the central Pacific, such as Kiribati (Lehodey et al., 2011). Therefore, understanding the relationship between ENSO and its impact on the catches, as well as the different fishing methods used, is critical to the effective management of these valuable resources in the WCP region.

This chapter aims to investigate the favorable ocean conditions in the equatorial Pacific that may lead to an increase in three tuna catches across the WCP between the FSM, located in the western part of the WCP, and the FOUR (Marshall Islands, Kiribati, Nauru, and Tuvalu), located in the eastern part of the WCP, considering the potential influence of different fishing methods.

3.2. Materials and methods

The annual catches of SKJ, YFT, and BET in each EEZ in the WCP from 1990 to 2018 were obtained from Sea Around Us (SAU, http://www.seaaroundus.org), which combines officially reported data from the Food and Agriculture Organization of the United Nations ((http://www.fao.org/fishery/statistics/en), obtained using the LL and the PS fishing methods, as well as estimates of unreported catches and major discards (Vali et al., 2014; Derrick et al., 2020). The EEZ-based annual dataset was compared to a spatially gridded monthly dataset provided by the Western Central Pacific Fisheries Commission (WCPFC, https://www.wcpfc.int/public-domain). The WCPFC data have a spatial resolution of 1° and include catch and effort data using the PS fishing method, as well as tuna school location information from Global Positioning System devices. However, the WCPFC data have an inconsistent number of empty grids over time in the gridded dataset. Therefore, the predictability of the three tuna species caught in the FSM and FOUR was examined using the SAU EEZ dataset. Comparison of the SAU EEZ annual catch data with the WCPFC catch per unit effort (CPUE, in this dissertation, catch per day) data for the corresponding grids in each EEZ showed similar temporal variability (Figure 3.4).

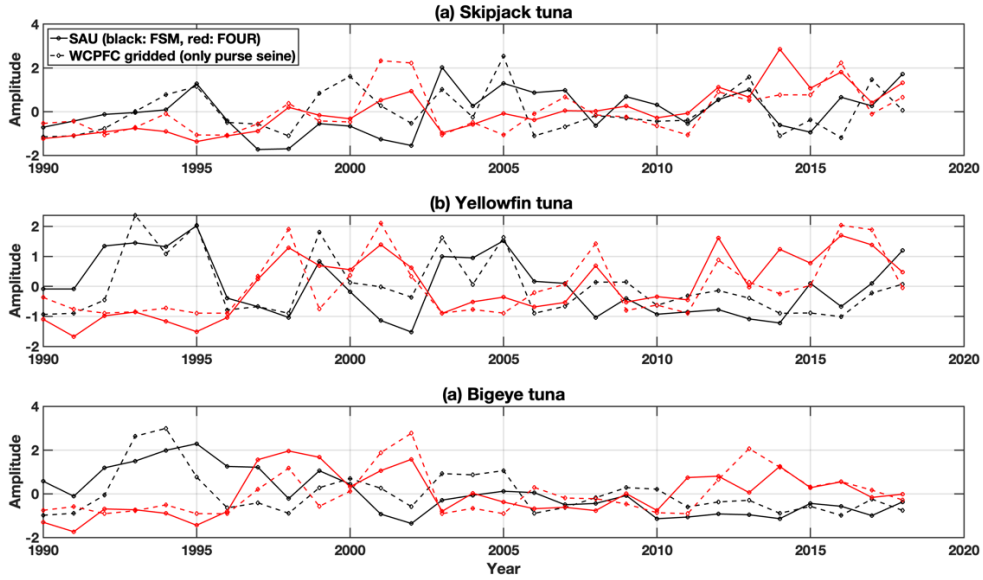

Figure 3.4 Comparison of normalized annual catches of tuna in the FSM and the FOUR during 1990–2018 SAU EEZ data (solid lines), WCPFC gridded data (dotted line): (a) SKJ, (b) YFT, and (c) BET. The black lines represent normalized data in the FSM, while the red lines represent normalized data in the FOUR.

This chapter analyzed monthly upper 500 m temperature, salinity, and current velocity data from the Simple Ocean Data Assimilation (SODA) 3.4.2, with a spatial resolution of 0.5° x 0.5°, from 1990-2018 (Carton et al., 2018). The thermocline depth was calculated using vertical linear interpolation of temperature at 1 m intervals at each grid point. Monthly chlorophyll concentration (CHL) and dissolved oxygen (DO) in the upper 500 m during 1993-2018 were obtained with a resolution of 0.25° x 0.25° from the Global Ocean Biogeochemistry Hindcast provided by the Copernicus Marine Environment Monitoring System Service. The CHL and the DO data were based on the PISCES biogeochemical model from the Nucleus for European Modelling of the Ocean modeling platform (Perruche et al., 2019). This chapter also used the ERA5 monthly averaged total precipitation (prep) and 10 m wind velocity data, with a horizontal resolution of 0.25°, from the ECMWF for the period 1990-2018 (Hersbach et al., 2020). This chapter investigated the statistical relationships between annual tuna catches in the FSM and the FOUR and ocean environmental variables in the equatorial Pacific (30° N-30° S, 100°-300° E) on the interannual time scale.

For the ocean environmental variables, the CSEOF analysis is used (Kim et al., 1996; Kim and North, 1997; see Appendix). To understand

the physical relationship between the target and predictor, regression analysis can be used. This results in a spatial pattern of predictor and target variables corresponding to their physical evolution.

3.3. Ocean conditions related to the tuna catches

Figure 3.5 shows the zonal distribution of the mean and interannual standard deviation (STD) of various ocean environmental variables in the equatorial Pacific from 1990 to 2018 (except chlorophyll concentration (CHL) and dissolved oxygen (DO), which are illustrated from 1993 to 2018). These variables, which include temperature, salinity, zonal current velocity (ZC), CHL, and DO, have been meridionally averaged from 15° N to 15° S.

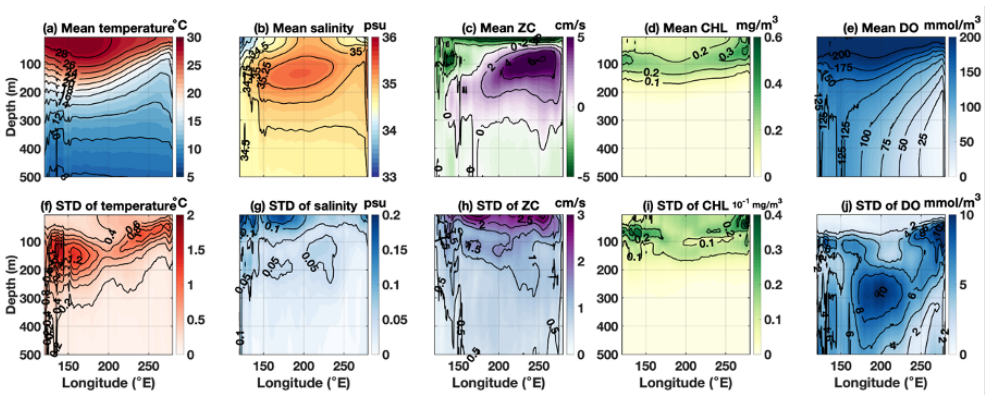

Figure 3.5 The zonal distribution of the mean (top panel) and standard deviation (bottom panel) of various ocean environmental variables in the equatorial Pacific during 1990–2018 (except for CHL and DO which are presented during 1993–2018). The variables are meridionally averaged from 15° N to 15° S and the standard deviations are calculated from the annual means. Each column represents different variables: temperature (a, f), salinity (b, g), ZC velocity (c, h), CHL (d, i), and DO (e, j).

In the equatorial Pacific, the mean temperature displays the warm pool with a deep thermocline in the western region and a shallow thermocline in the eastern region due to coastal upwelling (Toggweiler et al., 1991; Picaut et al., 1996). The STD of temperature in the equatorial Pacific reveals significant variability in the subsurface temperature from 100 to 200 m depth in the western region, and in the near-surface temperature in the eastern region because of coastal upwelling (Zeller et al., 2004) The STD of temperature also illustrates that the temporal variance of subsurface temperature is higher in the EEZ of the FSM (longitudinal band: approximately 135° -165° E) than that of the FOUR (longitudinal band: approximately 157° -183° E). Due to high amounts of precipitation (prep) caused by the Intertropical Convergence Zone (ITCZ) and South Pacific Convergence Zone (SPCZ) (top row in Figure 3.6) (Waliser et al., 1993; Vincent, 1994), the mean salinity is relatively low from the surface to near-surface layers (less than 100 m depth) in the western region. Due to the influence of the ITCZ and the SPCZ, the STD of salinity in the equatorial Pacific displays substantial fluctuation in the surface to near-surface layers in the western region (Delcroix et al., 1996; Delcroix & McPhaden, 2002). The mean ZC in the equatorial Pacific displays a westward surface current, the Equatorial Surface Current (Wyrtki, 1967;

Reverdin et al., 1994), with the easterly wind (top row in Figure 3.6). From the near-surface to approximately 200 m depth in the central to the eastern region, the subsurface ZC exhibits a considerable eastward current, the Equatorial Undercurrent (Taft et al., 1974; Lu et al., 1998). In the near-surface layer of the equatorial Pacific, the STD of ZC significantly varies, but the ZC below near the surface displays relatively modest variability.

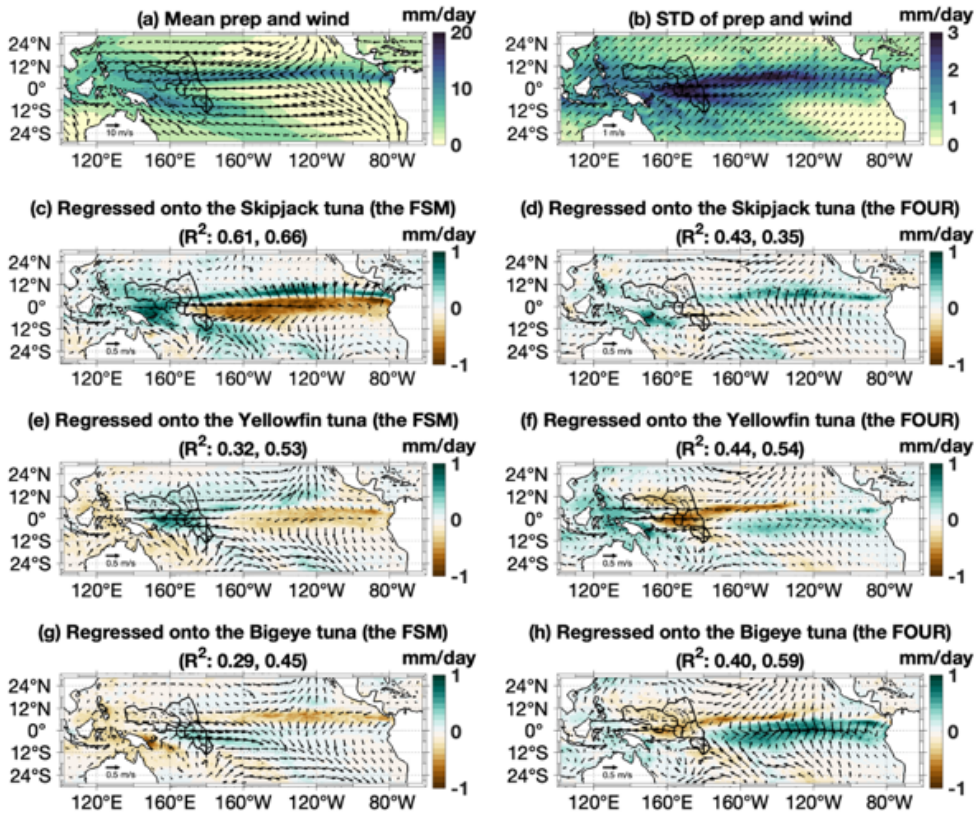

Figure 3.6 The mean (a) and standard deviation (b) of total precipitation and 10 m height wind velocity in the equatorial Pacific during 1990–2018. (c–h) regressed precipitation and wind anomalies with respect to the catch amounts of tuna in the EEZ of the FSM (left column) and the FOUR (right column). The standard deviation is calculated from the annual means. The R-squared values of total precipitation and 10 m height wind velocity for each regression are presented in parentheses, respectively.

The mean CHL in the equatorial Pacific is only explicable in the upper 200 m depth (shallower than the twilight zone) (Figure 3.5) (Martin et al., 2020). The CHL in the eastern region is greater than in other regions, probably because of coastal upwelling, which supplies nutrient-rich water near the surface (Fiedler et al., 1991). The mean DO increases from the subsurface to the surface and from east to west (Garcia et al., 2019). The western area has a higher mean DO from the surface to the subsurface than the eastern region. The temporal variability of the CHL exhibits substantial fluctuation only in the upper 200 m. In the western region, the STD of CHL is highly variable in the near-surface layer, but in the eastern region, it mostly varies around the surface layer. Below the surface, the STD of DO in the equatorial Pacific varies considerably (Schlitzer et al., 2004). In the western region, substantial variability is observed at approximately 100 m depth, whereas in the eastern region, it is observed near the surface at approximately 50 m depth. Notably, considerable DO variability is found between 200-400 m depth in the central Pacific. The temporal variance of CHL and DO in the equatorial Pacific indicates that there is a higher degree of temporal variability in the subsurface of the EEZ of the FSM compared to the EEZ of the FOUR, similar to the variance observed in temperature (Figure 3.5).

Figure 3.7 presents the catch amounts of SKJ, YFT, and BET with the trend (upper panel) and their detrended variability (lower panel) during 1990–2018 in FSM and FOUR. In both regions, the catch amounts of SKJ have increased over the past 30 years, with a stronger increasing trend observed in FOUR than in FSM (Figure 3.7a). Conversely, YFT catches have shown a decreasing trend in the FSM, but an increasing trend in the FOUR (Figure 3.7b). Similarly, the catches of BET in FSM have been decreasing while those in FOUR have been increasing (Figure 3.7c). In addition, the catch amounts of YFT caught by the PS method and BET caught by the PS and LL methods in FSM illustrate a decreasing trend, while those in FOUR show an increasing trend (Figure 3.3). The CPUE of YFT and BET in FSM and FOUR also exhibit a decreasing and increasing trend, respectively (Figure 3.4). When comparing the variability of the detrended catch amounts of all three tuna species in FSM and FOUR, negative correlations between the catches in the two regions can be observed, especially during the early 2000s (lower panel of Figure 3.3).

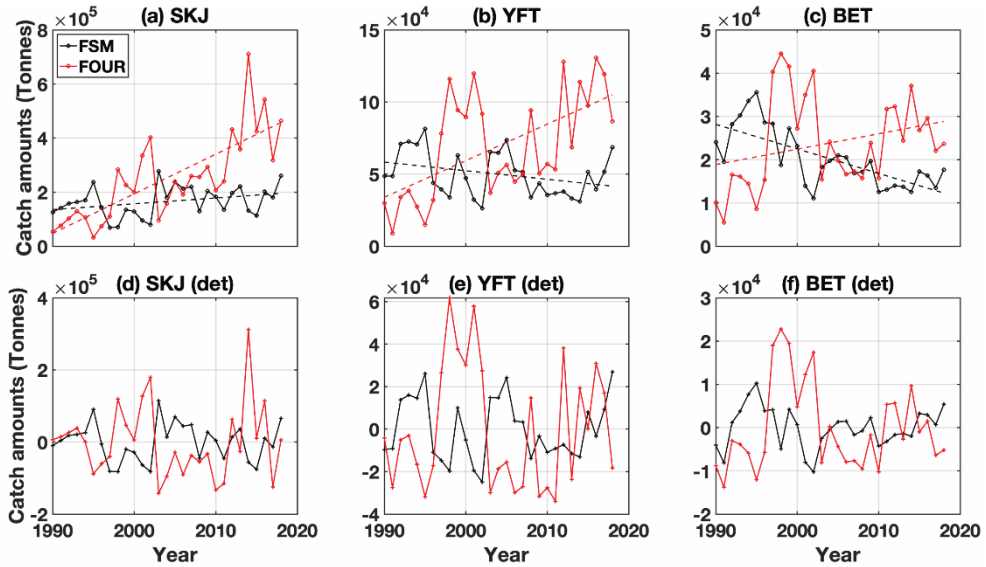

Figure 3.7 The catch amounts of the SKJ, YFT, and BET in the EEZs of the FSM and FOUR during 1990–2018: (top) the catch amounts (solid lines) and their linear trends (dotted lines) and (bottom) detrended (det) the catch amounts during the same period.

Table 3.1 presents the correlation coefficients of the catch amounts of the SKJ, the YFT, and the BET in the EEZs of the FSM and the FOUR from 1990 to 2018. Only statistically significant correlation coefficients ($p < .05$) are displayed. There is a positive relationship between the YFT and the BET catches in the EEZ of the FSM. However, there is no statistical correlation between the catches of the SKJ and the YFT, and between the catches of the SKJ and the BET. This may suggest that the ocean conditions contributing to an increase in the YFT and the BET catches in the FSM are similar, whereas those

driving an increase in the SKJ in this region are distinct. In the EEZ of the FOUR, catch amounts of all three tuna species also exhibit positive relationships. The correlation coefficients in this region suggest that ocean conditions leading to increased catches of all three species are comparable. The correlation coefficients between the catches in the FSM and the FOUR, except for the SKJ (FSM)-SKJ (FOUR) and SKJ (FSM)-YFT (FOUR) pairs, show significant inverse relationships, suggesting that there may be different ocean conditions that lead to increased the catches in each region.

Table 3.1 The correlation coefficients among the catch amounts of the SKJ, YFT, and BET in the EEZs of the FSM and FOUR during 1990–2018. Only statically significant correlation coefficients ($p < .05$) are shown.

	SKJ (FSM)	**YFT (FSM)**	**BET (FSM)**	**SKJ (FOUR)**	**YFT (FOUR)**	**BET (FOUR)**
SKJ (FSM)		0.53	-	-	-	-0.52
YFT (FSM)	0.53		0.68	-0.48	-0.54	-0.50
BET (FSM)	-	0.68		-0.68	-0.56	-0.35
SKJ (FOUR)	-	-0.48	-0.68		0.78	0.57
YFT (FOUR)	-	-0.54	-0.56	0.78		0.76
BET (FOUR)	-0.52	-0.50	-0.35	0.57	0.76	

It is worth noting that the correlation coefficient between SKJ catches in FSM and FOUR during the 1990–2018 period is insignificant, which contradicts previous studies (Lehodey et al., 1997; Kim et al., 2020). However, the correlation coefficients between the detrended catch amounts of SKJ during the same period in FSM and FOUR show a negative relationship (r = −0.48, p < .05), which is consistent with previous study (Lehodey et al., 1997; Kim et al., 2020) (Table 3.2). This may indicate that long-term trends and recent variability in SKJ catches in the FSM and FOUR have weakened the negative relationship between the FSM and FOUR regions. Because it is unclear whether this trend is a result of natural variability or anthropogenic factors (e.g., global warming, increased effort, etc.), this chapter investigates the detrend of tuna catch variability during 1990-2018.

Table 3.2 same as Table 3.1, but with detrended annual catch amounts of tuna during 1990–2018.

	SKJ (FSM)	YFT (FSM)	BET (FSM)	SKJ (FOUR)	YFT (FOUR)	BET (FOUR)
SKJ (FSM)		0.72	0.39	-0.48	-0.66	-0.67
YFT (FSM)	0.72		0.68	-0.38	-0.45	-0.45
BET (FSM)	0.39	0.68		-	-	-
SKJ (FOUR)	-0.48	-0.38	-		0.63	0.57
YFT (FOUR)	-0.66	-0.45	-	0.63		0.76
BET (FOUR)	-0.67	-0.45	-	0.57	0.76	

Figure 3.8 shows the R-squared values obtained from the regression of each depth with the detrended catch amounts of SKJ (black), YFT (blue), and BET (red) in the EEZ of the FSM (upper panel) and FOUR (lower panel) from 1990 to 2018, except for CHL and DO from 1993 to 2018. Overall, the R-squared values for the catches in the FSM and FOUR show statistically significant results. However, for SKJ in the FOUR, the R-squared values are generally insignificant, except for temperature at approximately 100-200 m depth, CHL near the surface, and DO near the surface to approximately 100 m depth (lower panel of Figure 3.8). In general, the R-squared values for the catches in the FSM are higher than those in the FOUR. Among the three tuna species, the R-squared values for the catches of BET tend to be the highest, followed by those for YFT and SKJ. Notably, the R-squared values for CHL and DO are higher than those for the other variables in both the FSM and the FOUR, suggesting that CHL and DO may have a stronger association with the biological responses of tuna catches than the other variables. In particular, temperature and CHL have particularly high R-squared values in the 100-200 m depth range and at the surface to approximately 100 m depth, respectively, where significant temporal variations are observed for these variables (Figure 3.5).

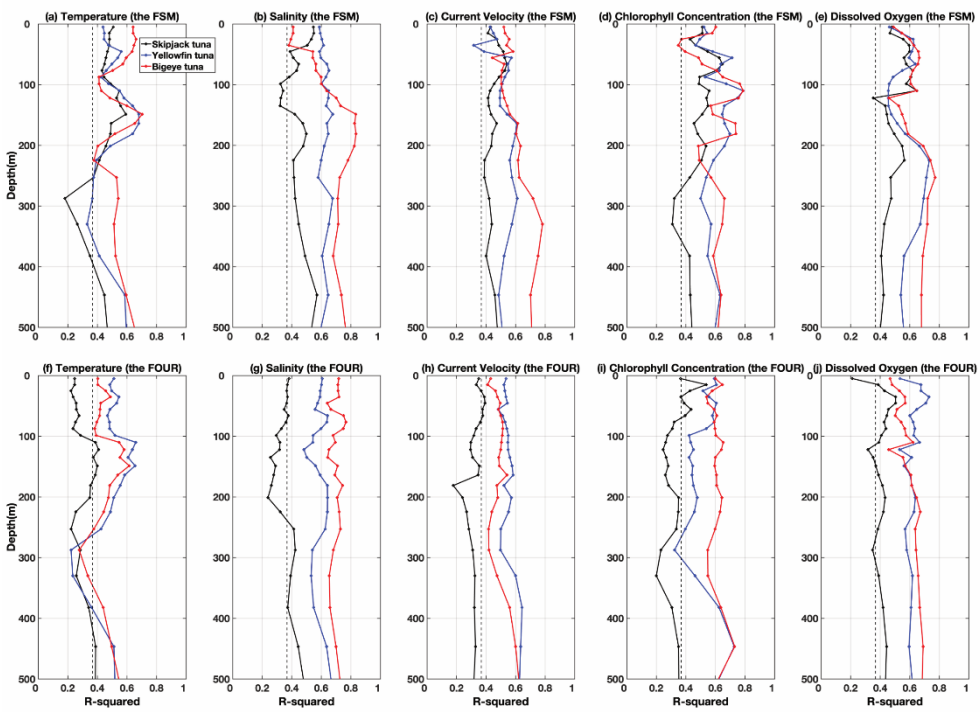

Figure 3.8 The R-squared values of the regression at each depth with respect to the SKJ, YFT, and BET in the EEZs of the FSM (top panel) and the FOUR (bottom panel) during 1990–2018 (except for chlorophyll concentration and dissolved oxygen during 1993–2018) for temperature (a, f), salinity (b, g), current velocity (c, h), CHL (d, i), and DO (e, j). The vertical dashed lines denote the e-folding value.

Figure 3.9 displays the zonal distributions of the regressed and reconstructed anomalies of ocean environmental variables in the equatorial Pacific during the periods of increased catches of SKJ (left column), YFT (middle column), and BET (right column) within the EEZ of the FSM. The vertical black lines indicate the longitudinal boundaries of the Five Nations (135-183° E), while the dotted gray lines indicate the boundaries of the FSM and FOUR regions (161° E). During an increase in SKJ catches, upper ocean warming has been observed in the central Pacific and cooling in the western and eastern Pacific, while for YFT and BET catches, cooling in the western Pacific and warming in the eastern Pacific is observed at 100-150 m depth (Figure 3.9a-c). In the FSM region, higher SKJ catches align with surface cooling to around 100 m depth, while increased YFT and BET catches correspond to surface to subsurface cooling, indicating a shallower thermocline in the FSM region. Salinity anomalies during the increase in all three species show surface to near-surface freshening from 150° E to 200° E, with larger amplitudes for YFT and BET. The precipitation anomaly, which is statistically significant only for SKJ, is positive in the western Pacific during an increase in SKJ (Figure 3.6c), consistent with near-surface freshening, indicating an intensification of the ITCZ and SPCZ (Cravatte et al., 2009; Yu et al., 2015).

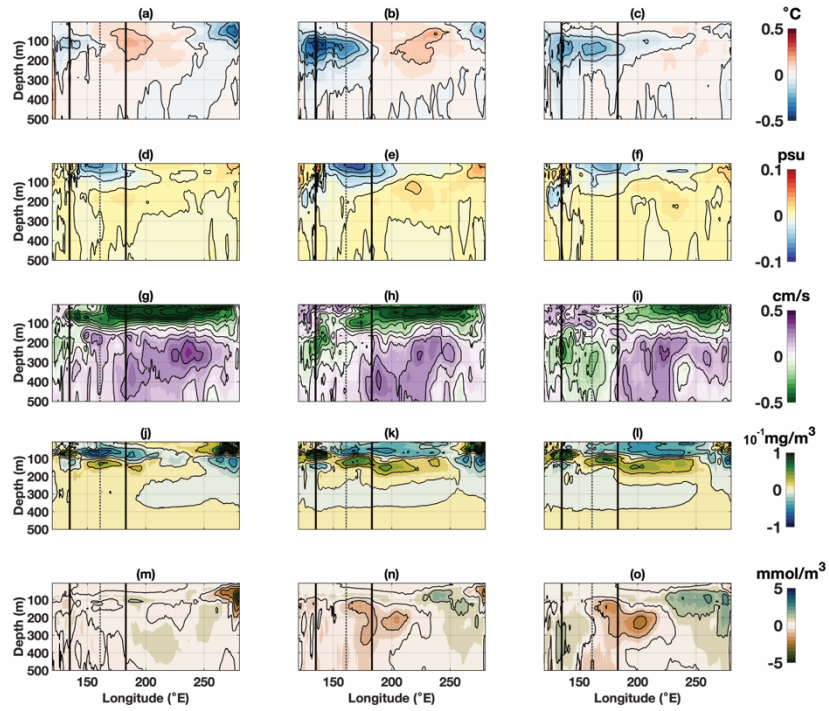

Figure 3.9 The zonal distributions of the regressed and reconstructed anomalies of the ocean environmental variables in the equatorial Pacific during 1990–2018 (except for CHL and DO during 1993–2018). Target time series are the annual catch amounts of the SKJ (left column), the YFT (middle column), and the BET (right column) in the EEZ of the FSM, respectively. The anomalies are presented after meridional averages from 15° N to 15° S. Each row represents a different variable: temperature (a–c), salinity (d–f), zonal current velocity (g–i), CHL (j–l), and DO (m–o).

During an increase in SKJ catches, the wind anomaly is westerly in the western Pacific and easterly in the central-eastern region (Figure 3.6c). Similarly, YFT and BET show westerly winds in the western Pacific, but the direction of the easterly winds in the central-eastern Pacific is unclear (Figure 3.6e-g). Anomalous westward currents are observed from the surface to approximately 100 m depth during the increase in SKJ catches, while eastward current anomalies are observed below approximately 100 m depth (Figure 3.9g). Conversely, the YFT and BET display upright, oblique patterns with eastward current anomalies in the western Pacific from the surface to approximately 100 m depth and westward current anomalies in the central-eastern Pacific below 100 m depth (Figure 3.9h-i). These current anomalies indicate an intensification of the Equatorial Surface Current and a weakening of the Equatorial Undercurrent during the increase in SKJ catches in the FSM and vice versa for the YFT and BET. The CHL and DO anomalies show increased CHL from the surface to approximately 100 m depth during an increase in SKJ catches in the FSM region and decreased DO below approximately 100 m depth. In the eastern Pacific, DO anomalies were significant (Figure 3.9m). During an increase in YFT and BET catches, CHL anomalies show increased CHL in the FSM region from approximately 50-150 m

depth and decreased CHL from the surface to approximately 100 m depth in the FOUR region (Figure 3.9k-l). DO shows a decrease in DO from 200-300 m depth in the central Pacific and an increase in DO from the surface to approximately 200 m depth, which is more pronounced in the BET (Figure 3.9n-o).

Figure 3.10 illustrates the zonal distributions of the regressed and reconstructed anomalies of ocean environmental variables in the equatorial Pacific during periods of increased catches of SKJ (left column), YFT (middle column), and BET (right column) within the EEZ of the FOUR. It is important to note that during an increase in SKJ catches in the FOUR, only temperature at approximately 100-200 m depth, CHL near the surface, and DO near the surface to approximately 100 m depth display statistical significance.

Ocean conditions during increased catches of YFT and BET exhibit similarities, as seen in the middle and right columns of Figure 3.10, which is consistent with the correlation coefficients among the tuna species in the FOUR, as shown in Table 3.1. However, ocean conditions during increased catches of SKJ are different from those of other species, as seen in the left column of Figure 3.10. During an increase in YFT and BET catches, the temperature anomalies show

upper-ocean warming in the western and eastern Pacific and cooling in the central Pacific (Figure 3.10b-c), while those in SKJ exhibit upper-ocean cooling in the western Pacific and warming in the eastern Pacific (Figure 3.10a). Saline conditions are present near the surface from 150° -200° E over the EEZs of five nations (Figure 3.10d-f), while the prep anomalies have a negative anomaly over the EEZs of five nations during increases in YFT and BET catches, and prep anomaly is positive in the EEZs of the FOUR during an increase of SKJ catches (Figure 3.6c-g), consistent with the presence of near-surface freshening in that region (Figure 3.10d-f). This suggests that the ITCZ and the SPCZ are weakened during an increase in YFT and BET catches. The wind anomalies associated with increased SKJ catches are westerlies in the EEZs of the FOUR and central Pacific, while those in YFT and BET display easterlies over the EEZs of five nations and westerlies equatorial central Pacific to eastern Pacific (Figure 3.6d-h).

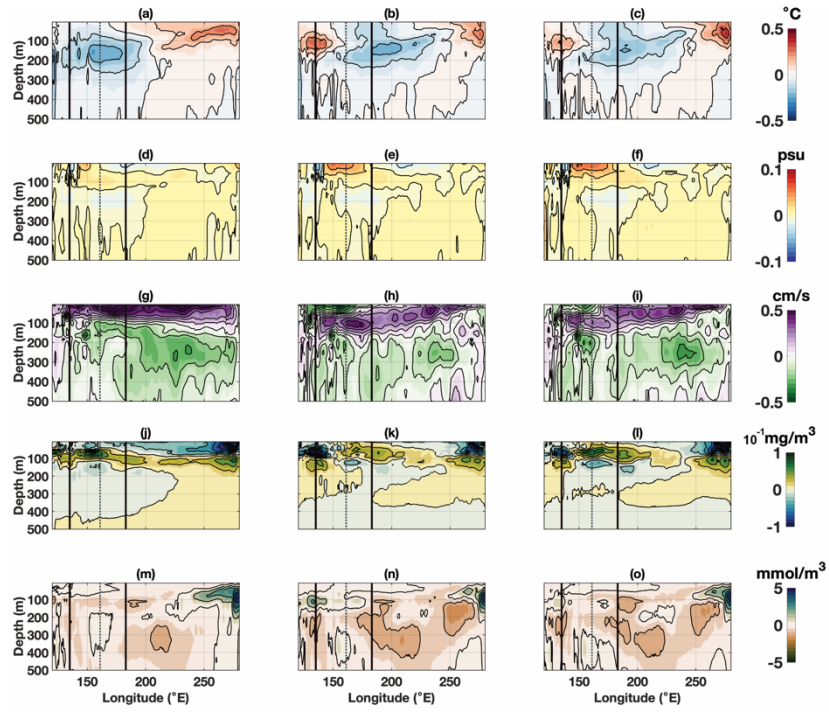

Figure 3.10 same as Figure 3.9, but for the FOUR.

During an increase in YFT and BET catches, the current anomalies show upright patterns that are skewed, with westward anomalies in the western Pacific from the surface to 200 m depth and eastward anomalies in the central to eastern Pacific, mostly below 100 m depth (Figure 3.10h-i). Therefore, these current anomalies show the strengthening of the Equatorial Surface Current and the Equatorial Undercurrent during increased YFT and BET catches in the FOUR. With respect to CHL anomalies, an increase in CHL from the surface to 100 m depth and a decrease below 100 m are observed in the FOUR region during an increase in YFT and BET catches, while the FSM region shows a decrease from the surface to approximately 100 m depth and an increase below approximately 100 m (Figure 3.10k-l). In addition, DO anomalies show negative DO anomalies in the central Pacific and positive DO anomalies in the eastern Pacific during an increase in all three tuna species (Figure 3.10m-o).

As illustrated in Figures 3.9 and 3.10, ocean conditions during increases in the catches in the FSM and FOUR show similar ocean conditions in the YFT and BET, while those in the SKJ are different from other species. The ocean conditions during an increase in YFT and BET catches in the FSM and FOUR are generally opposite to each other (e.g., upper ocean temperature anomaly and surface to near-

surface CHL), which is consistent with the negative relationship between the catches in each EEZ (Table 3.1). It is noteworthy that the relationship between ENSO and tuna catches in the FSM and FOUR is evident from the comparable ocean environmental patterns observed in the equatorial Pacific (Figure 3.11). The catch of SKJ in the FSM is known to increase during La Niña-like ocean conditions (left column of Figure 3.9), which is consistent with previous studies (Lehodey et al., 1997; Kim et al., 2020). Conversely, catches of YFT and BET tend to increase during El Niño-like ocean conditions (middle and right columns of Figure 3.9). In the FOUR, an increase in YFT and BET catches is associated with La Niña-like ocean conditions (middle and right columns of Figure 3.10), while an increase in SKJ catches may be associated with El Niño-like ocean conditions, as indicated by the temperature at approximately 100-200 m depth, CHL near the surface, and DO near the surface to approximately 100 m depth (left column of Figure 3.10). The ocean conditions associated with the increase in the catches suggest a possible relationship between ENSO and tuna catches in the FSM and FOUR.

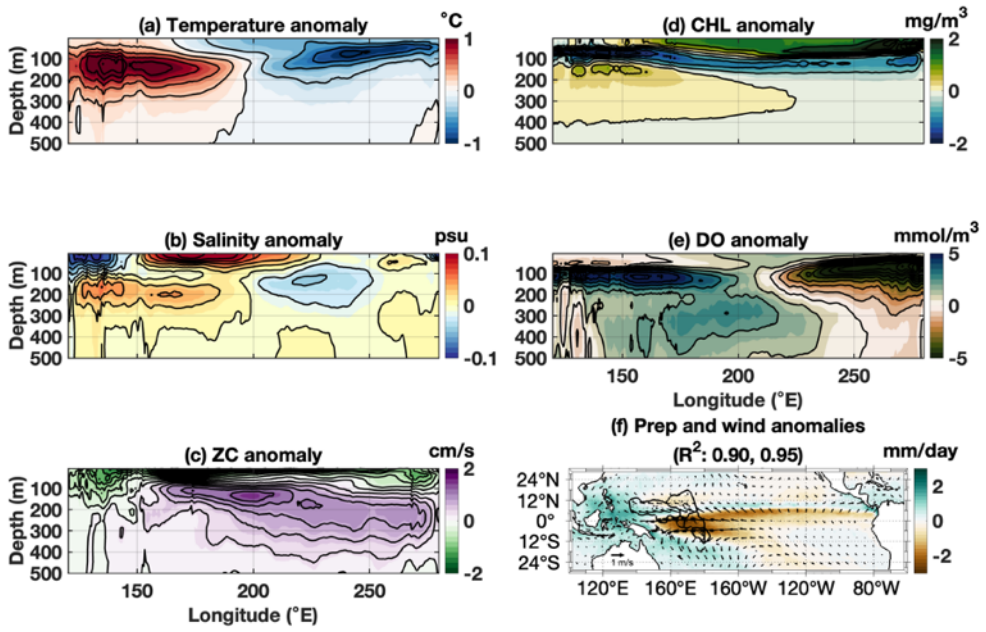

Figure 3.11 The zonal distributions of the regressed and reconstructed anomalies of the ocean environmental variables in the equatorial Pacific with respect to 2-yr low-pass filtered Southern Oscillation Index during 1990–2018 (except for CHL and DO during 1993–2018). The ocean conditions during the La Niña years can be observed through the regressed and reconstructed anomalies of the ocean environmental variables. The anomalies are presented after meridional averages from 15° N to 15° S: temperature (a), salinity (b), zonal current (ZC) velocity (c), CHL (d), DO (e), and precipitation with the 10 m height wind (f). The R-squared values of total precipitation and 10 m height wind velocity for each regression are presented in parentheses, respectively.

The R-squared values for the regression of ocean environmental variables on the catches in the FSM were found to be statistically significant for both the LL and PS methods (upper panel of Figure 3.12). Among the two tuna species, the R-squared values were highest for BET using the LL method, followed by those for BET using the PS method, YFT using the LL method, and YFT using the PS method. The ocean conditions during an increase in YFT and BET catches in the FSM using both the LL and PS methods are similar to the total YFT and BET catches in the FSM (Figure 3.13), as shown in Figure 3.9.

In the FOUR, the LL method produced statistically insignificant R-squared values, while the PS method was statistically significant (lower panel of Figure 3.12). Among the two species in the FOUR, the R-squared values for the BET using the PS method were highest, followed by those for the YFT using the PS method. In the EEZs of Kiribati and the Marshall Islands, which account for a significant proportion of total YFT and BET catches in the FOUR (56% and 53% in Kiribati and 14% and 18% in the Marshall Islands, respectively), YFT and BET using the LL method contributed statistically insignificant R-squared values to the catches in the FOUR using the LL method. In the FOUR, the ocean conditions during an increase in the YFT and BET catches using the PS method are also similar to the total YFT and BET

catches in the FOUR (Figure 3.14), as shown in Figure 3.10.

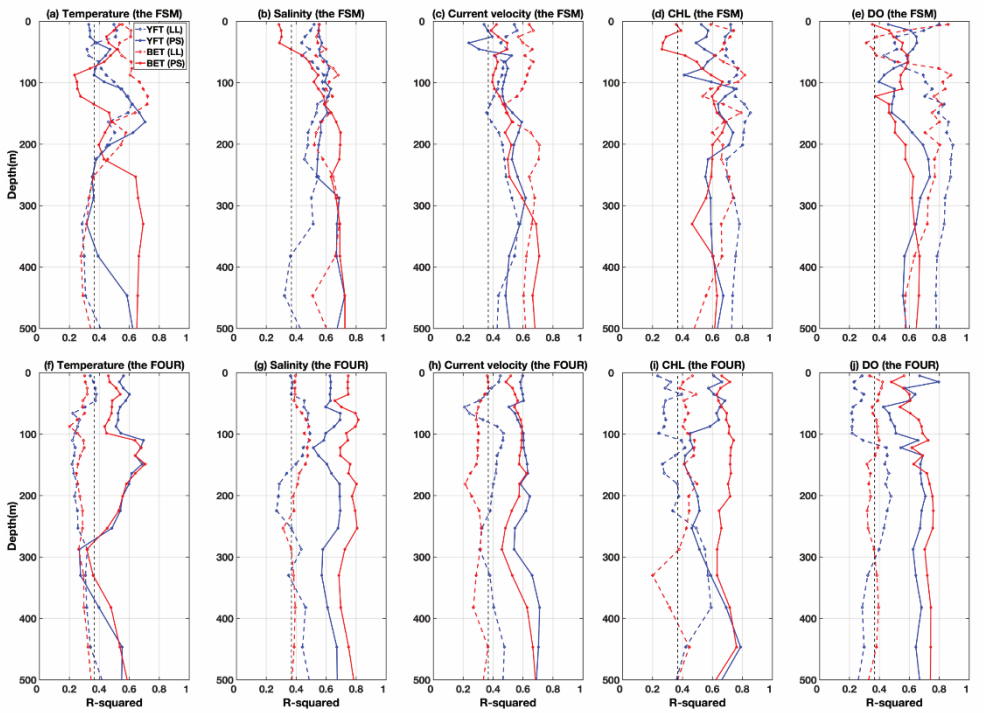

Figure 3.12 The R-squared values of the regression at each depth with respect to the YFT (blue) and the BET (red) caught by the LL (dotted lines) and the PS (solid lines) fishing methods in the EEZ of the FSM (top panel) and the FOUR (bottom panel) during 1990–2018 (except for CHL and DO during 1993–2018) for temperature (a, f), salinity (b, g), current velocity (c, h), CHL (d, i), DO (e, j). The vertical dashed lines denote the e-folding value.

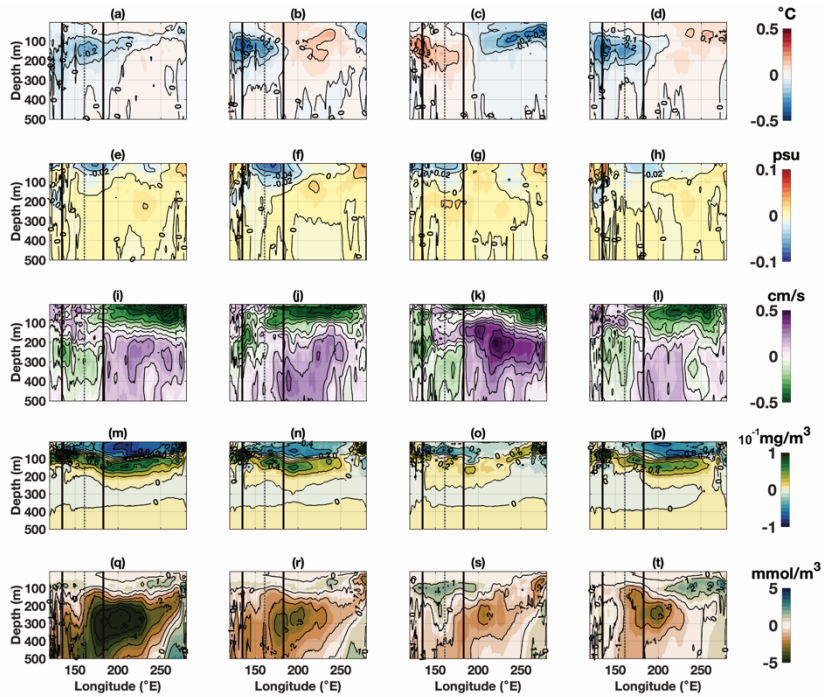

Figure 3.13 The zonal distributions of the regressed and reconstructed anomalies of the ocean environmental variables in the equatorial Pacific during 1990–2018 (except for CHL and DO during 1993–2018). Target time series are the annual catch amounts of the YFT caught by the LL (the first column) and PS (the second column) fishing methods and the BET caught by the LL (the third column) and PS (the fourth column) methods in the EEZ of the FSM, respectively. The anomalies are presented after meridional averages from 15° N to 15° S. Each row represents a different variable: temperature (a–d), salinity (e–h), zonal current velocity (i–l), chlorophyll concentration (m–p), and dissolved oxygen (q–t).

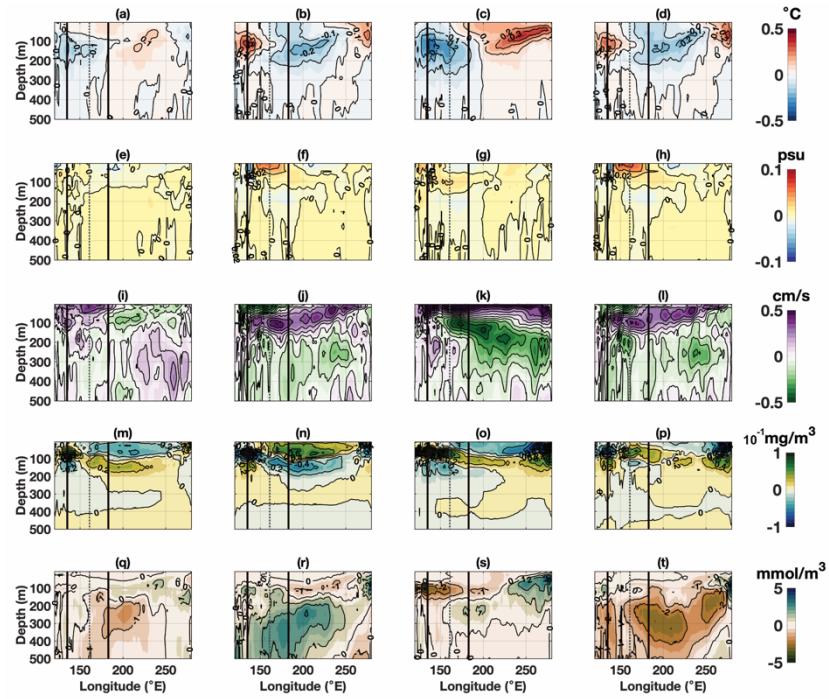

Figure 3.14 same as Figure 3.13, but for the FOUR.

3.4. Discussion

The habitat suitable for tuna may be determined by a variety of factors, including the species' temperature tolerance, diving capabilities, and oxygen tolerance (Senina et al., 2018). The vertical habitat characteristics of the species, such as the depth of the isotherm and the thermocline, may also be relevant (Schaefer & Fuller, 2010). The distinct habitats of each tuna species may result in unique relationships between ocean environmental variability and the abundance of each species (Bertignac et al., 1998). Factors that may impact tuna catches include the availability of sufficient plankton, rich levels of the DO, and accumulation of preferred prey (Lehodey et al., 2003; Lehodey et al., 2008). However, this chapter primarily demonstrates the statistical relationship between ocean environment in the equatorial Pacific and tuna catches in the FSM and FOUR, without considering the physiological conditions of the tuna in the region.

This chapter shows that the negative relationship is not statistically significant in SKJ catches during 1990-2018 (Table 3.1) which is in contrast to previous studies that there is an inverse relationship (zonal difference) between the catches in the FSM and the

FOUR (Lehodey et al., 1997, Kim et al., 2020). This suggests a lack of zonal variation in the distribution of SKJ in the WCP, in contrast to the significant zonal variation observed in the catches of the YFT and BET (middle and right columns of Figure 3.9-10). Nevertheless, detrended catch amounts of SKJ in the FSM and FOUR show a negative relationship (r = -0.48, $p < .05$; Table 3.2), which is consistent with previous reports of zonal variation in SKJ catches (Lehodey et al., 1997; Kim et al., 2020). Similarly, regression results of detrended SKJ catches in FSM and FOUR show La Niña-like and El Niño-like ocean conditions (left column in Figure 3.9-10), indicating that warm pool contraction and expansion can still explain variability in SKJ catches in the WCP region (Lehodey et al., 1997).

The expansion of the Pacific warm pool due to upper ocean warming in recent years has been suggested as a contributing factor to warm pool variability and its impact on SKJ habitat (Lehodey et al., 1997). The warm pool has continued to expand eastward possibly due to ongoing climate change (Weller et al., 2016). This expansion has caused SKJ to migrate eastward, following the warm pool, resulting in a higher increasing trend in catches in the eastern region of the WCP (the FOUR region) compared to the western region of the WCP (the FSM region). The zonal difference in SKJ catches between the FSM

and FOUR regions was evident from 1990 to 2014, but lost statistical significance by 2018. This disappearance of the zonal difference can be attributed to the pronounced positive trend in SKJ catch observed in the FOUR region (Figure 3.7a), which was influenced by the recent expansion of the warm pool and the occurrence of high-temperature regions in the eastern area of the WCP since 2014 (Figure 3.15). In particular, the expansion of the warm pool along with the occurrence of high-temperature regions in recent years likely contributed to a significant increase in SKJ catches in the FOUR region (Figure 3.7a). This, in turn, has caused the difference in the catches between the FSM and FOUR regions to become uni-sign, leading to the disappearance of the zonal difference between the two regions in recent years. These results highlight the complex relationship between warm pool expansion, SKJ habitat shifts, and resulting changes in catch patterns, and emphasize the need for further study and monitoring in the context of climate change.

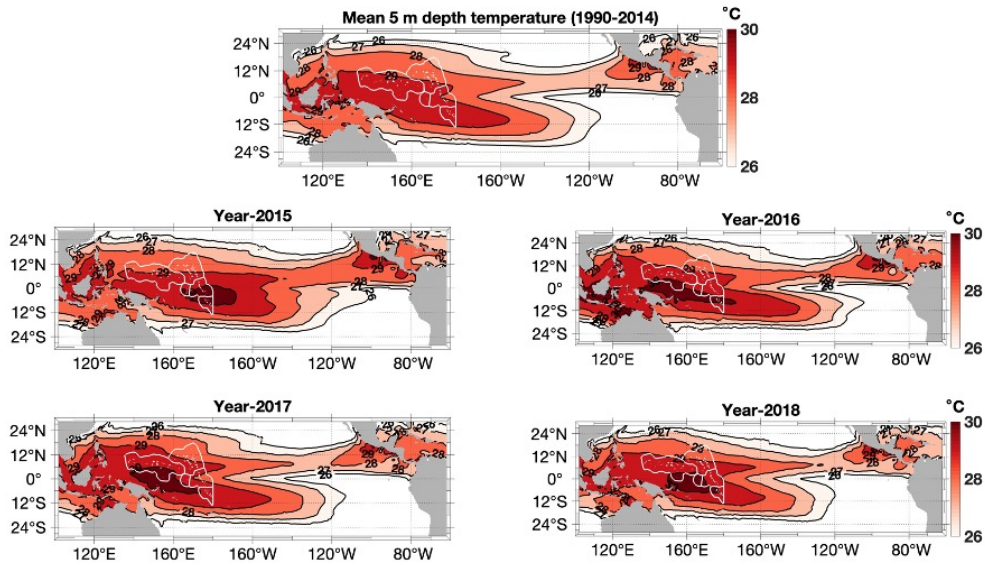

Figure 3.15 Mean 5 m depth temperature during 1990–2014 and yearly averaged 5 m depth temperature in 2015, 2016, 2017, and 2018. Only the temperature exceeding 26℃ is displayed.

The correlation coefficients and regression results may suggest that the previously established inverse relationship between SKJ catches in the FSM and FOUR is not robust and may not have been consistently evident in recent decades. This may be due to anthropogenic effects such as increased fishing efforts. If there were a rapid increase in the number of fishing vessels in the fishery, it would be expected that the CPUE would decrease significantly due to the finite availability of fish. To mitigate the effects of this increase in vessels, this chapter focused on analyzing relatively recent data beginning in 1990. No significant decrease in CPUE was observed when examining the CPUE data obtained from the WCPFC gridded data. In addition, the analysis results showed statistically significant R-squared values, indicating that the anthropogenic factors resulting from the increase in fishing vessels did not have a significant impact in explaining the relationship between the ocean environment and tuna catch.

The spatial patterns of ocean conditions associated with increases in YFT and BET catches exhibit opposite characteristics in the FSM and FOUR, consistent with the negative correlation observed between the catches in these two regions (Table 3.1). Specifically, in the FSM region, an increase in YFT and BET catches is associated with a

cooling of the subsurface temperature (shallow thermocline) and an increase in CHL from the near-surface to the subsurface (approximately 50 to 150 m depth) (middle and right columns of Figure 3.9). Conversely, the FOUR region experiences a decrease in CHL from the surface to approximately 100 m depth with relatively weak subsurface cooling. Similarly, as YFT and BET catches increase in the FOUR region, the ocean environment in the FOUR region shows subsurface cooling accompanied by an increase in CHL concentrations from the surface to approximately 100 m depth (the middle and right columns of Figure 3.10). In contrast, the FSM region experiences subsurface warming with a decrease in CHL from the surface to the subsurface (approximately 50 to 150 m depth).

In terms of temperature, the notable variability is attributed to the thermocline and warm pool in the WCP region, posing a challenge in identifying the optimal temperature range associated with tuna catches. Consequently, the investigation focused on examining the relationship between the expansion and contraction of the warm pool, which is influenced by SST, and the variability in thermocline depth, which influences the subsurface temperature, about tuna catches.

The migration pattern of SKJ is closely linked to the warm pool,

which is characterized by sea surface temperatures above 26° C (Lehodey et al., 1997). Consequently, the catch of SKJ tends to increase in the eastern region and decrease in the western region, depending on the east-west expansion and contraction of the warm pool (Lehodey et al., 1997; Kim et al., 2020). While YFT and BET cannot dive through the thermocline until they reach maturity, as adults they have the ability to dive to depths beyond the thermocline (Senina et al., 2018). Variability in thermocline depth can affect the vertical distribution of YFT and BET, resulting in shifts in their habitat depth (Senina et al., 2018). In the WCP region, purse seine fisheries dominate YFT and BET catches, accounting for 90% and 70%, respectively (Lehodey, 2000; Lennert-Cody & Hall, 2000). Purse seine nets are typically deployed at depths of approximately 200 m, making YFT or BET closer to the surface more susceptible to capture (increased catchability). The depth of the thermocline plays a role in the vertical habitat distribution of YFT and BET. As the thermocline becomes shallower, the proximity of YFT and BET to the surface increases, creating favorable conditions for purse seine catchability.

In addition, variations in chlorophyll concentration can be considered as a biological factor associated with improved catchability. Regions with higher chlorophyll concentrations indicate a more

productive marine ecosystem characterized by an abundance of nutrients and prey for tuna (Lehodey, 2001; Lehodey et al., 2011). Such conditions provide an optimal environment for tuna, resulting in increased catch potential. Therefore, chlorophyll concentration serves as an indicator of the biological productivity of the ocean, causing schools of tuna to migrate to areas with elevated chlorophyll concentrations, thereby increasing potential catchability.

The ocean conditions associated with increases in YFT and BET catches in the WCP are similar to those of the ENSO (Figure 3.9-14). During El Niño-like conditions, the YFT and BET catches in the FSM region increase while those in the FOUR region decrease. Conversely, during La Niña-like conditions, the YFT and BET catches in the FOUR region increase while those in the FSM region decrease. These opposing catch-related ocean conditions suggest that the habitat of tuna (the catch-favorable ocean condition) in the WCP has a zonal fluctuation, contracting westward during El Niño-like conditions and expanding eastward during La Niña-like conditions (Lehodey et al., 1997; Lehodey, 2000; Lu et al., 2001; Gouriou & Delcroix, 2002; Leung et al., 2019). As a result of this zonal expansion and contraction of fishing ground, catch amounts of the YFT and the BET in the FOUR may increase during La Niña-like conditions and increase in the FSM

during El Niño-like conditions (Figure 3.16). This suggests that the ENSO plays a role in the tuna catches in the FSM and the FOUR through zonal habitat (fishing ground) shifts (Lehodey et al., 1997; Lehodey et al., 2011).

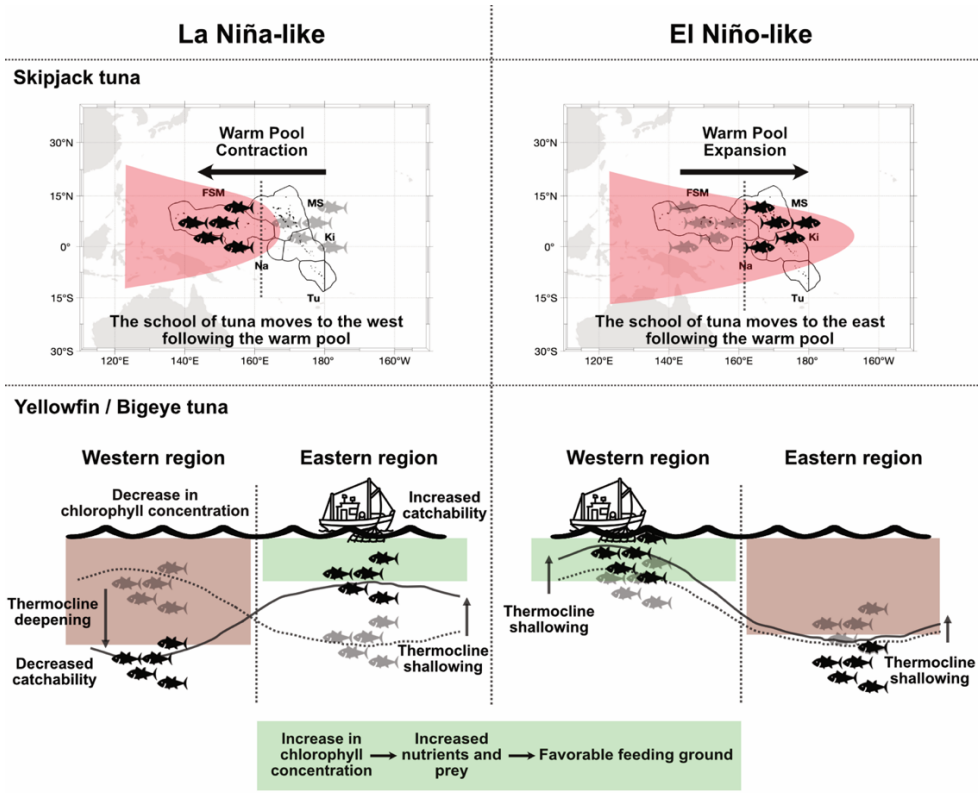

Figure 3.16 Schematic representation of the shift in habitat of the SKJ, YFT, and BET and the corresponding warm pool, thermocline depth and CHL anomalies during ENSO-like ocean conditions. The left panel depicts La Niña-like ocean conditions while the right panel shows El Niño-like ocean conditions. Arrows indicate the direction of vertical tuna habitat movement.

The ocean environment in the EEZ of the FSM exhibits higher temporal variability in subsurface temperature and the CHL compared to the EEZ of the FOUR (Figure 3.5). This is also reflected in the overall R-squared values for environmental variables (Figure 3.8), which tend to be higher in the FSM than in the FOUR. This may suggest that regions with higher environmental variability have a stronger ability to predict and explain variations in the catches using ocean environmental variables (Kim and Na, 2022). The use of different fishing techniques has little effect on tuna catches within the EEZ of the FSM (Figure 3.13). However, it may be challenging to explain the catches using the LL method in the EEZ of the FOUR (Figure 3.14), possibly due to the low quantities of tuna caught by this method (e.g., the YFT in the FOUR) and the relatively stable ocean condition in the FOUR.

The BET has higher overall R-squared values than the YFT and the SKJ among ocean environmental variables (Figure 3.8), indicating that it may be more sensitive to temporal ocean environmental variability. It is worth noting that each tuna species may have distinct responses and sensitivities to ocean environmental variability and that catch amounts may also be influenced by the fluctuation and movement of their prey, which is related to ocean conditions (Schaefer & Fuller,

2005; Senina et al., 2018). Further studies could benefit from defining the dynamics between each tuna species and ocean environmental variability based on the response of the prey during specific ocean conditions.

It is worth noting that each tuna species may have distinct responses and sensitivities to ocean conditions and that catch amounts may also be influenced by the fluctuation and movement of their prey, which is related to ocean conditions (Schaefer & Fuller, 2005; Senina et al., 2018). Although the ocean environmental variables perform good at prediction, relying on these variables would not always be the best option for an operational application because of their limited availability and/or accuracy over longer time periods. An alternative option would be to obtain a statistical relationship between the ocean environmental variables from the long-term best available dataset and then apply the relationship to predict the target tuna catch variability. Moreover, further studies could benefit from defining the dynamics between each tuna species and ocean environmental variables based on the response of the prey during specific ocean conditions.

3.5. Conclusions

This chapter investigates the relationship between ocean environmental variability in the equatorial Pacific and the tuna catches (skipjack, yellowfin, and bigeye tuna) in the WCP. This chapter shows the favorable ocean conditions of the annual catch amounts of the SKJ, the YFT, and the BET in the WCP region. The habitat of the YFT and the BET in the WCP may expand eastward during La Niña-like conditions and contract westward during El Niño-like conditions, resulting in a negative relationship between the catches in the FSM and the FOUR. However, previously observed zonal differences in ocean conditions for an increase in SKJ catches in the WCP are not evident in recent decades, which may be due to the eastward expansion of the warm pool as a result of warm pool expansion in recent years.

The region with relatively high ocean environmental variability exhibits higher levels of explanation and predictability of the catches using ocean environmental variables. The use of different fishing techniques has little effect on the catches within the EEZ of the FSM. However, it may be challenging to explain the catches using the LL method in the EEZ of the FOUR, possibly due to the low quantities of tuna caught by this method (e.g., the YFT in the FOUR) and the

relatively stable ocean environmental variability in the FOUR.

The statistical relationships observed in this chapter between tuna catches and ocean environmental variability in the equatorial Pacific have significant implications for the sustainable management of tuna fisheries in the WCP. These findings can be used to make informed predictions and implement effective strategies for the long-term sustainability of tuna fisheries in the WCP in the context of climate change.

4. Potential predictability of the tuna catches in the Western Central Pacific

4.1. Introduction

The ENSO events have a significant impact on the spatial distribution of skipjack tuna (SKJ) catches in the Western Central Pacific (WCP), as evidenced by their habitat expansion towards the east during El Niño and contraction towards the west during La Niña (Lehodey et al., 1997). Given that the EEZ of the Federated States of Micronesia (FSM) is situated in the western region of the WCP, SKJ catches in FSM are expected to increase (decrease) when the warm pool shift westward (eastward) during La Niña (El Niño) events (Lehodey et al., 1997).

If this ENSO-dependent availability of SKJ catches in the WCP is robust on an interannual time scale, then the annual catch in the WCP should have a significant correlation with ENSO indices. However, the catch amounts of the FSM show insignificant correlation coefficients of -0.30 with the Southern Oscillation index and 0.11 with the multivariate ENSO index during 1990-2014. Correlations with the Niño 3, Niño 3.4, and Niño 4 indices are also insignificant, with correlation coefficients of -0.23, 0.25, and 0.03, respectively. This suggests that

the catch amounts of SKJ cannot be explained by analyzing their relationship with ENSO indices alone. Instead, it is necessary to investigate the connection between the ENSO-related ocean environment and the catch amounts of SKJ.

This chapter examines the interannual relationship between SKJ catches in the FSM, the western part of the WCP, and the equatorial Pacific. Statistical analysis is used to examine the relationship between SKJ catches in the FSM and ocean environmental variables, including temperature, current velocity, salinity, and precipitation on the interannual time scale. Finally, the catch amounts of SKJ in the FSM is presented to be potentially predictable on an interannual time scale based on the statistical relationship between the catch amounts and ocean environmental variables in the equatorial Pacific.

4.2. Materials and methods

The annual catches of SKJ in the EEZ of the FSM from 1990 to 2014 were obtained from Sea Around Us (SAU, http://www.seaaroundus.org), which combines officially reported data from the Food and Agriculture Organization of the United Nations ((http://www.fao.org/fishery/statistics/en), as well as estimates of unreported catches and major discards (Vali et al., 2014; Derrick et al., 2020). The EEZ-based annual dataset was compared to a spatially gridded monthly dataset provided by the WCPFC. The autocorrelations of the SKJ catches in the FSM, which is the target time series for evaluating potential predictability, show a significant decrease over time (Figure 4.1). The e-folding time scale over the period 1990-2014 is approximately one year.

Monthly mean values of upper-ocean (5-200 m) temperature and salinity were acquired from EN4.1.1, and those of current velocity were obtained from Simple Ocean Data Assimilation (SODA) 3.4.2. Surface precipitation data were obtained from CPC Merged Analysis of Precipitation (CMAP). The EN4.1.1 dataset is spatially gridded based on quality-controlled in situ vertical profiles of temperature and salinity. The SODA 3.4.2 dataset is a reanalysis product with ERA-Interim forcing and the National Oceanic and Atmospheric

Administration (NOAA)/Geophysical Fluid Dynamics Laboratory CM2.5 coupled model. The CMAP dataset is a merged product of precipitation estimates from satellites, gauges, and NCEP/NCAR reanalysis. All ocean environmental datasets were analyzed from 1990 to 2014 over the equatorial Pacific Ocean (30° S-30° N, 100° E-60° W) to determine the statistical correlations between the ocean environmental variability and the catch amounts of the SKJ.

The ocean environmental variables are analyzed using CSEOF analysis (Kim et al., 1996; Kim and North, 1997; see Appendix). Regression analysis is then used to investigate the physical relationship between the target and predictor variables and to extract the spatial patterns that correspond to their physical evolution. The prediction was conducted by using the statistical relationship α_m during the learning period, L, within the total length of the time series of the regression analysis. The learning period, L is 24, 23, and 22 years (1990-2013, 1990-2012, and 1990-2011) years and the prediction period, P is 1, 2, or 3 years (2014, 2013-2014, and 2012-2014), respectively (Kim, 2000; see Appendix). The number of modes that were used in the regression was set to 10. Note that the regression error during the learning period would be reduced by increasing the number of modes used for the regression (i.e., a greater

m), but this does not guarantee better predictive accuracy during the predictive period, P.

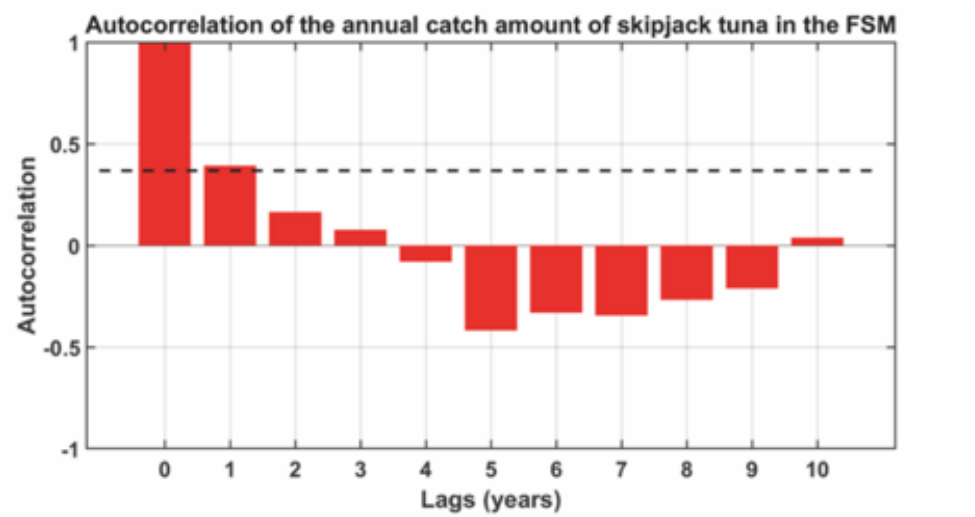

Figure 4.1 The autocorrelations of the annual mean catch amount of the FSM during 1990–2014.

4.3. Results

Figure 4.2 exhibit the R-squared values of ocean environmental variables at different depths regressed onto the SKJ catches in the FSM during 1990-2014 without detrending. Generally, temperature and salinity show higher R-squared values in comparison to those of current velocity. The subsurface temperature at approximately 100 m and near-surface salinity present stronger statistical relationships with the target time series, and the interannual variability of SKJ catches in the FSM. Note that the near-surface temperature exhibits lower R-squared values than the subsurface temperature and surface salinity. The different depths of maximum R-squared values for different variables suggest that the regression results can be a reflection of both/either the favorable habitat of SKJ and/or the representability of the particular variable at a particular depth.

Figure 4.3 shows the reconstructed anomalies of 100 m temperature, 60 m current velocity, 5 m salinity, and surface precipitation regressed onto the SKJ catches in the FSM during 1990-2014 without detrending. Thus, the spatial patterns in Figure 4.3 are related to the interannual variability of the SKJ catches in the FSM with the corresponding R-squared values. The depths of each variable (except precipitation) are chosen to be displayed based on their high

R-squared values (100 m temperature 0.75; 60 m current velocity: 0.53; 5 m salinity: 0.77; precipitation: 0.55). 100 m temperature anomalies show positive values in the western to central equatorial Pacific and negative values in the eastern equatorial Pacific (Figure 4.3). Regression results indicate that under these La Niña-like ocean conditions (McPhaden and Picaut, 1990; Picaut et al., 1996), tuna catches increase in the FSM. The 60 m current velocity shows westward anomalies along the equator, also indicating La Niña-like conditions. Negative anomalies of the 5 m salinity in the western equatorial Pacific and positive anomalies in the eastern equatorial Pacific suggest a westward shift of the ITCZ associated with La Niña (Figure 4.3) (Choi et al., 2015). The westward shift of the ITCZ can also be seen in precipitation anomalies, which show consistent spatial patterns similar to those of 5 m salinity. All of these ocean environmental variables at different depths are independently regressed on the annual catches of SKJ in the FSM and show La Niña-like ocean conditions, suggesting that the interannual variability in tuna catches is associated with ENSO-like variability.

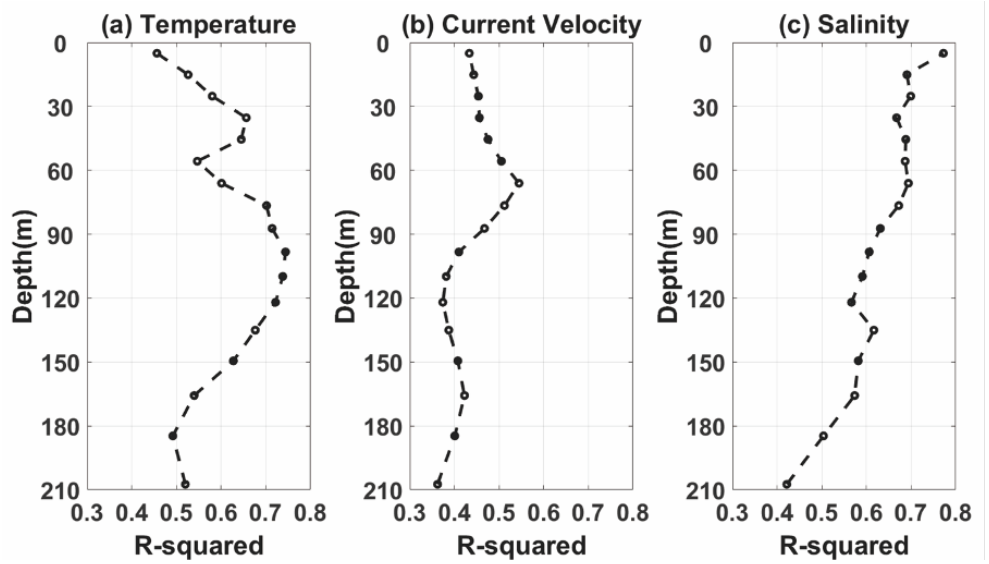

Figure 4.2 R-squared values of the regression at each depth with respect to the SKJ catches in the FSM from 1990 to 2014 for (a) temperature, (b) current velocity, and (c) salinity.

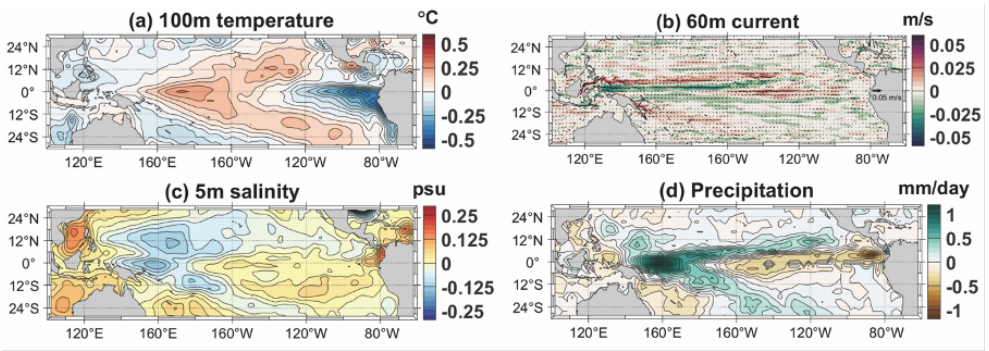

Figure 4.3 Regressed and reconstructed anomalies of ocean environmental variables in the equatorial Pacific Ocean with respect to the SKJ catches in the FSM from 1990–2014: (a) temperature at 100 m, (b) current velocity at 60 m (shading: zonal velocity), (c) salinity at 5 m, and (d) precipitation.

The statistical relationship between SKJ catches in the FSM and ENSO-like variability (Figure 4.3) can be used to predict the amount of catch given information about the ocean environment, specifically the 100 m temperature or 5 m salinity in the equatorial Pacific. Figure 4.4 shows the regression results for the 25 years of the data set (1990-2014). The correlation coefficients between the observed annual catches and those estimated from 100 m temperature and 5 m salinity are 0.87 and 0.88, respectively. By performing the regression analysis of temperature or salinity on the catch for a limited period (i.e., shorter than the total length of the dataset), called the learning period, the catch for the remaining years can be predicted and the performance for the prediction years can be evaluated. Figure 4.4b-d shows the regression relationship obtained from different learning periods and their application for annual predictions up to 3 years. The 1-year prediction based on the regression relationship for a 24-year learning period (Figure 4.4b) shows plausible results; the correlation coefficients for the entire period (24-year prediction plus 1-year prediction) based on 100 m temperature and 5 m salinity are 0.84 and 0.83, respectively. Predictions based on 23- and 22-year learning periods also show acceptable results, although the actual values are higher than the predicted catch amounts (Figure 4.4c-d).

Also, the regression coefficients of each mode of 5 m salinity and 100 m temperature show no significant change during the different learning periods (Table 4.1-2), which indicates that the main ocean variability that explains the variability of tuna catch amounts does not change even if the learning period is different. Therefore, it suggests the robustness of the statistical prediction using the ocean environmental variables.

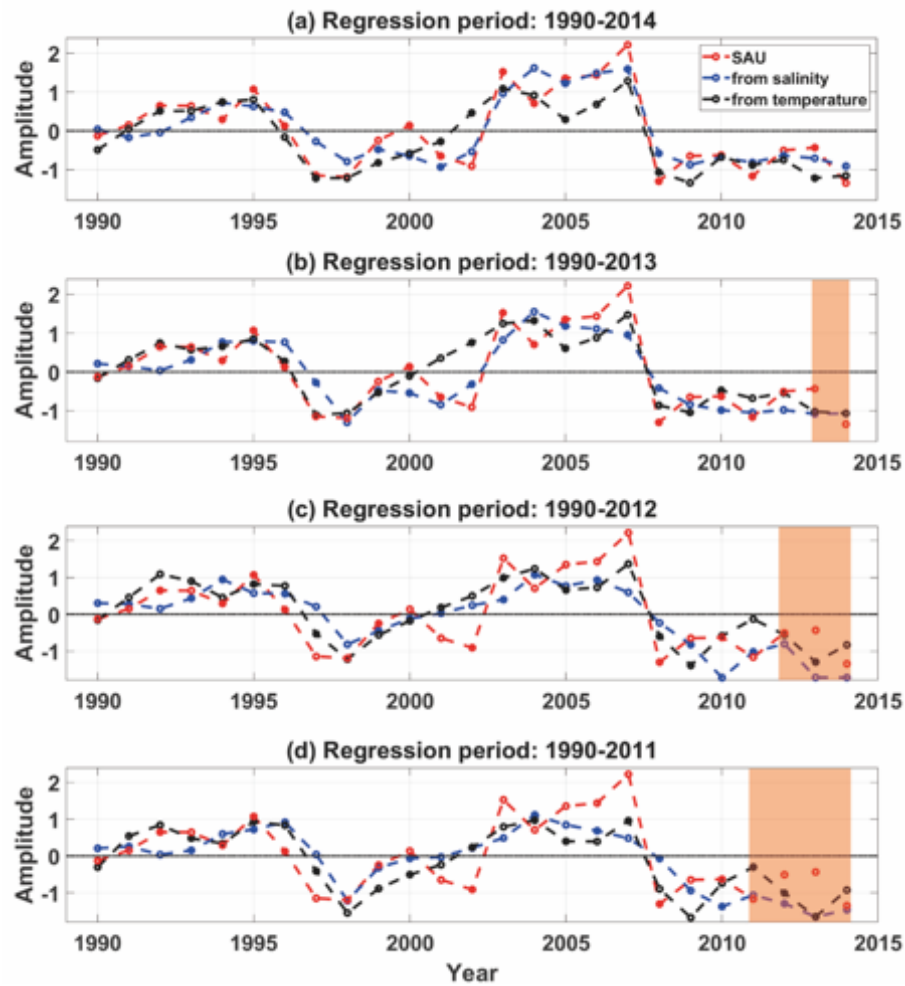

Figure 4.4 Observed (red), estimated and predicted annual catch amount of SKJ in the FSM based on the relationship with the 5 m salinity (blue) and 100 m temperature (black): (a) regression during 1990–2014, (b) regression during 1990–2013 and prediction for 2014, (c) regression during 1990–2012 and prediction for 2013–2014, and (d) regression during 1990–2012 and prediction for the 2012–2014 period. The prediction period is shaded in orange.

Table 4.1 Regression coefficients of each mode of 5 m salinity to the catch amounts of SKJ in the FSM during the learning period.

	Mode 1	Mode 2	Mode 3	Mode 4	Mode 5	Mode 6	Mode 7	Mode 8	Mode 9	Mode 10
1990-2018	0.387	0.256	0.150	0.270	0.034	0.268	0.291	0.109	0.136	0.286
1990-2017	0.356	0.284	0.147	0.312	0.032	0.290	0.325	0.106	0.164	0.329
1990-2016	0.347	0.280	0.167	0.300	0.035	0.281	0.314	0.093	0.156	0.336
1990-2015	0.323	0.277	0.165	0.317	0.006	0.276	0.307	0.098	0.160	0.335

Table 4.2 Regression coefficients of each mode of 100 m temperature to the catch amounts of SKJ in the FSM during the learning period.

	Mode 1	Mode 2	Mode 3	Mode 4	Mode 5	Mode 6	Mode 7	Mode 8	Mode 9	Mode 10
1990-2018	0.077	0.056	0.071	0.283	0.328	0.235	0.377	0.147	0.320	0.134
1990-2017	0.097	0.021	0.006	0.285	0.373	0.314	0.429	0.134	0.306	0.208
1990-2016	0.079	0.014	0.021	0.300	0.357	0.358	0.365	0.223	0.263	0.179
1990-2015	0.094	0.030	0.064	0.270	0.369	0.310	0.404	0.234	0.234	0.269

The FSM region experienced abrupt changes in SKJ catches during the 2007-2008 period, suggesting that predictability using statistical relationships between the catches and ocean environmental variables may be low during this period. To investigate the continued potential predictability of SKJ catches based on ocean environmental variables, several learning periods were established before and after the catch reduction period. The learning periods consisted of 1990-2007/1990-2008/1990-2009, and subsequent predictions were conducted for durations of 3 years (2008-2010)/2 years (2009-2010)/1 year (2010) (Figure 4.5). Using 5m salinity and 100m temperature, the potential predictability of SKJ catches in the FSM region was assessed. The correlation coefficients between the target SKJ catch and the predicted SKJ catch were found to be 0.81 and 0.75 (for 5m salinity and 100m temperature, respectively) based on the 1990-2009 learning period, 0.79 and 0.76 for the 1990-2008 learning period, and 0.74 and 0.73 for the 1990-2007 learning period. These prediction results indicate the existence of potential predictability for SKJ catches during periods of sudden catch changes when using ocean environmental variables over 3 years.

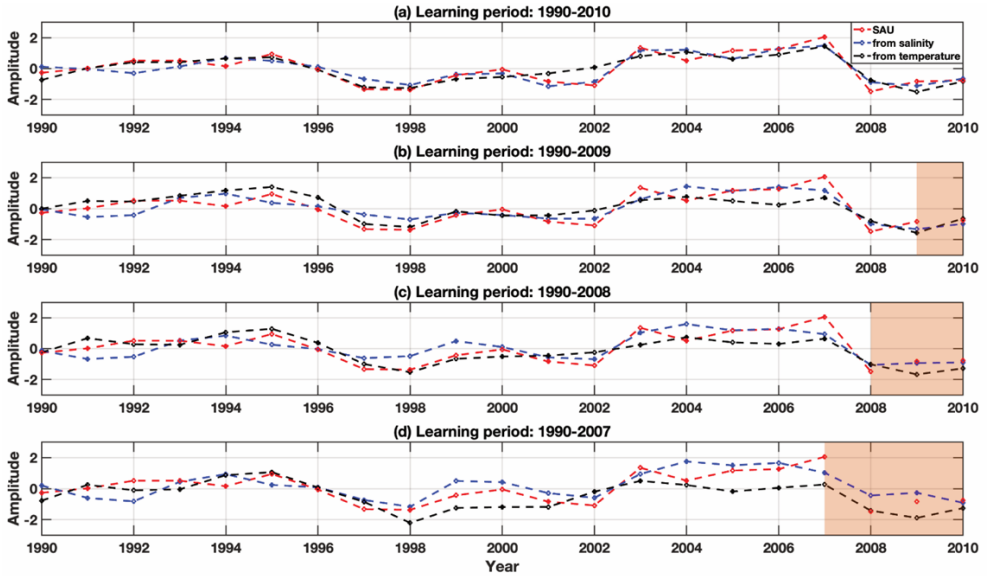

Figure 4.5 Observed (red), estimated, and predicted annual catch amount of SKJ in the FSM based on the relationship with the 5 m salinity (blue) and 100 m temperature (black): (a) regression during 1990–2010, (b) regression during 1990–2009 and prediction for 2010, (c) regression during 1990–2008 and prediction for 2009–2010, and (d) regression during 1990–2007 and prediction for the 2008–2010 period. The prediction period is shaded in orange.

Similar to the bootstrap method, the potential predictability was examined by excluding the intermediate 3 years (2007-2009)/5 years (2006-2010) during the learning period (Figure 4.6). The 5m salinity and 100m temperature were also used to estimate the potential predictability of SKJ catches in the FSM. The correlation coefficients between the target SKJ catch and the predicted SKJ catch were found to be 0.82 and 0.75 (for 5m salinity and 100m temperature, respectively) based on the 1990-2006 and 2007-2009 learning period and 0.85 and 0.61 for the 1990-2005 and 2011-2014 learning period. It suggests that despite the exclusion of the intermediate data, the potential predictability of SKJ catch in FSM was evident using ocean environment variables.

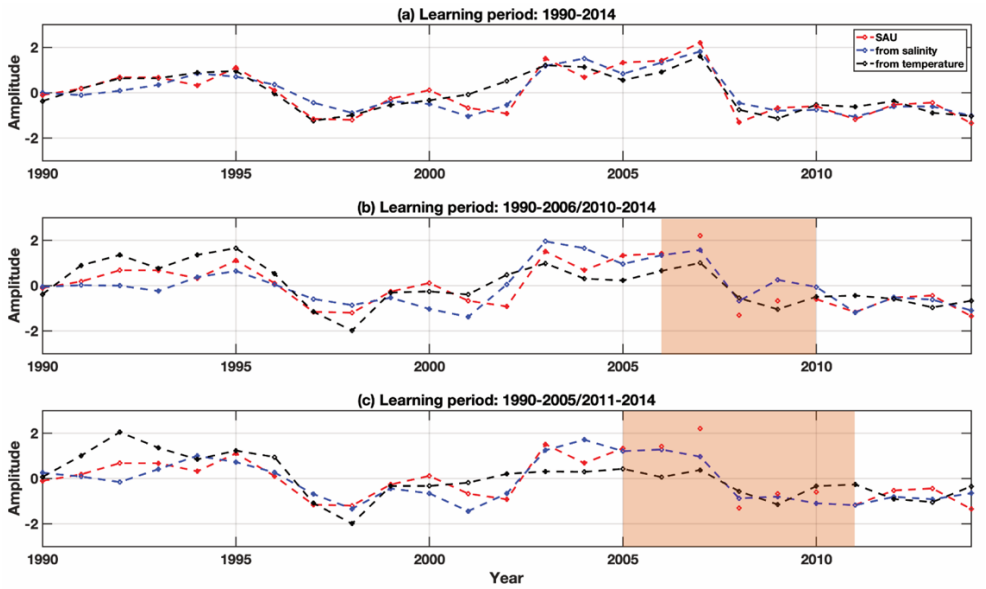

Figure 4.6 Observed (red), estimated, and predicted annual catch amount of SKJ in the FSM based on the relationship with the 5 m salinity (blue) and 100 m temperature (black): (a) regression during 1990–2014, (b) regression during 1990–2006 and 2010–2014 and prediction for 2007–2009 and (c) regression during 1990–2005 and 2011–2014 and prediction for 2006–2010 period. The prediction period is shaded in orange.

4.4. Discussion

One of the most successful fishing grounds for SKJ is located in the convergence zone between the warm pool and equatorial upwelling in the central Pacific where the warm, low-salinity water and the cold, saline water converge in the upper ocean. It should be pointed out that, however, this analysis is not based on a prior understanding of the physiological conditions of SKJ caught in the equatorial Pacific. Rather, the higher R-squared values of the specific variables at specific depths (Figure 4.2) suggest that they would be associated with favorable conditions for SKJ, for example, regions with enhanced availability of food, sufficient plankton, and an accumulation of preferred prey. The warm pool, however, is known to be oligotrophic with low chlorophyll and primary production, which can be counter-intuitive. Studies have indicated that chlorophyll may be advected to the warm pool region by the westward current during the transition phase of the ENSO in the equatorial Pacific. Regression analysis of surface chlorophyll, conducted only from 1998 to 2014 only due to the shorter length of the available chlorophyll dataset, indeed exhibits relatively high R-squared values of 0.76 (not shown). This suggests that sea surface chlorophyll variability could also be a potential predictor when longer data is available to obtain a robust statistical relationship.

The predictability of SKJ catches in the FSM was estimated by utilizing the statistical relationships between ocean environmental variables, specifically upper ocean temperature, and salinity, and SKJ catches in the FSM, which represents ENSO-like variability (Figure 4.3). In particular, the ENSO-like variability represented by 100 m temperature and 5 m salinity in the equatorial Pacific showed significant predictability for the annual catch in the FSM over several years, with a learning period of over 20 years (Figure 4.4).

To evaluate the possibility of predicting abrupt changes in SKJ catch in the FSM region during 2007-2008, different learning periods were established both before and after the catch reduction period (Figure 4.5). The learning periods included 1990-2007/1990-2008/1990-2009, and predictions were made for 3 years (2008-2010)/2 years (2009-2010)/1 year (2010), respectively. By analyzing ocean variables such as 5m salinity and 100m temperature, the potential predictability of SKJ catches in the FSM region was evaluated. The results indicated a high level of predictability, especially when predicting changes over 3 years following sudden variations in SKJ catches. Similarly, predictability was examined by excluding the intermediate 3 years (2007-2009)/5 years (2006-2010) during the learning period (Figure 4.6). The potential predictability of SKJ catch

in FSM using ocean environmental variables was evident despite the exclusion of intermediate data. Therefore, utilizing the relationship between the catches and ocean environmental variables demonstrates strong predictive performance for future tuna catches.

Most of the climate indices associated with ENSO are computed using sea surface temperature. Notably, the low correlation, thus low predictability, between the single ENSO indices and the catch amount is explained by the lower R-squared values of the sea surface temperature compared to those of the subsurface temperature. The higher R-squared values of the subsurface temperature compared to that of surface temperature would be partly due to the larger temporal variability of the subsurface temperature. The smaller amplitude of temperature anomalies at the sea surface may not be great enough to induce physiological or behavioral responses of the SKJ. Indeed, the surface salinity exhibits a larger temporal variability and a higher R-squared value with the catch amount compared to the subsurface salinity. Furthermore, this chapter highlights that surface salinity can provide a better basis for predicting the SKJ catch amount in the FSM than the surface temperature, possibly because the amplitude of sea surface temperature anomalies tends to decrease rapidly due to active heat exchanges between the ocean and the atmosphere.

4.5. Conclusions

This chapter focused on evaluating the potential predictability of SKJ catches in the WCP region using statistical relationships with ocean environmental variables. The results revealed a strong statistical relationship between SKJ catches and ENSO-like ocean conditions, specifically the contraction of the warm pool during La Niña-like periods. This chapter used ocean variables such as 5 m salinity and 100 m temperature as potential predictors, which showed better predictability for SKJ catches in the FSM compared to ENSO indices based on sea surface temperature.

Although a statistical relationship generally becomes more robust when the analysis is conducted using a longer dataset, the inclusion of catch data prior to 1990s is not helpful for increasing the predictability. This is because temporal changes in the anthropogenic effect, which are not depicted in the ocean environment, would be larger. However, if the anthropogenic effect is something that is depicted in the ocean environment (e.g. if the temperature and salinity variability related to the SKJ catches somehow occurs more frequently in the future induced by the anthropogenic effect), then the prediction would tell the catch amount of SKJ would increase in the FSM.

The predictability presented in this chapter is based on the statistical relationship established between annual catches and ocean environmental variability in the equatorial Pacific. Future predictions can be made if future ocean environmental data are available, particularly for the equatorial Pacific, although the quality and perspectives of such data may vary. Extending the time series of ocean environmental variables using methods such as autoregressive modeling can improve prediction capabilities. The accuracy of predictions depends primarily on the extent to which the selected variables represent the ocean environmental variability associated with the target variability, assuming that SKJ abundance is adequately represented by the target time series.

It is important to acknowledge that the presence of anthropogenic effects, such as illegal fishing, may affect the SKJ population and introduce regression errors into the predictions, as the target time series may not fully capture the natural variability in catch amounts. However, the statistical significance of the regression relationship established in this study indicates that the target time series can effectively represent the variability of SKJ during the learning period.

Overall, the statistical relationships identified in this study provide

a solid foundation for making informed predictions and developing effective strategies for the long-term sustainable management of tuna fisheries in the WCP region. By considering the complex interactions between SKJ and ocean environmental variables, stakeholders can make informed decisions and adapt their approaches to the challenges posed by climate change and anthropogenic impacts in the future.

5. Conclusions

The suitability of tuna habitats is determined by a variety of factors, including the availability of food sources and the physical characteristics of the ocean environment. The availability of food sources, such as plankton and preferred prey plays a role in the distribution of tuna in the oceans. Temperature, depth, and oxygen concentrations are among the important environmental variables that affect habitat suitability for tuna. The ocean currents and vertical mixing are also related to the habitat. However, each tuna species has specific physiological requirements that influence its habitat preferences.

The primary objective of this dissertation is to investigate the relationship between ocean environmental variables and the catch amounts of three tuna species (the SKJ, YFT, and BET) in different regions of the tropical oceans. The statistical relationships between ocean environmental variables and annual catches of tuna are presented using regression and reconstruction analysis. The results of this dissertation highlight that the climate variability, including the ENSO, plays an important role in influencing the horizontal and vertical distribution of tuna and, in turn, the catch amount.

Both in the SWTIO and WCP, chlorophyll concentration increases at certain depths when the YFT and BET catch increase, indicating enrichment of biological factors associated with tuna (nutrients, prey, etc.). The increase of chlorophyll concentration is observed at the subsurface in the SWTIO and at the near-surface in the WCP. In the SWTIO, the increase in the subsurface chlorophyll concentration and suppression of upwelling contribute to a vertical extension of the tuna fishery, thus an increase of the YFT and BET catch. However, in the WCP, the increase in chlorophyll concentration from surface to near-surface and enhancement of upwelling (shallowing of thermocline) shift the location of favorable fishing grounds to near-surface and surface, increasing catchability in the WCP (Figure 5.1).

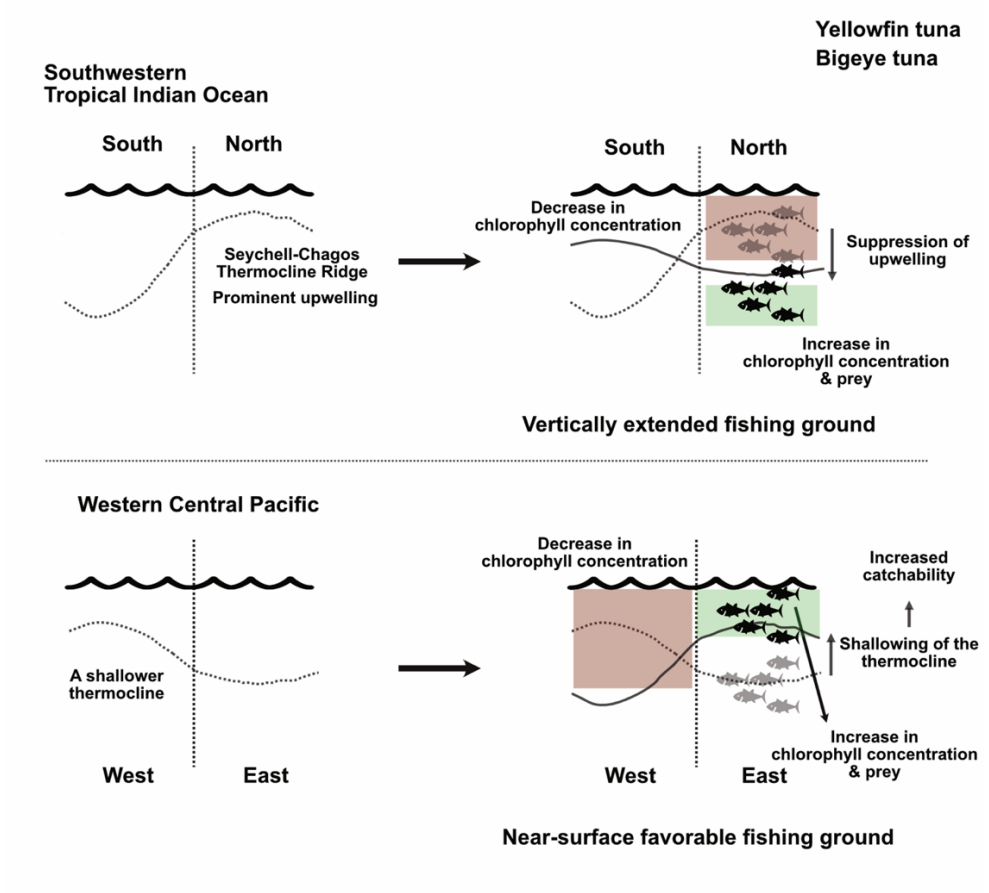

Figure 5.1 Schematics of ocean conditions during an increase in yellowfin and bigeye tuna catches in the northern region of the southwestern tropical Indian Ocean and the eastern region of the western central Pacific. Dotted lines indicate the mean thermocline depth and black lines indicate the thermocline depth during an increase in tuna catches. Vertical dashed lines indicate the boundaries of the regions. Green and brown shading indicate the positive and negative chlorophyll concentration anomaly, respectively, during an increase in tuna catches.

This dissertation also presents how much variability of the annual catch amount can be explained and predicted based on the relationship with ocean conditions. The results indicate that regions with higher environmental variability are more effective in explaining and predicting variations in tuna catch. However, it is difficult to identify favorable ocean conditions for the catches in regions with low variability in the ocean environmental variables. More studies are required to fully understand the complex relationship between ocean environmental variables and catch amounts, especially in the areas where the environmental variability is relatively weak.

In the tuna fishery, the IOTC and the WCPFC implement species-specific quotas to reduce the overfishing. Therefore, it is important to examine whether these quotas have an impact when examining the relationship between the ocean environment and catch data. If the anthropogenic effects of species-specific quotas outweigh the natural variability, regression analyses would be expected to have low explainability. However, the regression showed statistically significant R-squared values in both the SWTIO and the WCP regions. This suggests that the anthropogenic effects such as the quota system did not significantly affect the results of this dissertation.

The available data, which includes information from the SAU and WCPFC, lacks specific details on the use of certain types of fishing gear, such as fish aggregating devices (FADs). The FADs play an important role in the tuna fishery as a means of increasing fishing efficiency and reducing operating costs (Morgan, 2011). This reliance on FADs can be attributed to the migratory nature of tuna, as they travel long distances, making them difficult to track and catch. By strategically positioning their nets and lines near FADs, tuna vessels can achieve significant improvements in catch rates and reduce time at sea, ultimately increasing CPUE.

However, this reliance on FADs poses a challenge in explaining the variability of tuna catches based on natural variability in the ocean environment. Therefore, in order to fully understand the variability of the catches, it is essential to first assess the potential impact of anthropogenic factors associated with the deployment of FADs. It should be noted that, due to the lack of data, this dissertation confirms the limited anthropogenic impact of quotas and the use of specific fishing gears on tuna catches only using statistical methods. If the use of a particular fishing gear had a significant impact on the catch, it would be expected to reduce the explainability of the catches using ocean environmental variables. However, the R-squared values in the

regression analysis using the ocean environmental variables are statistically significant in the target regions of this dissertation. Future studies are recommended to use numerical models for a more comprehensive confirmation of the effects of anthropogenic impacts on tuna fisheries.

The relationship between SKJ catches in the WCP and ocean environmental variables in this dissertation is statistically robust. Chapter 3 examined catch data from 1990 to 2018 to investigate the ocean conditions that are associated with the increase in SKJ catches in the FSM region. Chapter 4 examined catch data from 1990 to 2014 in the FSM region to evaluate the predictability of SKJ catches. The four-year difference in data coverage between the two studies was considered to evaluate its impact on the results. Both studies showed the presence of La Niña-like ocean conditions during periods of increased SKJ catches in the FSM region from 1990 to 2014 and 1990 to 2018, respectively. Despite the data gap, the two studies exhibit similar results, indicating a statistically robust relationship between SKJ catches and ENSO in the FSM region. Therefore, assuming no future changes in the ocean environment that differ from current conditions, the favorable ocean conditions and potential predictability of SKJ catches in the FSM region are expected to continue.

The La Niña occurred from the late 2010s through 2022. If the robust relationship between ocean conditions and tuna continues beyond 2018, then certain trends would be expected. Specifically, in the northern region of the SWTIO, there would be a decreasing trend in YFT and BET catches from the late 2010s through 2022 (L' Heureux_2019; Li et al., 2022). In contrast, the western/eastern region of the WCP would experience an increase/decrease in SKJ catches and a decrease/increase in YFT and BET catches during the same period. Given the predicted transition from La Niña to El Niño in 2023 (NOAA, n.d.), YFT and BET catch are expected to increase in the northern region of the SWTIO and the western region of the WCP in 2023.

This study uses statistical methods to examine the relationship between the catches and ocean environmental variables. While these methods effectively capture the favorable ocean conditions associated with catch variability, they do not provide insight into the specific habitat suitability for particular tuna species or allow forecasting of future habitat distribution. Alternative methods such as the maximum entropy method and the habitat suitability index have been used in various studies to model the geographic distribution of species (Phillips et al., 2006) and to assess habitat quality and make

predictions (Chen et al., 2008). In addition to the statistical methods used in this study, the incorporation of different modeling approaches proves beneficial in understanding the tuna fishery by exploring the relationship between ocean environment and fishery, as well as examining habitat variability driven by surrounding environmental factors.

Previous studies have highlighted the potential impact of future ocean conditions influenced by ongoing global warming on extreme ENSO events (Grothe et al., 2020; Cai et al., 2021). This dissertation examines the robust statistical relationship between ocean conditions and the catches, even in the presence of extreme ocean variability. Consequently, the study expects a corresponding variability in catch amounts within the SWTIO and WCP regions. The results gained from this dissertation will facilitate the development of effective management strategies and accurate projections of future tuna populations and yields, allowing for informed decision-making. These findings will help protect and conserve tuna populations in the face of changing ocean conditions and climate change, ensuring their long-term sustainability.

References

Abascal, F., Peatman, T., Leroy, B., Nicol, S., Schaefer, K., Fuller, D., & Hampton, J. (2018). Spatiotemporal variability in bigeye vertical distribution in the Pacific Ocean. Fisheries Research, 204, 37–79.

Andutta, F. P., de Miranda, L. B., Franca Schettini, C. A., Siegle, E., da Silva, M. P., Izumi, V. M., & Chagas, F. M. (2013). Temporal variations of temperature, salinity and circulation in the peruipe river estuary (nova vicosa, ba). Continental Shelf Research, 70, 36–45. doi:10.1016/j.csr.2013.03.013

Aoki, Y., Aoki, A., Ohta, I., & Kitagawa, T. (2020). Physiological and behavioural thermoregulation of juvenile yellowfin tuna Thunnus albacares in subtropical waters. Marine Biology, 167(6), 71.

Ashida, H., Tanabe, T., & Suzuki, N. (2009). Recent progress on reproductive biology of skipjack tuna in the tropical region of the Western and Central Pacific Ocean. Scientific Comitte Fifth Regular Session, Port Vila, Vanuatu.

Behrenfeld, M. J., Randerson, J. T., McClain, C. R., Feldman, G. C., Los, S. O., Tucker, C. J., Falkowski, P. G., Field, C. B., Frouin, R., & Esaias, W. E. (2001). Biospheric primary production during an ENSO transition. Science, 291(5513), 259–597.

Bell, J. D., Reid, C., Batty, M. J., Lehodey, P., Rodwell, L., Hobday, A. J., Johnson, J. E., & Demmke, A. (2013). Effects of climate change on oceanic fisheries in the tropical Pacific: implications for economic development and food security. Climatic change, 119, 19–12.

Bertignac, M., Lehodey, P., & Hampton, J. (1998). A spatial population dynamics simulation model of tropical tunas using a habitat index based on environmental parameters. Fisheries Oceanography, 7(3-4), 32–34.

Boistol, L., Harper, S., Booth, S., & Zeller, D. (2011). Reconstruction of marine fisheries catches for Mauritius and its outer. Fisheries Centre Research Reports, 19(4), 39.

Bosc, C., Delcroix, T., & Maes, C. (2009). Barrier layer variability in the western Pacific warm pool from 2000 to 2007. Journal of Geophysical Research: Oceans, 114(C6).

Boyce, D. G., Tittensor, D. P., & Worm, B. (2008). Effects of temperature on global patterns of tuna and billfish richness. Marine Ecology Progress Series, 355, 26–76.

Brander, K. M. (2007). Global fish production and climate change. Proceedings of the National Academy of Sciences, 104(50), 1970–9714.

BRILL, R. W. (1994). A review of temperature and oxygen tolerance studies of tunas pertinent to fisheries oceanography, movement models and stock assessments. Fisheries Oceanography, 3(3), 20–16.

Brill, R. W., Bigelow, K. A., Musyl, M. K., Fritsches, K. A., & Warrant, E. J. (2005). Bigeye tuna (Thunnus obesus) behavior and physiology and their relevance to stock assessments and fishery biology. Col. Vol. Sci. Pap. ICCAT, 57(2), 14–61.

Brill, R., Block, B., Boggs, C., Bigelow, K., Freund, E. V., & Marcinek, D. J. (1999). Horizontal movements and depth distribution of large adult yellowfin tuna (Thunnus albacares) near the Hawaiian Islands, recorded using ultrasonic telemetry: implications for the physiological ecology of pelagic fishes. Marine Biology, 133, 39–08.

Cai, W., Santoso, A., Collins, M., Dewitte, B., Karamperidou, C., Kug, J.-S., Lengaigne, M., McPhaden, M. J., Stuecker, M. F., & Taschetto, A. S. (2021). Changing El Niño–Southern oscillation in a warming climate. *Nature Reviews Earth & Environment*, *2*(9), 628-644.

Carton, J. A., Chepurin, G. A., & Chen, L. (2018). SODA3: A new ocean climate reanalysis. Journal of Climate, 31(17), 696–983.

Chen, B., Lin, X., & Bacmeister, J. T. (2008). Frequency distribution of daily ITCZ patterns over the western–central Pacific. Journal of Climate, 21(17), 420–222.

Chen, X., Li, G., Feng, B., & Tian, S. (2009). Habitat suitability index of Chub mackerel (Scomber japonicus) from July to September in the East China Sea. *Journal of Oceanography*, *65*, 93-102.

Choi, K.-Y., Vecchi, G. A., & Wittenberg, A. T. (2015). Nonlinear zonal wind response to ENSO in the CMIP5 models: Roles of the zonal and meridional shift of the ITCZ/SPCZ and the simulated climatological precipitation. Journal of Climate, 28(21), 855–573.

Clarke, A. J., & Van Gorder, S. (2001). ENSO prediction using an ENSO trigger and a proxy for western equatorial Pacific warm pool movement. Geophysical research letters, 28(4), 57–82.

Cravatte, S., Delcroix, T., Zhang, D., McPhaden, M., & Leloup, J. (2009). Observed freshening and warming of the western Pacific warm pool. Climate Dynamics, 33, 56–89.

Dagorn, L., Bach, P., & Josse, E. (2000). Movement patterns of large

bigeye tuna (Thunnus obesus) in the open ocean, determined using ultrasonic telemetry. Marine Biology, 136(2), 36–71.
De Anda-Montañez, J. A., Amador-Buenrostro, A., Martínez-Aguilar, S., & Muhlia-Almazán, A. (2004). Spatial analysis of yellowfin tuna (Thunnus albacares) catch rate and its relation to El Niño and La Niña events in the eastern tropical Pacific. Deep Sea Research Part II: Topical Studies in Oceanography, 51(–), 57–86.
Delcroix, T., & McPhaden, M. (2002). Interannual sea surface salinity and temperature changes in the western Pacific warm pool during 1992–2000. Journal of Geophysical Research: Oceans, 107(C12), SRF –-SRF –7.
Delcroix, T., Cravatte, S., & McPhaden, M. J. (2007). Decadal variations and trends in tropical Pacific sea surface salinity since 1970. Journal of Geophysical Research: Oceans, 112(C3).
Delcroix, T., Henin, C., Porte, V., & Arkin, P. (1996). Precipitation and sea-surface salinity in the tropical Pacific Ocean. Deep Sea Research Part I: Oceanographic Research Papers, 43(7), 112–141.
Derrick, B., Khalfallah, M., Relano, V., Zeller, D., & Pauly, D. (2020). Updating to 2018 the 195–010 marine catch reconstructions of the Sea Around Us. Part II: The Americas and Asia-Pacific.
Evans, K., Langley, A., Clear, N. P., Williams, P., Patterson, T., Sibert, J., Hampton, J., & Gunn, J. S. (2008). Behaviour and habitat preferences of bigeye tuna (Thunnus obesus) and their influence on longline fishery catches in the western Coral Sea. Canadian Journal of Fisheries and Aquatic Sciences, 65(11), 242–443.
Farley, J., Eveson, P., Krusic-Golub, K., Sanchez, C., Roupsard, F., McKechnie, S., Nicol, S., Leroy, B., Smith, N., & Chang, S. (2017). Age, growth and maturity of bigeye tuna in the western and central Pacific Ocean.
Fiedler, P. C., Philbrick, V., & Chavez, F. P. (1991). Oceanic upwelling and productivity in the eastern tropical Pacific. Limnology and oceanography, 36(8), 183–850.
Folland, C., Renwick, J., Salinger, M., & Mullan, A. (2002). Relative influences of the interdecadal Pacific oscillation and ENSO on the South Pacific convergence zone. Geophysical research letters, 29(13), 2—-4.
Food and Agriculture Organization. Review of the state of world marine fishery resources 2011 (2013). Marine resources - Western

Central Pacific. FIRMS Reports. In: Fisheries and Resources Monitoring System (FIRMS). http://firms.fao.org/firms/resource/13333/en

Garcia, H., Weathers, K., Paver, C., Smolyar, I., Boyer, T., Locarnini, M., Zweng, M., Mishonov, A., Baranova, O., & Seidov, D. (2019). World Ocean Atlas 2018, Volume 3: Dissolved Oxygen, Apparent Oxygen Utilization, and Dissolved Oxygen Saturation.

Garnesson, P., Mangin, A., Fanton d'Andon, O., Demaria, J., & Bretagnon, M. (2019). The CMEMS GlobColour chlorophyll a product based on satellite observation: Multi-sensor merging and flagging strategies. Ocean Science, 15(3), 81–30.

Gibbon J., & Galland G. (2020, October 6). Netting Billions 2020: A Global Tuna Valuation. Pewtrust. https://www.pewtrusts.org/en/research-and-analysis/reports/2020/10/netting-billions-2020-a-global-tuna-valuation

Good, S. A., Martin, M. J., & Rayner, N. A. (2013). EN4: Quality controlled ocean temperature and salinity profiles and monthly objective analyses with uncertainty estimates. Journal of Geophysical Research: Oceans, 118(12), 670–716.

Gordon, A. L., Ma, S., Olson, D. B., Hacker, P., Ffield, A., Talley, L. D., Wilson, D., & Baringer, M. (1997). Advection and diffusion of Indonesian throughflow water within the Indian Ocean South Equatorial Current. Geophysical research letters, 24(21), 257–576.

Gouriou, Y., & Delcroix, T. (2002). Seasonal and ENSO variations of sea surface salinity and temperature in the South Pacific Convergence Zone during 1976–2000. Journal of Geophysical Research: Oceans, 107(C12), SRF 1–1–SRF 1–4.

Graham, J. B., & Dickson, K. A. (2004). Tuna comparative physiology. Journal of experimental biology, 207(23), 401–024.

Green, R. E. (1967). Relationship of the thermocline to success of purse seining for tuna. Transactions of the American Fisheries Society, 96(2), 12–30.

Grothe, P. R., Cobb, K. M., Liguori, G., Di Lorenzo, E., Capotondi, A., Lu, Y., Cheng, H., Edwards, R. L., Southon, J. R., & Santos, G. M. (2020). Enhanced El Niño–Southern oscillation variability in recent decades. *Geophysical research letters*, *47*(7), e2019GL083906.

Hampton, J., & Gunn, J. (1998). Exploitation and movements of yellowfin tuna (Thunnus albacares) and bigeye tuna (T. obesus)

tagged in the north-western Coral Sea. Marine and Freshwater Research, 49(6), 47–89.
Harley, S., Williams, P. G., Nicol, S., & Hampton, J. (2013). The western and central Pacific tuna fishery: 2011 overview and status of stocks. Secretariat of the Pacific Community, Ocean Fisheries Programme.
Hermes, J., & Reason, C. (2008). Annual cycle of the South Indian Ocean (Seychelles-Chagos) thermocline ridge in a regional ocean model. Journal of Geophysical Research: Oceans, 113(C4).
Hersbach, H., Bell, B., Berrisford, P., Hirahara, S., Horányi, A., Muñoz-Sabater, J., Nicolas, J., Peubey, C., Radu, R., & Schepers, D. (2020). The ERA5 global reanalysis. Quarterly Journal of the Royal Meteorological Society, 146(730), 199–049.
Juillet-Leclerc, A., Thiria, S., Naveau, P., Delcroix, T., Le Bec, N., Blamart, D., & Corrège, T. (2006). SPCZ migration and ENSO events during the 20th century as revealed by climate proxies from a Fiji coral. Geophysical research letters, 33(17).
Kim, J., & Na, H. (2022). Interannual Variability of Yellowfin Tuna (Thunnus albacares) and Bigeye Tuna (Thunnus obesus) Catches in the Southwestern Tropical Indian Ocean and Its Relationship to Climate Variability. Frontiers in Marine Science, 9.
Kim, J., Na, H., Park, Y.-G., & Kim, Y. H. (2020). Potential predictability of skipjack tuna (Katsuwonus pelamis) catches in the Western Central Pacific. Scientific reports, 10(1), 3193.
Kim, K.-Y. (2000). Statistical prediction of cyclostationary processes. Journal of Climate, 13(6), 109–115.
Kim, K.-Y., & North, G. R. (1997). EOFs of harmonizable cyclostationary processes. Journal of the atmospheric sciences, 54(19), 241–427.
Kim, K.-Y., Hamlington, B., & Na, H. (2015). Theoretical foundation of cyclostationary EOF analysis for geophysical and climatic variables: concepts and examples. Earth-science reviews, 150, 20–18.
Kim, K.-Y., Hamlington, B., & Na, H. (2015). Theoretical foundation of cyclostationary EOF analysis for geophysical and climatic variables: concepts and examples. Earth-science reviews, 150, 20–18.
Kim, K.-Y., North, G. R., & Huang, J. (1996). EOFs of one-dimensional cyclostationary time series: Computations, examples, and

stochastic modeling. Journal of Atmospheric Sciences, 53(7), 100–017.
Kumari, B., Raman, M., Narain, A., & Sivaprakasam, T. (1993). Location of tuna resources in Indian waters using NOAA AVHRR data. International Journal of Remote Sensing, 14(17), 330–309.
L'Heureux, M. (2019). Overview of the 2017–18 La Niña and El Niño Watch in Mid-2018. *Climate Prediction S&T Digest*, 97.
Lan, K. W., Lee, M. A., Chou, C. P., & Vayghan, A. H. (2018). Association between the interannual variation in the ocean environment and catch rates of bigeye tuna (Thunnus obesus) in the Atlantic Ocean. Fisheries Oceanography, 27(5), 39–07.
Lan, K.-W., Chang, Y.-J., & Wu, Y.-L. (2020). Influence of oceanographic and climatic variability on the catch rate of yellowfin tuna (Thunnus albacares) cohorts in the Indian Ocean. Deep Sea Research Part II: Topical Studies in Oceanography, 175, 104681.
Lan, K.-W., Chang, Y.-J., & Wu, Y.-L. (2020). Influence of oceanographic and climatic variability on the catch rate of yellowfin tuna (Thunnus albacares) cohorts in the Indian Ocean. Deep Sea Research Part II: Topical Studies in Oceanography, 175, 104681.
Lan, K.-W., Evans, K., & Lee, M.-A. (2013). Effects of climate variability on the distribution and fishing conditions of yellowfin tuna (Thunnus albacares) in the western Indian Ocean. Climatic change, 119, 6–7.
Langley, A., Harley, S., Hoyle, S., Davies, N., Hampton, J., & Kleiber, P. (2009). Stock assessment of yellowfin tuna in the western and central Pacific Ocean. WCPFC SC5 SA WP-3, Port Vila, Vanuatu, 1–1.
Le Manach, F., Bach, P., Barret, L., Guyomard, D., Fleury, P. G., Sabarros, P. S., and Pauly, D. (2015). Reconstruction of the domestic and distant water fisheries catch of La Réunion (France), 1950–2010. Fisheries Centre Research Reports 23(2), University of British Columbia, 83–98.
Le Manach, F., Bach, P., Boistol, L., Robinson, J., and Pauly, D. (2015). Artisanal fisheries in the world's second largest tuna fishing ground-Reconstruction of the Seychelles' marine fisheries catch, 1950–2010. Fisheries Centre Research Reports 23(2), University of British Columbia, 99–110.
Lehodey, P. (2000). Impacts of the El Niño Southern Oscillation on tuna populations and fisheries in the tropical Pacific Ocean.

Secretariat of the Pacific Community No. RG-1.
Lehodey, P. (2001). The pelagic ecosystem of the tropical Pacific Ocean: dynamic spatial modelling and biological consequences of ENSO. Progress in Oceanography, 49(–), 43–68.
Lehodey, P. et al. (2011). Vulnerability of oceanic fisheries in the tropical Pacific to climate change. In J. D. Bell, J. E. Johnson, & A. J. Hobday (Eds.), Vulnerability of oceanic fisheries in the tropical Pacific to climate change (pp. 433–492). Secretariat of the Pacific Community, Noumea, New Caledonia.
Lehodey, P., Alheit, J., Barange, M., Baumgartner, T., Beaugrand, G., Drinkwater, K., Fromentin, J.-M., Hare, S., Ottersen, G., & Perry, R. (2006). Climate variability, fish, and fisheries. Journal of Climate, 19(20), 500–030.
Lehodey, P., Bertignac, M., Hampton, J., Lewis, A., & Picaut, J. (1997). El Niño Southern Oscillation and tuna in the western Pacific. Nature, 389(6652), 71–18.
Lehodey, P., Chai, F., & Hampton, J. (2003). Modelling climate-related variability of tuna populations from a coupled ocean–biogeochemical-populations dynamics model. Fisheries Oceanography, 12(4-5), 48–94.
Lehodey, P., Senina, I., & Murtugudde, R. (2008). A spatial ecosystem and populations dynamics model (SEAPODYM)–Modeling of tuna and tuna-like populations. Progress in Oceanography, 78(4), 30–18.
Lehodey, P., Senina, I., Calmettes, B., Hampton, J., & Nicol, S. (2013). Modelling the impact of climate change on Pacific skipjack tuna population and fisheries. Climatic change, 119, 9–09.
Lehodey, P., Senina, I., Sibert, J., Bopp, L., Calmettes, B., Hampton, J., & Murtugudde, R. (2010). Preliminary forecasts of Pacific bigeye tuna population trends under the A2 IPCC scenario. Progress in Oceanography, 86(–), 30–15.
Lennert-Cody, C., & Hall, M. (2000). The development of the purse seine fishery on drifting Fish Aggregating Devices in the eastern Pacific Ocean: 199–998. Pêche thonière et dispositifs de concentration de poissons, Caribbean-Martinique, 1–9 Oct 1999 1–9 octobre 1999,
Leung, S., Thompson, L., McPhaden, M. J., & Mislan, K. (2019). ENSO drives near-surface oxygen and vertical habitat variability in the tropical Pacific. Environmental Research Letters, 14(6), 064020.
Li, X., Hu, Z. Z., Tseng, Y. h., Liu, Y., & Liang, P. (2022). A historical

perspective of the La Niña event in 2020/2021. *Journal of Geophysical Research: Atmospheres*, *127*(7), e2021JD035546.
Loukos, H., Monfray, P., Bopp, L., & Lehodey, P. (2003). Potential changes in skipjack tuna (Katsuwonus pelamis) habitat from a global warming scenario: modelling approach and preliminary results. Fisheries Oceanography, 12(4-5), 47–82.
Lu, H. J., Lee, K. T., Lin, H. L., & Liao, C. H. (2001). Spatio-temporal distribution of yellowfin tuna Thunnus albacares and bigeye tuna Thunnus obesus in the Tropical Pacific Ocean in relation to large-scale temperature fluctuation during ENSO episodes. Fisheries Science, 67(6), 104–052.
Lu, P., McCreary Jr, J. P., & Klinger, B. A. (1998). Meridional circulation cells and the source waters of the Pacific Equatorial Undercurrent. Journal of Physical Oceanography, 28(1), 6–4.
Maes, C., & Belamari, S. (2011). On the impact of salinity barrier layer on the Pacific Ocean mean state and ENSO. Sola, 7, 9–00.
Maes, C., Ando, K., Delcroix, T., Kessler, W. S., McPhaden, M. J., & Roemmich, D. (2006). Observed correlation of surface salinity, temperature and barrier layer at the eastern edge of the western Pacific warm pool. Geophysical research letters, 33(6).
Makarim, S., Sprintall, J., Liu, Z., Yu, W., Santoso, A., Yan, X.-H., & Susanto, R. D. (2019). Previously unidentified Indonesian Throughflow pathways and freshening in the Indian Ocean during recent decades. Scientific reports, 9(1), 7364.
Marsac, F., & Le Blanc, J. (1999). Oceanographic changes during the 1997–1998 El Niño in the Indian Ocean and their impact on the purse seine fishery. IOTC Proc(2), 14–57.
Marsac, F., & Le Blanc, J.-L. (1998). Dynamics of ENSO events in the Indian ocean: To what extent would recruitment and catchability of tropical tunas be affected?
Marsac, F., and Le Blanc, J. L. (1999). Oceanographic changes during the 199–998 El Niño in the Indian Ocean and their impact on the purse seine fishery. 1st session of the IOTC working party on tropical tunas, Seychelles, 4–8.
Martin, A., Boyd, P., Buesseler, K., Cetinic, I., Claustre, H., Giering, S., Henson, S., Irigoien, X., Kriest, I., & Memery, L. (2020). The oceans' twilight zone must be studied now, before it is too late. Nature, 580(7801), 2–8.
McIlgorm, A., Hanna, S., Knapp, G., Le Floc'H, P., Millerd, F., & Pan, M. (2010). How will climate change alter fishery governance? Insights from seven international case studies. Marine Policy,

34(1), 17–77.
McPhaden, M., & Picaut, J. (1990). El Niño-Southern Oscillation displacements of the western equatorial Pacific warm pool. Science, 250(4986), 138–388.
Ménard, F., Marsac, F., Bellier, E., & Cazelles, B. (2007). Climatic oscillations and tuna catch rates in the Indian Ocean: a wavelet approach to time series analysis. Fisheries Oceanography, 16(1), 9–04.
Mohri, M., & Nishida, T. (2000). Consideration on distribution of adult yellowfin tuna (Thunnus albacares) in the Indian Ocean based on Japanese tuna longline fisheries and survey information. J Natl Fish Univ, 49, 1–11.
Morato, T., Hoyle, S. D., Allain, V., & Nicol, S. J. (2010). Tuna longline fishing around West and Central Pacific seamounts. PloS one, 5(12), e14453.
Morgan, A. (2011). Fish aggregating devices and tuna: impacts and management options. *Ocean science division, Pew Environment Group, Washington, DC*, *18*.
Na, H., Jang, B.-G., Choi, W.-M., & Kim, K.-Y. (2011). Statistical simulations of the future 50-year statistics of cold-tongue El Niño and warm-pool El Niño. Asia-Pacific Journal of Atmospheric Sciences, 47, 22–33.
Nakano, H., Okazaki, M., & Okamoto, H. (1997). Analysis of catch depth by species for tuna longline fishery based on catch by branch lines. Bull. Nat. Res. Inst. Far Seas Fish, 34, 4–2.
Nicol, S., Lehodey, P., Senina, I., Bromhead, D., Frommel, A. Y., Hampton, J., Havenhand, J., Margulies, D., Munday, P. L., & Scholey, V. (2022). Ocean futures for the world's largest yellowfin tuna population under the combined effects of ocean warming and acidification. Frontiers in Marine Science, 9.
NOAA Climate Prediction Center. (n.d.). ENSO: Recent Evolution, Current Status and Predictions. Retrieved from https://www.cpc.ncep.noaa.gov/products/analysis_monitoring/enso_advisory/ensodisc.shtml, , accessed on 5/28/23.
Park, J. Y., Kug, J. S., Park, J., Yeh, S. W., & Jang, C. J. (2011). Variability of chlorophyll associated with El Niño–Southern Oscillation and its possible biological feedback in the equatorial Pacific. Journal of Geophysical Research: Oceans, 116(C10).
Pauly, D., & Zeller, D. (2016). Catch reconstructions reveal that global marine fisheries catches are higher than reported and declining. Nature communications, 7(1), 10244.

Perruche, C., Szczypta, C., Paul, J., and Drévillon, M. (2019). Global Production Centre GLOBAL_REANALYSIS_BIO_001_029. Copernicus Marine Environment Monitoring Service.

Phillips, J. S., Gupta, A. S., Senina, I., van Sebille, E., Lange, M., Lehodey, P., Hampton, J., & Nicol, S. (2018). An individual-based model of skipjack tuna (Katsuwonus pelamis) movement in the tropical Pacific ocean. Progress in Oceanography, 164, 6–4.

Phillips, S. J., Anderson, R. P., & Schapire, R. E. (2006). Maximum entropy modeling of species geographic distributions. *Ecological modelling*, *190*(3-4), 231-259.

Picaut, J., Ioualalen, M., Menkès, C., Delcroix, T., & Mcphaden, M. J. (1996). Mechanism of the zonal displacements of the Pacific warm pool: Implications for ENSO. Science, 274(5292), 148–489.

POSEIDON, MRAG, NFDS, and COFREPECHE. (2014). Review of tuna fisheries in the western Indian Ocean. Framework contract MARE/2011/01 - Lot 3 specific contract 7, Brussels, 165.

Radenac, M. H., Léger, F., Singh, A., & Delcroix, T. (2012). Sea surface chlorophyll signature in the tropical Pacific during eastern and central Pacific ENSO events. Journal of Geophysical Research: Oceans, 117(C4).

Remolà, A. O., & Gudmundsson, A. (2018). Global review of safety at sea in the fisheries sector. Food and Agriculture Organization of the United Nations.

Reverdin, G., Frankignoul, C., Kestenare, E., & McPhaden, M. J. (1994). Seasonal variability in the surface currents of the equatorial Pacific. Journal of Geophysical Research: Oceans, 99(C10), 2032–0344.

Ritchie H., & Roser M. (2021, October). Fish and Overfishing. Out World In Data. https://ourworldindata.org/fish-and-overfishing

Saji, N., Goswami, B. N., Vinayachandran, P., & Yamagata, T. (1999). A dipole mode in the tropical Indian Ocean. Nature, 401(6751), 36–63.

Schaefer, K. M., & Fuller, D. W. (2005). Conventional and archival tagging of bigeye tuna (Thunnus obesus) in the eastern equatorial Pacific Ocean. Col. Vol. Sci. Pap. ICCAT, 57(2), 6–4.

Schaefer, K. M., & Fuller, D. W. (2010). Vertical movements, behavior, and habitat of bigeye tuna (Thunnus obesus) in the equatorial eastern Pacific Ocean, ascertained from archival tag data. Marine Biology, 157, 262–642.

Schaefer, K. M., & Oliver, C. W. (1998). Shape, volume, and resonance frequency of the swimbladder of yellowfin tuna (Thunnus alabacares). Fishery Bulletin, 98, 364–374

Schaefer, K. M., & Oliver, C. W. (1998). Shape, volume, and resonance frequency of the swimbladder of yellowfin tuna (Thunnus alabacares).

Schaefer, K. M., Fuller, D. W., & Block, B. A. (2011). Movements, behavior, and habitat utilization of yellowfin tuna (Thunnus albacares) in the Pacific Ocean off Baja California, Mexico, determined from archival tag data analyses, including unscented Kalman filtering. Fisheries Research, 112(–), 2–7.

Schlitzer, R. (2004). Export production in the equatorial and North Pacific derived from dissolved oxygen, nutrient and carbon data. Journal of Oceanography, 60, 5–2.

Senina, I., Lehodey, P., Calmettes, B., Dessert, M., Hampton, J., Smith, N., Gorgues, T., Aumont, O., Lengaigne, M., & Menkes, C. (2018). Impact of climate change on tropical Pacific tuna and their fisheries in Pacific Islands waters and high seas areas. 14th Regular Session of the Scientific Committee of the Western and Central Pacific Fisheries Commission, WCPFC-SC14.

Song, L. M., Zhang, Y., Xu, L. X., Jiang, W. X., & Wang, J. Q. (2008). Environmental preferences of longlining for yellowfin tuna (Thunnus albacares) in the tropical high seas of the Indian Ocean. Fisheries Oceanography, 17(4), 23–53.

Song, L., Zhou, J., Zhou, Y., Nishida, T., Jiang, W., & Wang, J. (2009). Environmental preferences of bigeye tuna, Thunnus obesus, in the Indian Ocean: an application to a longline fishery. Environmental Biology of Fishes, 85, 15–71.

Sprintall, J., & Tomczak, M. (1992). Evidence of the barrier layer in the surface layer of the tropics. Journal of Geophysical Research: Oceans, 97(C5), 730–316.

Syamsuddin, M. L., Saitoh, S.-I., Hirawake, T., Bachri, S., & Harto, A. B. (2013). Effects of El Niño–Southern Oscillation events on catches of bigeye tuna (Thunnus obesus) in the eastern Indian Ocean off Java.

Taft, B., Hickey, B., Wunsch, C., & Baker Jr, D. (1974). Equatorial undercurrent and deeper flows in the central Pacific. Deep Sea Research and Oceanographic Abstracts,

Takahashi, K., & Battisti, D. S. (2007). Processes controlling the mean tropical Pacific precipitation pattern. Part I: The Andes and the eastern Pacific ITCZ. Journal of Climate, 20(14), 343–451.

Toggweiler, J., Dixon, K., & Broecker, W. (1991). The Peru upwelling and the ventilation of the South Pacific thermocline. Journal of Geophysical Research: Oceans, 96(C11), 2046–0497.

Tremblay-Boyer, L., McKechnie, S., Pilling, G., & Hampton, J. (2017). Stock assessment of yellowfin tuna in the western and central Pacific Ocean. Report to the 13th Regular Session of the Scientific Committee of the Western & Central Pacific Fisheries Commission, Rarotonga, Cook Islands, 9(17), 125.

Vali, S., Rhodes, K., Au, A., Zylich, K., Harper, S., & Zeller, D. (2014). Reconstruction of total fisheries catches for the Federated States of Micronesia (195–010). Fisheries-Centre of The University of British Columbia, Working paper, 6.

Varghese, S. P., Mukesh, Pandey, S., and Ramalingam, L. (2019). Recent studies on the population delineation of yellowfin tuna in the Indian Ocean considerations for stock assessment, IOTC-2019-WPM1–8.

Vialard, J., & Delecluse, P. (1998). An OGCM study for the TOGA decade. Part II: Barrier-layer formation and variability. Journal of Physical Oceanography, 28(6), 108–106.

Vialard, J., Duvel, J., Mcphaden, M., Bouruet-Aubertot, P., Ward, B., Key, E., Bourras, D., Weller, R., Minnett, P., & Weill, A. (2009). Cirene: air–sea interactions in the Seychelles–Chagos thermocline ridge region, B. Am. Meteorol. Soc., 90, 45–61. In.

Vincent, D. G. (1994). The South Pacific convergence zone (SPCZ): A review. Monthly weather review, 122(9), 194–970.

Waliser, D. E., & Gautier, C. (1993). A satellite-derived climatology of the ITCZ. Journal of Climate, 6(11), 216–174.

Wang, C.-c., & Magnusdottir, G. (2006). The ITCZ in the central and eastern Pacific on synoptic time scales. Monthly weather review, 134(5), 140–421.

Weller, E., Min, S.-K., Cai, W., Zwiers, F. W., Kim, Y.-H., & Lee, D. (2016). Human-caused Indo-Pacific warm pool expansion. *Science advances*, *2*(7), e1501719.

Wexler, J. B., Margulies, D., & Scholey, V. P. (2011). Temperature and dissolved oxygen requirements for survival of yellowfin tuna, Thunnus albacares, larvae. Journal of Experimental Marine Biology and Ecology, 404(–), 6–2.

Wild, A., & Hampton, J. (1994). A review of the biology and fisheries for skipjack tuna, Katsuwonus pelamis, in the Pacific Ocean. FAO Fisheries Technical Paper (FAO).

Williams, P., & Terawasi, P. (2010). Overview of tuna fisheries in the

western and central Pacific Ocean, including economic conditions–2009. WCPFC-SC-010-GN-WP-01, Western and Central Pacific Fisheries Commission Scientific Committee Sixth Regular Session, Nuku'alofa, Kingdom of Tonga, 10–19 August 2010.

Williams, P., & Terawasi, P. (2010). Overview of tuna fisheries in the western and central Pacific Ocean, including economic conditions–2009.

Wyrtki, K. (1967). Equatorial pacific ocean1. Int J Oceanol & Limnol, 1, 11–47.

Xie, P., & Arkin, P. A. (1997). Global precipitation: A 17-year monthly analysis based on gauge observations, satellite estimates, and numerical model outputs. Bulletin of the american meteorological society, 78(11), 253–558.

Yu, L. (2015). Sea-surface salinity fronts and associated salinity-minimum zones in the tropical ocean. Journal of Geophysical Research: Oceans, 120(6), 420–225.

Zelle, H., Appeldoorn, G., Burgers, G., & van Oldenborgh, G. J. (2004). The relationship between sea surface temperature and thermocline depth in the eastern equatorial Pacific. Journal of Physical Oceanography, 34(3), 64–55.

Zeller, D., & Pauly, D. (2016). Catch reconstruction: concepts, methods, and data sources. Global Atlas of Marine Fisheries: A Critical Appraisal of Catches and Ecosystem Impacts. Island Press, Washington, DC, 1–3.

Zhang, T., Hoell, A., Perlwitz, J., Eischeid, J., Murray, D., Hoerling, M., & Hamill, T. M. (2019). Towards probabilistic multivariate ENSO monitoring. Geophysical research letters, 46(1–8), 1053–0540.

Zhang, Y., Du, Y., & Qu, T. (2016). A sea surface salinity dipole mode in the tropical Indian Ocean. Climate Dynamics, 47, 257–585.

Zheng, F., Zhang, R.-H., & Zhu, J. (2014). Effects of interannual salinity variability on the barrier layer in the western-central equatorial Pacific: A diagnostic analysis from Argo. Advances in Atmospheric Sciences, 31, 53–42.

Abstract (in Korean)

열대서인도양과 열대서태평양 상층 해양 변동성과 다랑어류 어획량 사이의 관계

다랑어류 어획량은 해수 온도, 수온약층의 깊이, 해류와 같은 물리적 해양 환경 변수에 크게 영향을 받는다. 따라서 다랑어류 어획량과 해양 환경 변동성 사이의 관계를 이해하는 것은 다랑어류 어업 변동을 설명하는 데 매우 중요하다. 이 논문에서는 다랑어류 어획량이 가장 많은 열대 서인도양과 서태평양에서 가장 많이 잡히는 어종인 가다랑어(*Katsuwonus pelamis*), 황다랑어(*Thunnus albacares*), 눈다랑어(*Thunnus obesus*)를 대상으로 해양 환경 변동성과 연간 어획량 간의 통계적 상관성을 25년에 걸쳐 조사하였다.

열대 남서인도양의 해양 환경과 연간 다랑어류 어획량 변동성 분석 결과, 북부 해역에서 수온약층 및 20° C 등수온선 수심이 깊어질수록 황다랑어와 눈다랑어 어획량이 증가하는 것으로 나타났다. 추가 분석 결과, 다랑어류 어획에 유리한 해양 조건은 엘니뇨 기간 동안 발생하며, 그 다음 해에도 지속되는 것으로 나타났다. 그러나 남부 해역 다랑어류 어획량의 변동성은 해양 환경의 변동만으로는 설명하기 어려웠으며,

이는 남부 해역에서 해양 환경 변동성이 약하기 때문인 것으로 생각된다.

열대서태평양 가다랑어 연간 어획량은 서부 해역에서는 라니냐와 유사한 조건일때 증가하는 반면, 동부 해역에서는 엘니뇨와 유사한 조건에서 증가하는 것으로 나타났다. 이는 가다랑어 어획에 유리한 조건이 해역에 따라 다름을 보여준다. 또한 황다랑어와 눈다랑어 어획량은 가다랑어와 비교했을 때 해양 환경 변동성과의 관계에서 반대의 특성을 보였다.

이러한 통계적 상관성을 바탕으로 열대서태평양에서 가다랑어 연간 어획량의 예측 가능성을 평가하였다. 그 결과 아표층 수온 또는 해수면 근처 염분이 가다랑어 어획량 변동성을 예측하는 좋은 지표가 될 수 있음을 보였다. 이 결과는 가다랑어 뿐만 아니라 황다랑어, 눈다랑어와 같은 다른 다랑어류의 연간 어획량도 통계적으로 예측 가능할 수 있음을 보여준다.

이 논문은 해양 환경 변동성과 다랑어류 어획량 간의 통계적 관계를 이해하는 데 기여하여 다랑어류 어업의 관리 및 지속 가능성 향상에 도움이 될 수 있을 것이다. 또한 해양 환경 변동성이 큰 해역일수록 어획량 예측 가능성이 높을 수 있다는 결과를 주요 시사점으로 제시하고자 한다.

주요 단어 : 다랑어류 어획량, 엘니뇨-남방 진동, 열대 남서 인도양, 열대 중앙 서태평양

학 번 : 2019-28546

Appendix I: Cyclostationary EOF analysis

A cyclostationary empirical orthogonal function (CSEOF) analysis (Kim et al., 1996; Kim and North, 1997) was conducted for extracting the spatio-temporal variability of ocean environmental variables. The CSEOF method has been utilized by various studies to investigate the relationship between a specific time series and the physical variability of the environmental variables (Kim et al., 2015; Kim et al., 2020; Kim and Na, 2022). The geophysical variables, $G(r,t)$, are decomposed into cyclostationary loading vectors (CSLVs), $A_n(r,t)$ and their corresponding principal component (PC) time series, $B_n(t)$ as in Eq. (1):

$$G(r,t) = \sum_n A_n(r,t)B_n(t), \qquad (1)$$

where n, r, and t denote the mode number, 2-dimensional space, and time, respectively. The current velocity was analyzed as a single variable by combining both the zonal and meridional components. The CSEOF analysis was conducted separately on each environmental

variable at each depth, and the CSLVs were obtained to demonstrate the physical evolution of environmental variables over a nested period d of 12 months. The nth mode of the CSLVs is expressed with periodicity d, as in Eq. (2):

$$A_n(r,t) = A_n(r,t+d) \qquad (2)$$

Thus, $A_n(r,t)$ consists of 12 monthly spatial patterns which that illustrate the spatio-temporal evolution of the nth mode. Its corresponding PC time series, $B_n(t)$, illustrates the temporal variation of the nth mode of spatial variation. Each of the PC time series is statistically independent and the CSLVs are perpendicular to one another.

Appendix II: Regression analysis and statistical prediction

The statistical relationship between the annual tuna catches in the each EEZ, $F(t)$, and ocean environmental variability was obtained by conducting regression analysis in the CSEOF space, as described by Eq. (3):

$$F(t) \approx \sum_{m=1}^{10} \alpha_m \tilde{B}_m(t), \qquad (3)$$

where m denotes the mode number, α_m is the regression coefficient, and $\tilde{B}_m(t)$ is annually averaged the PC time series of each ocean environmental variable. Through the regression coefficient, α_m, the regressed and reconstructed ocean environmental variability, $R(r,t)$, can be obtained as in Eq. (4):

$$R(r,t) = \sum_{m=1}^{10} \alpha_m A_m(r,t), \qquad (4)$$

Thus, the resulting physical evolutions of the ocean environment, $R(r,t)$, share the long-term variability of the fishery data, $F(t)$, with some regression error. In this dissertation, the first ten CSEOF PC time series of the predictors were used for the regression analysis to minimize the chance of overfitting, which can lead to unstable predictability. If the R-squared value is relatively low for a specific variable at a specific depth, it indicates that the ocean environmental variables at the depth is not closely related to the target variability. To investigate the interannual relationship between the tuna catches and ocean conditions, the annual mean spatial patterns of $R(r,t)$ are illustrated.

The annual catch amount of tuna, $F(t)$, was predicted for the prediction period, P, using the statistical relationship, β_m, derived from each training period (learning period), L, which is a subset of the total length of the time series used in the regression analysis (Kim et al., 2000). The estimated and predicted annual catch amount, $\bar{F}(t)$, including the prediction period, P can be written as in Eq. (5):

$$\bar{F}(t) = \sum_{m=1}^{M} \beta_m \tilde{B}_m(t), \qquad t \in L + P. \quad (5)$$

The first ten modes were utilized for the prediction (M = 10). In this dissertation, the prediction period, P, was set to 3, 2, and 1 years.